Quantitative Laser Diagnostics for Combustion Chemistry and Propulsion

Lecture 7: Electronic Spectra of Diatomics

1. Term symbols for diatomic molecules
2. Common molecular models for diatomics
3. Improved treatments
4. Quantitative absorption

Fortrat parabola, $^1\Delta \leftarrow {}^1\Delta$ (Symmetric Top)

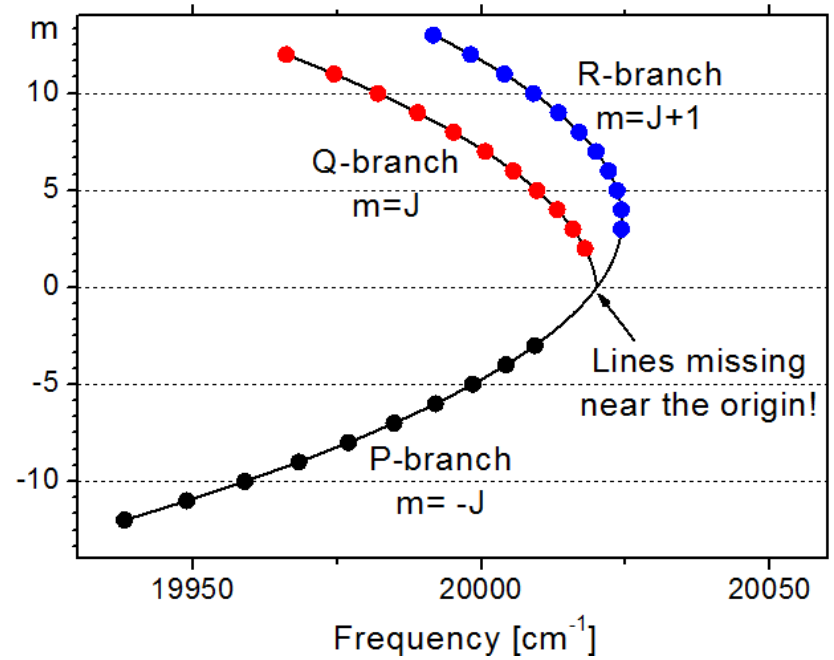

1. Term symbols for diatomic molecules

- Term symbols characterize key features of electron spin and orbital angular momentum

For an atom: $^{2S+1}L_J$

For a diatomic: $^{2S+1}\Lambda_\Omega$

Important terms

$\vec{\Lambda}$ projection of orbital angular momentum onto the internuclear axis.

Magnitude: $|\vec{\Lambda}| = \Lambda\hbar$

Symbols:

Λ	0	1	2
Symbol	Σ	Π	Δ

Atoms	L	0	1	2
	Symbol	S	P	D

$\vec{S}$ total electronic spin angular momentum (the sum of electron spin in unfilled shells)

Magnitude: $|\vec{S}| = S\hbar$, S will have 1/2-integer values

$\vec{\Sigma}$ projection of $\vec{S}$ onto the internuclear axis (only defined when Λ ≠ 0).

Magnitude: $|\vec{\Sigma}| = \Sigma\hbar$

Allowed values: $\Sigma = S, S-1, \ldots, -S \; (2S+1 \text{ values})$

$\vec{\Omega}$ sum of projections along the internuclear axis of electron spin and orbital angular momentum

$$\vec{\Omega} = \vec{\Sigma} + \vec{\Lambda}$$

$$\Omega = \Lambda + S, \Lambda + S - 1, \ldots, |\Lambda - S| \quad (2S+1 \text{ values for } \Lambda \geq S)$$

1. Term symbols for diatomic molecules

- Examples

For a diatomic: $^{2S+1}\Lambda_{\Omega}$

NO The ground state for NO is $X^2\Pi$

$S = 1/2$, $\Lambda = 1$, $\Omega = 3/2, 1/2$

There are two spin-split sub-states: $^2\Pi_{1/2}$, $^2\Pi_{3/2}$

Separation: $121 cm^{-1}$

CO The ground state for CO is $X^1\Sigma^+$

$S = 0$ and $\Lambda = 0$, therefore Ω is unnecessary. This is a rigid rotor molecule. <u>Easiest case!</u>

O_2 The ground state for O_2 is $X^3\Sigma_g^-$

$S = 1$, $\Lambda = 0$

The $^-$ and $_g$ are notations about symmetry properties of wave functions. This is an example of a molecule that is modeled by Hund's case **b**

2. Common molecular models for diatomics

- Four common molecular models

Rigid Rotor	$\Lambda = 0$, $S = 0$
Symmetric Top	$\Lambda \neq 0$, $S = 0$
Hund's *a*	$\Lambda \neq 0$, $S \neq 0$
Hund's *b*	$\Lambda = 0$, $S \neq 0$

2S+1 = 1 ➡ "singlets"
no influence of electron spin on spectra

Spin important through interaction of Λ and Σ

- This lecture:

  Rigid Rotor

  Symmetric Top

  Followed by:

  Hund's *a*

  Hund's *b*

2. Common molecular models for diatomics

- Rigid rotor ($^1\Sigma$)

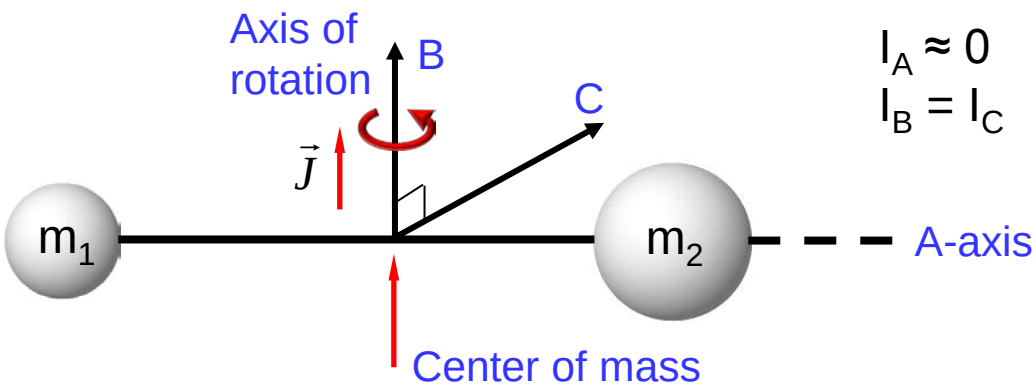

$I_A \approx 0$
$I_B = I_C$

- $\Lambda = 0$, $S = 0$ ➡ $^1\Sigma$ type, Ω is not defined
- $\Lambda = 0$ means the projection of the orbital angular momentum onto the A-axis is zero, and rotation must thus be around the B-axis

2. Common molecular models for diatomics

- Rigid rotor ($^1\Sigma$)

Rotational Energy $F(J) = B_v J(J+1) - D_v J^2 (J+1)^2$

Total Energy $E(T_e, \mathrm{v}, J) = T_e + G(\mathrm{v}) + F(J)$

Energy Change $\Delta E = \Delta T_e + \Delta G + \Delta F$

Selection Rules

Rotational spectra: $\Delta J = J' - J'' = +1$

Rovibrational spectra: $\Delta \mathrm{v} = \mathrm{v}' - \mathrm{v}'' = +1$

$\Delta J = \pm 1$

Rovibronic spectra: $\Delta \mathrm{v}$ determined by Frank-Condon factors

$\Delta J = \pm 1$

✐Note: an alternate form is sometimes used

$$\Delta\alpha = \alpha_{\text{final}} - \alpha_{\text{initial}}$$
$$\alpha = J \text{ or } \mathrm{v}$$

2. Common molecular models for diatomics

- Rigid rotor ($^1\Sigma$)

Intensity Distribution

Within each band (v', v''), the intensity distribution follows the Boltzmann distribution for J modified by a J-dependent branching ratio (i.e., for the P and R branch), known as the Hönl-London factor.

The relative intensities among all the vibrational bands originating from a single initial level $v_{initial}$ to all possible final levels v_{final} are given by Franck-Condon factors.

The relative total emission or absorption from $v_{initial}$ depends directly on the Boltzmann fraction in that level, i.e., $n_{v\ initial}/n$

Examples

Most stable diatomics: CO, Cl_2, Br_2, N_2, H_2 are rigid rotors
Exceptions: NO ($X^2\Pi$), $O_2(X^3\Sigma)$

Note: no $X\Delta$ states for diatomics – all X states are Σ or Π!
Some linear polyatomics: $CO_2(\tilde{X}^1\Sigma_g^+)$, HCN and N_2O $(\tilde{X}^1\Sigma^+)$ are rigid rotors with $^1\Sigma$ ground states.

Nuclear spin will have an impact on the statistics of homonuclear diatomic molecules

2. Common molecular models for diatomics

- Symmetric top

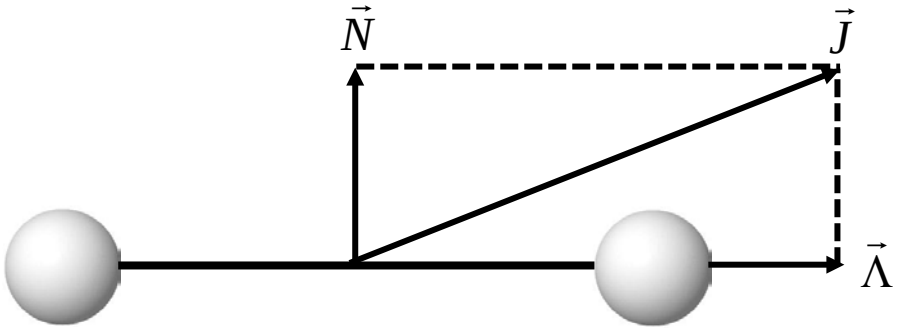

$I_A \neq 0$
$I_A \neq I_B = I_C$

- $\Lambda \neq 0$, $S = 0$ (non-zero projection of orbital angular momentum on the internuclear axis and zero spin) ➡ ground states $^1\Pi$, $^1\Delta$
- Important components

$\vec{N}$ angular momentum of nuclei

$\vec{\Lambda}$ A-axis projection of electron orbital angular momentum

$\vec{J}$ total angular momentum; $\vec{J} = \vec{N} + \vec{\Lambda}$

Only the axial component of orbital angular momentum is used, because only $\vec{\Lambda}$ is a “good” quantum number, i.e., a constant of the motion

2. Common molecular models for diatomics

- Symmetric top ($\Lambda \neq 0$, $S = 0$)

Rotational Energy

$$F(J) = BJ(J+1) + (A-B)\Lambda^2, \; J = \Lambda, \Lambda+1, \ldots$$

$$A, B = \frac{h}{8\pi^2 c I_{A,B}}$$

Same spacing as the rigid rotor, but with a constant offset

Since $I_A < I_B$, $A > B$, lines with $J < \Lambda$ are missing, as $J = \Lambda, \Lambda+1, \ldots$

Selection Rules

$$\Delta\Lambda = 0, \Delta J = \pm 1, 0 \quad (\Delta J = 0 \text{ is weak})$$

$$\Delta\Lambda = \pm 1, \Delta J = \pm 1, 0$$

As a result of having a Q branch (i.e., $\Delta J = 0$), the bands for a symmetric top will be double-headed, in contrast to the single-headed character of rigid rotor bands

2. Common molecular models for diatomics

- Symmetric top ($\Lambda \neq 0$, $S = 0$)

Spectra for $\Delta\Lambda = 0$ ($^1\Pi \leftarrow {}^1\Pi$ or $^1\Delta \leftarrow {}^1\Delta$)

$$T' = B' J'(J'+1) + (A'-B')\Lambda^2 + G(\mathrm{v}') + T_e'$$

$$T'' = B'' J''(J''+1) + (A''-B'')\Lambda^2 + G(\mathrm{v}'') + \boxed{T_e''}$$

= 0 for ground state

$$\bar{\nu}_\infty = \text{upper}(\text{for } J' = 0) - \text{lower}(\text{for } J'' = 0) = \text{constant}$$

$$P(J'') = \bar{\nu}_\infty - (B'+B'')J + (B'-B'')J^2$$

$$Q(J'') = \bar{\nu}_\infty + (B'-B'')J + (B'-B'')J^2$$

$$R(J'') = \bar{\nu}_\infty + (B'+B'')(J+1) + (B'-B'')(J+1)^2$$

$$m_P = -J$$

$$m_Q = +J$$

$$m_R = J+1$$

P and R branches: $\bar{\nu} = \bar{\nu}_\infty + am + bm^2$

Q branch: $\bar{\nu} = \bar{\nu}_\infty + bm + bm^2$

where $a = B'+B'', b = B'-B''$

2. Common molecular models for diatomics

- Symmetric top ($\Lambda \neq 0$, $S = 0$)

Spectra for $\Delta\Lambda = 0$

P and R branches: $\bar{\nu} = \bar{\nu}_\infty + am + bm^2$

Q branch: $\bar{\nu} = \bar{\nu}_\infty + bm + bm^2$

where $a = B' + B'', b = B' - B''$

Notes:

- Band heads in the Q and R branches for the typical case of B'<B".
- $m_P = -J$, $m_Q = +J$, $m_R = J+1$
- $J_{min} = 2$ for $^1\Delta \leftarrow {}^1\Delta$
  - ➡ $m_{min}=3$ for R branch
    $m_{min}=2$ for Q branch
    $|m_{min}|=3$ for P branch
  - ➡ missing lines near the origin

Fortrat parabola, $^1\Delta \leftarrow {}^1\Delta$

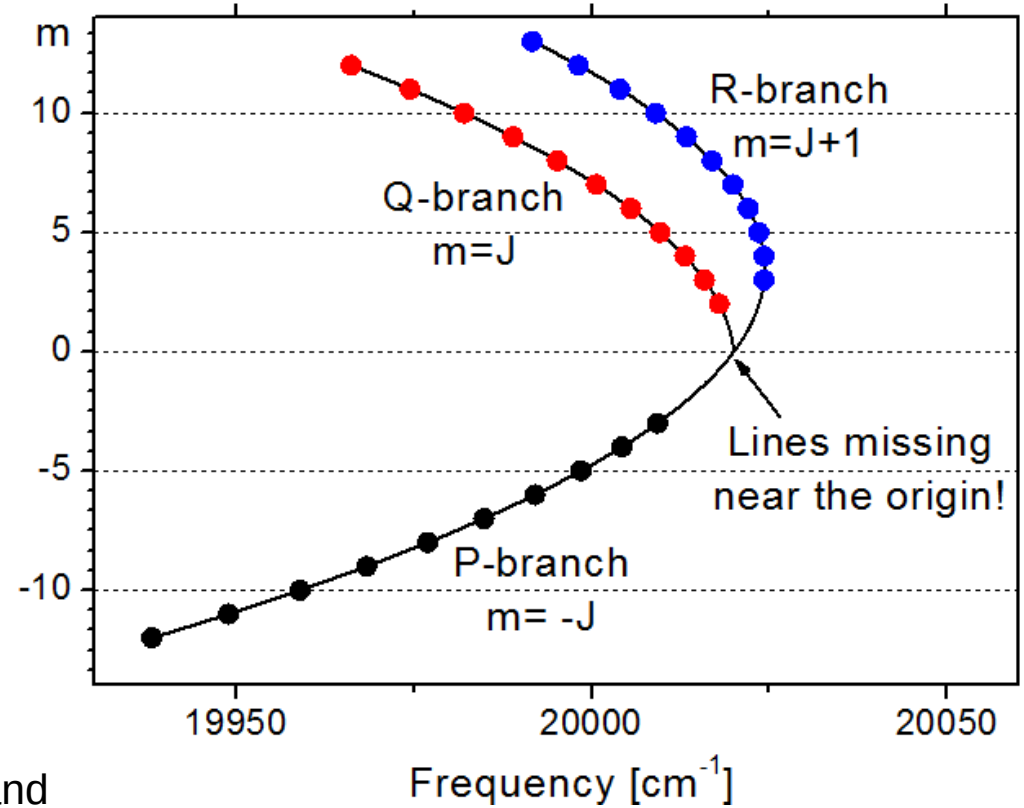

Intensity Distribution

Relative intensities depend on
- n_J/n, and
- Hönl-London factors ($S_J^{P,Q,R}$) - "relative intensity factors / line strengths" ➡ breakdown of the principle of equal probability

2. Common molecular models for diatomics

- Example – 1: Hönl-London Factors for Symmetric Top (see Herzberg)

For ΔΛ = 0

$$\left.\begin{aligned} S_J^R &= \frac{(J+1+\Lambda)(J+1-\Lambda)}{J+1} \approx J+1 \quad (J >> \Lambda) \\ S_J^Q &= \frac{(2J+1)\Lambda^2}{J(J+1)} \approx \frac{2\Lambda^2}{J} \approx 0 \qquad \text{for large } J \\ S_J^P &= \frac{(J+\Lambda)(J-\Lambda)}{J} \approx J \qquad \text{for large } J \end{aligned}\right\} \sum S_J = 2J+1$$

Notes:

1. $\Sigma S_J = 2J+1$, the total degeneracy!
2. The R-branch line for a specific J, is ~ J+1/J times as strong as the P-branch line
3. For ΔΛ=±1, J>>Λ

$$\left.\begin{aligned} S_J^R &= \frac{(2J+1)}{4} \\ S_J^Q &= \frac{(2J+1)}{2} \\ S_J^P &= \frac{(2J+1)}{4} \end{aligned}\right\} \sum S_J = 2J+1$$

Q branch lines are twice as strong as P and R lines!

ΔΛ value is important in determining the relative line and branch strengths of rovibronic spectra.

2. Common molecular models for diatomics

- Example – 2: Symmetric Top Ground State

If X = $^1\Pi$, possible transitions (Recall $\Delta\Lambda = 0, \pm 1$)

$^1\Pi \leftarrow {}^1\Pi$	$^1\Delta \leftarrow {}^1\Pi$	$^1\Sigma \leftarrow {}^1\Pi$
$\Delta\Lambda = 0$	$\Delta\Lambda = 1$	$\Delta\Lambda = -1$

1. Three separate "systems" of bands possible from $X^1\Pi$
2. Hönl-London factors for $\Delta\Lambda = \pm 1$ differ from for $\Delta\Lambda = 0$ (see previous page)

3. Electronic Spectra of Diatomic Molecules: Improved Treatments (add Spin)

1. Review of angular momentum
2. Interaction of Λ and Σ
3. Hund's case a (Λ ≠ 0, S ≠ 0)
4. Hund's case b (Λ = 0, S ≠ 0)
5. Λ-doubling

Hund's case a

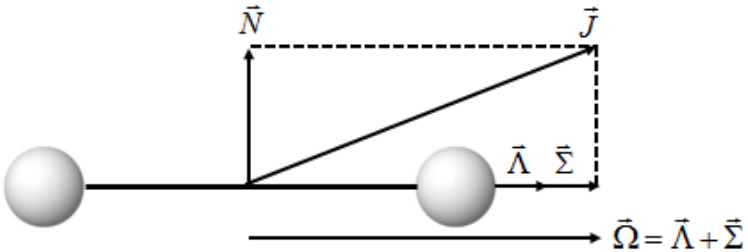

Hund's case b

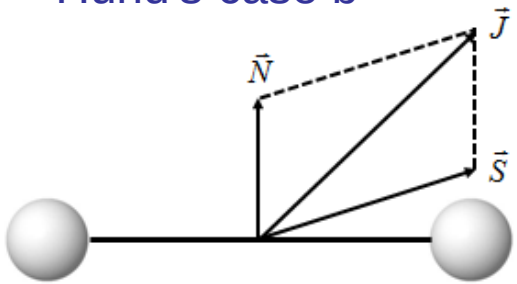

3.1. Review of angular momentum

- Review – then add spin
  - Term symbol

"Multiplicity" of state

$$\boxed{\text{Term Symbol} = {}^{2S+1}\Lambda_{\Omega}}$$

Sum of projections on A axis when $\Lambda \neq 0$

$$\vec{\Omega} = \vec{\Lambda} + \vec{\Sigma}$$

$$\Omega = \Lambda + S, \Lambda + S - 1, \ldots, |\Lambda - S|$$

Projection of electron orbital angular momentum on A axis

Λ	**0**	**1**	**2**
Symbol	Σ	Π	Δ

  - 4 models
    - Rigid Rotor $\Lambda = S = 0$ e.g., N_2, H_2: $X^1\Sigma$
    - Symmetric Top $\Lambda \neq 0$; $S = 0$ e.g., $^1\Pi$
    - Hund's a $\Lambda \neq 0$; $S \neq 0$ e.g., OH, NO (both $X^2\Pi$)
    - Hund's b $\Lambda = 0$; $S \neq 0$ e.g., O_2: $X^3\Sigma$

Add spin

3.1. Review of angular momentum

- Electronic angular momentum for molecules
  - Orbital angular momentum of electrons

    1. Separate from spin and nuclear rotation
    2. Strong electrostatic field exists between nuclei.

       So $\vec{L}$ precesses about field direction (internuclear axis) with "allowed" components along axis

       ➡ m_l = L, L-1, …, -L ≡ Λ

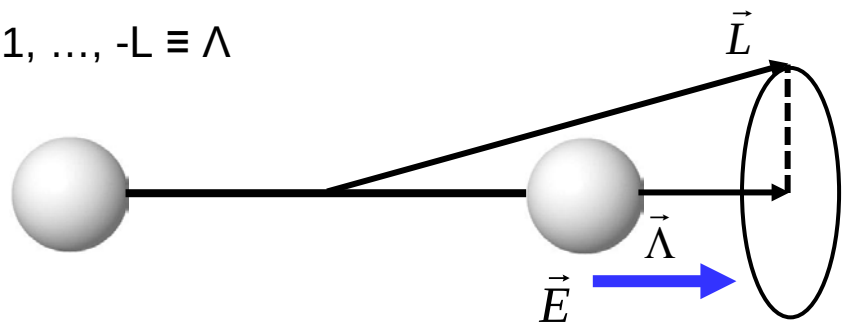

    3. If we reverse direction of electron orbit in $\vec{E}$ field, we get the same energy but Λ → –Λ (Λ doubling)

3.1. Review of angular momentum

- Electronic angular momentum for molecules
  - Spin of electrons

    1. To determine L and S for molecule, we usually sum l & s for all electrons. e.g., $S = \sum_i s_i$

       So even number of electrons ➡ integral spin

       odd number of electrons ➡ half-integral spin

    2. For $\Lambda \neq 0$, precession of L about internuclear axis ➡ magnetic field along axis. So m_s is defined. $m_s \equiv \Sigma = S, S-1, \ldots -S$.

       Note for change of orbital direction, energy of electron spinning in magnetic field changes ➡ no degeneracy ➡ 2S+1 possibilities (multiplets)

    3. For $\Lambda = 0$, no magnetic field exists and the projection of S on the nuclear axis is not conserved (Σ not defined)

3.1. Review of angular momentum

- Electronic angular momentum for molecules
  - Total electronic angular momentum

    1. Total electronic angular momentum along internuclear axis is $\vec{\Omega} = \vec{\Lambda} + \vec{\Sigma}$

       But since all in same direction, use simple addition

       $$\Omega = |\Lambda + \Sigma|$$

    2. For $\Lambda \neq 0$, magnetic field $H \propto \Lambda$.

       Magnetic moment of "spinning" electron $\mu_H \propto \Sigma$.

       So interaction energy is proportional to $E \sim \mu H \sim \Lambda\Sigma$, or

       $T_e = T_0 + A\Lambda\Sigma$ (more on this later)

       For $A > 0$, "Regular" state

       For $A < 0$, "Inverted" state

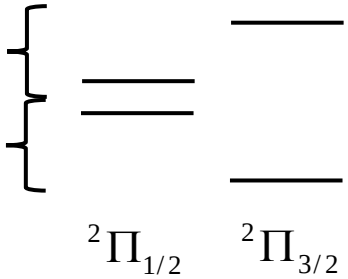

3.2. Interaction of Λ and Σ

- This interaction is key to modeling the influence of spin on the electronic state structure.

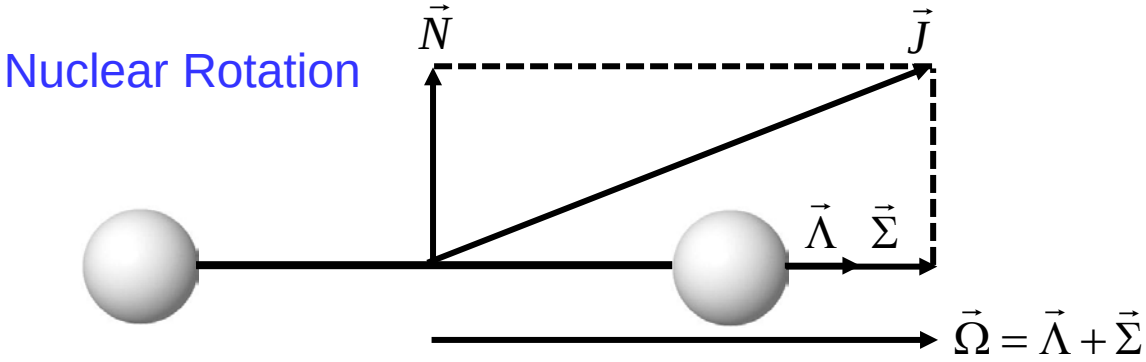

When Λ ≠ 0, S ≠ 0, they combine to form a net component of Ω.

Λ ≠ 0 ➡ an associated magnetic field due to net current about the axis. This field interacts with spinning electrons.

➡ Spin-orbit coupling (spin-splitting of energy levels)

Comments:

- Models are only approximations.
- Coupling may change as J ranges from low to high values

3.2. Interaction of Λ and Σ

- Examples

$^3\Delta$ ⟨
- $^3\Delta_3$ ⬅ S = 1, Λ = 2, Ω = 3 (Σ = 1)
- $^3\Delta_2$ ⬅ S = 1, Λ = 2, Ω = 2 (Σ = 0)
- $^3\Delta_1$ ⬅ S = 1, Λ = 2, Ω = 1 (Σ = –1)

Electronic energies $T_e = T_0 + A\Lambda\Sigma$

T_0: Energy without interaction

A: Spin-orbit coupling constant, generally increases with molecular weight and the number of electrons

$^3\Delta$ ➡ S = 1, Λ = 2, Σ = 1,0,–1

$$T_e = T_0 + A(2)\begin{pmatrix}1\\0\\-1\end{pmatrix}$$

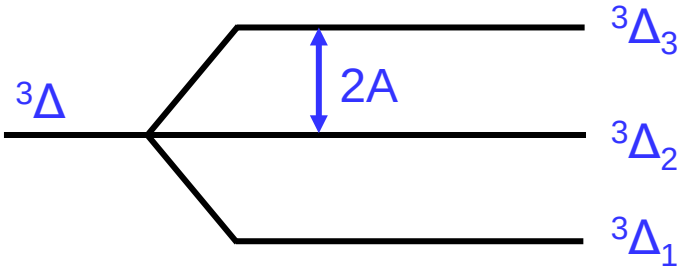

For A>0

Sample constants

$A_{BeH} \approx 2\ cm^{-1}$
$A_{NO} \approx 124\ cm^{-1}$
$A_{HgH} \approx 3600\ cm^{-1}$
$A_{OH} \approx -140\ cm^{-1}$ ← Negative!

Notes:
1. The parameter Y is often specified, where $Y = A/B_v$
2. Values for A given in Herzberg, Vol.I

Now, consider Hund's cases where S ≠ 0

3.3. Hund's case a

- $\Lambda \neq 0$, $S \neq 0$, $\Sigma = S, S-1, \ldots, -S$

$$F(J) = BJ(J+1) + (A-B)\Omega^2$$

$$\Omega = \Lambda + S, \Lambda + S - 1, \ldots, |\Lambda - S|$$

$$J = \Omega, \Omega + 1, \ldots$$

- Recall

$$A = \frac{h}{8\pi^2 I_A c}, B = \frac{h}{8\pi^2 I_B c}$$

Not to be confused with spin-orbit constant

P, Q, R branches for each value of Ω.

Example:

$^2\Pi$ ➡ Ω = 3/2 and 1/2, two electronic sub-states

➡ a total of 2 x 3 = 6 branches

3.4. Hund's case b

- Applies when spin is *not* coupled to the A-axis
  - E.g., 1. For Λ = 0, $\vec{\Sigma}$ is not defined, must use $\vec{S}$

    2. At high J, especially for hydrides, even with Λ ≠ 0

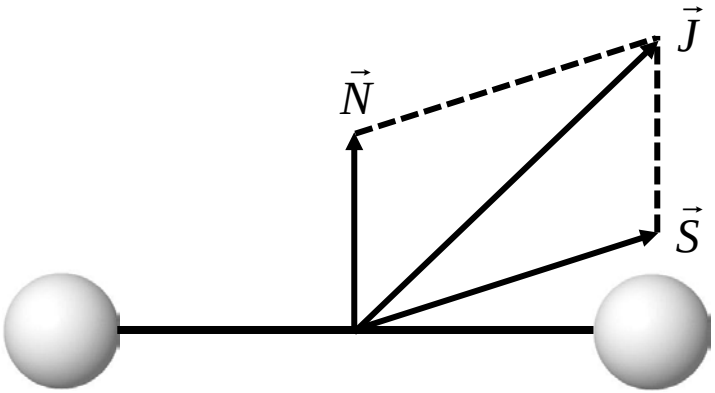

Allowed J: J = N+S, N+S-1, …, N-S, J ≥ 0 only

For this case, $\vec{S}$ and $\vec{N}$ couple directly,

3.4. Hund's case b

- Example – O_2
  - Ground state $X^3\Sigma$ has three J's for each N!

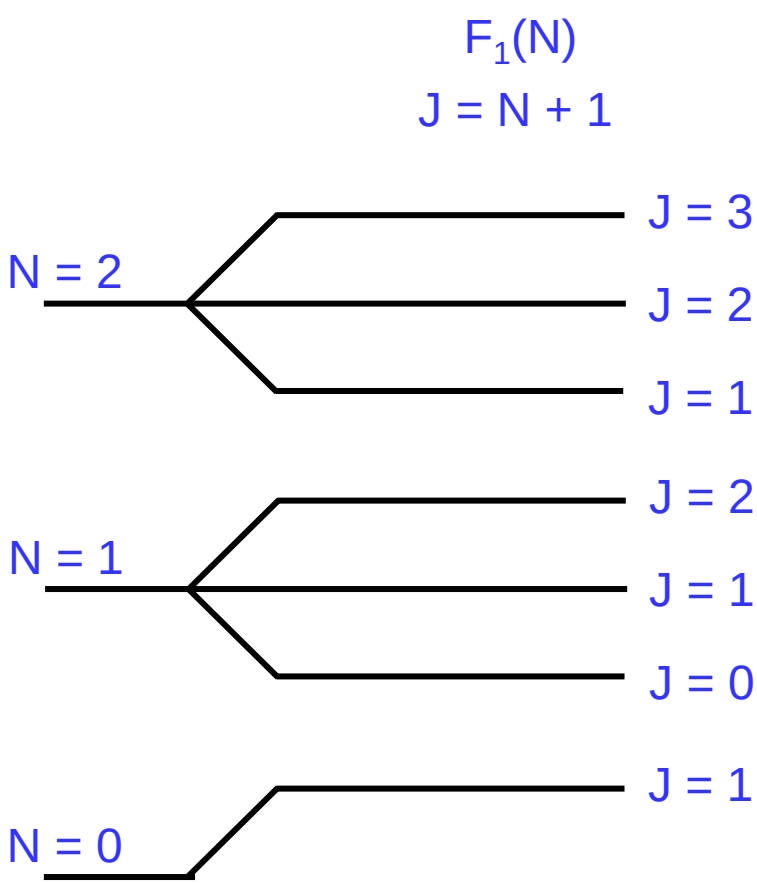

Notes:

- Split rotational levels for N > 0
- Each level has a degeneracy of 2J + 1, and a sum of Hönl-London factors of 2J + 1
- Minimum J is |N-S|
- In N = 0 level, only spin is active (S = 1), this is the minimum value of J

3.5. Λ – doubling

- Further complexity in the energy levels resulting from Λ-doubling
  - Different coupling with nuclear rotation ($\vec{N}$ and $\vec{\Lambda}$ interaction)

    ➡ The two orientations of $\vec{\Lambda}$ (± Λ along the A-axis) have slightly different energies

$$F(J) \rightarrow F_c(J) \text{ and } F_d(J)$$

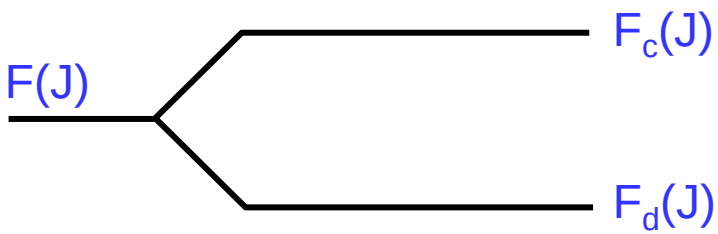

  - By definition, $F_c(J)>F_d(J)$ (c,d replaced by e,f in some literature)
  - Lambda doubling usually results in a very small change in energy, affecting Boltzmann distribution only slightly.
  - Change of parity between Λ-doubled states – reduces the accessible fraction of molecules for a given transition (due to selection rules)

4. Quantitative absorption

- Review of Beer's law and spectral absorption as interpreted for molecules with multiplet structure
  - Beer's Law

$$\left(\frac{I}{I^0}\right)_\nu = \exp\left(-k_\nu L\right)$$

  - For two-level system

$$n_1 = \frac{n_1}{n_i} n_i$$

$$k_\nu = S_{12}\phi(\nu) = \left(\frac{\pi e^2}{m_e c}\right) n_1 f_{12} \left(1 - \exp\left(-h\nu / kT\right)\right)\phi(\nu)$$

$f_{ij}, i - \text{initial}, j - \text{final}$

Integrated absorption intensity [$cm^{-1}s^{-1}$]

For a complex, multiple level system, we have 2 quantities to specify:

- *Boltzmann fraction?*
- *Oscillator strength for a specific transition?*

4. Quantitative absorption

- Boltzmann fraction
- $$n_1 = n_i \frac{n_1}{n_i}$$

  n_i = the total number density of species I

  n_1/n_i = the fraction of species i in state/level 1

- $$\frac{n_1}{n_i} = \frac{N_i(n, \mathrm{v}, \Sigma, \Lambda, J, N)}{N_i}$$

<u>Quantum numbers</u>:

n – electronic
v – vibrational
Σ – spin
Λ – orbital
J – total angular momentum
N – nuclear rotation
c or *d* – Λ-component

We will illustrate this in the next lecture!

4. Quantitative absorption

- Oscillator strength
  - Strength of a *specific*, single transition (i.e., from *one* of the J" substrates to a specific J' substrate), $f_{J''J'}$

$$f_{12} = f_{(m,\mathrm{v}'',J'')(n,\mathrm{v}',J')} = f_{J''J'}$$

$$= \underbrace{f_{el}}_{\text{"system" osc. strength}} \times \underbrace{q_{\mathrm{v}''\mathrm{v}'}}_{\text{Franck-Condon factor}} \times \underbrace{\frac{S_{J''J'}}{2J''+1}}_{\text{normalized H-L factor or line strength}}$$

Notes:

- $\sum_{\mathrm{v}'} q_{\mathrm{v}''\mathrm{v}'} = 1$
- $\sum_{J'} S_{J''J'} = (2J''+1)[(2S+1)\delta]$ $\delta = 1$ for Σ-Σ, otherwise $\delta = 2$ (Λ-doubling).

  $[(2S+1)\delta] = 4$ for OH's $A^2\Sigma \leftarrow X^2\Pi$ system.
- $\sum_{\mathrm{v}',J''} f_{J''J'} = [(2S+1)\delta] f_{el}$ sum is f_{el} for a single J" substate.

4. Quantitative absorption

- Oscillator strength

Remarks

1. Band oscillator strength $f_{v''v'} = f_{el} q_{v''v'}$ → often is tabulated
   e.g., f_{00} = 0.001 (OH $A^2\Sigma \leftarrow X^2\Pi$)

2. $$f_{J''J'} = f_{v''v'} \left(\frac{S_{J''J'}}{2J''+1} \right)$$
   e.g., if only P and R are allowed $S^P_{J''J'} = J'', S^R_{J''J'} = J''+1$

3. In some cases, an additional "correction term" $T_{J''J'}$ is used, e.g., in OH
   $$f_{J''J'} = f_{v''v'} \left(\frac{S_{J''J'}}{2J''+1} \right) T_{J''J'}, T_{J''J'} \text{ always near } 1$$

4. In terms of A-coefficient $$f_{v''v'} = \left(\frac{m_e c \lambda^2}{8\pi^2 e^2} \right) A_{v'v''} \left(\frac{g_{e'}}{g_{e''}} \right)$$
   $$= \frac{g_{e'}}{g_{e''}} f_{v'v''}$$

Next: Case Study of Molecular Spectra

- Ultraviolet: OH

Quantitative Laser Diagnostics for Combustion Chemistry and Propulsion

Lecture 8: Case Study: UV - OH

UV absorption of OH: $A^2\Sigma^+ – X^2\Pi$ (~300nm)

1. Introduction
2. OH energy levels
   - Upper level
   - Lower level
3. Allowed radiative transitions
   - Transition notations
   - Allowed transitions
4. Working example - OH

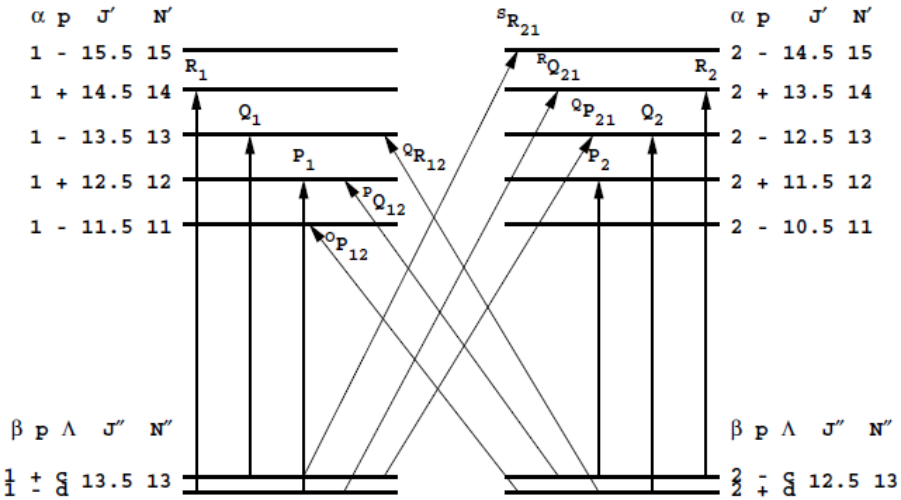

Allowed rotational transitions from N"=13 in the $A^2\Sigma^+ \leftarrow X^2\Pi$ system

1. Introduction

- OH, a prominent flame emitter, absorber.
  Useful for T, X_{OH} measurements.

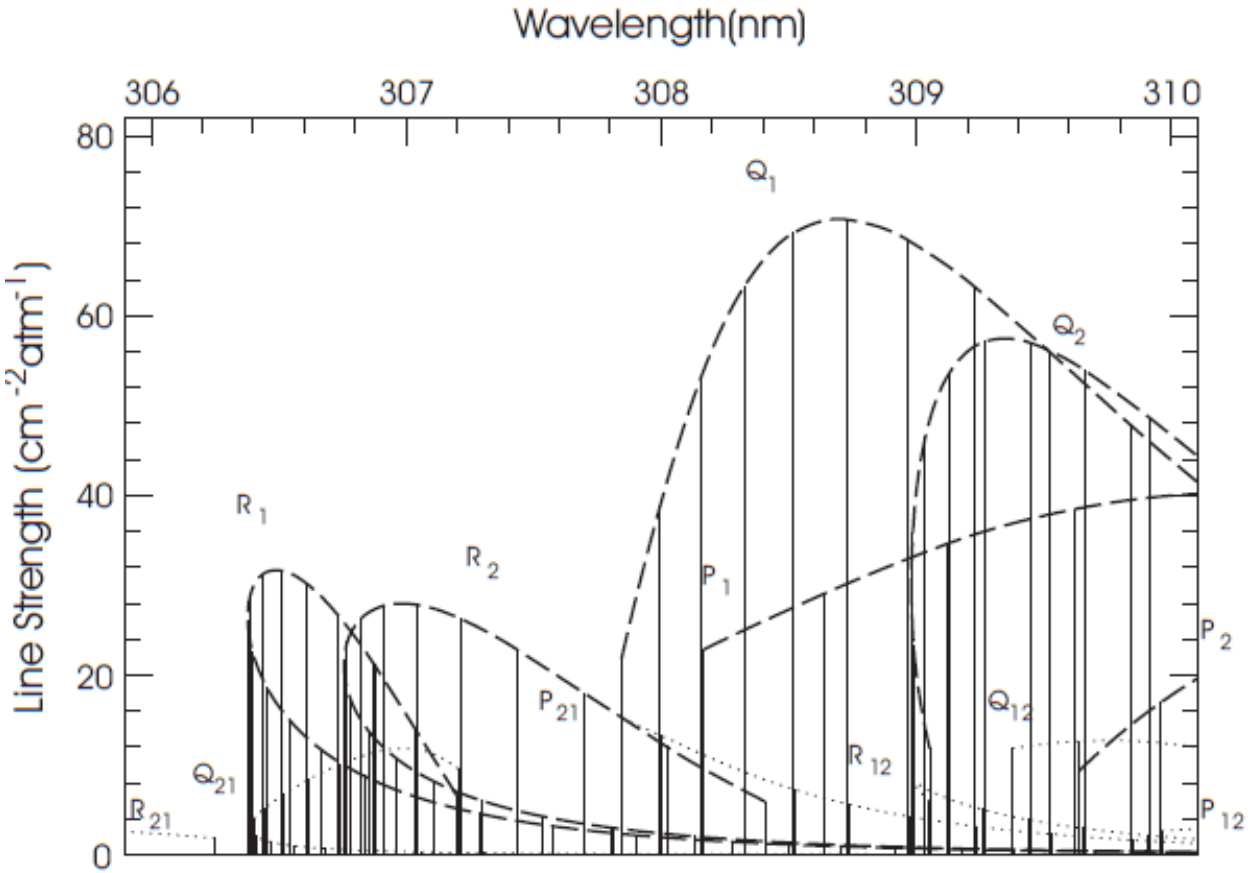

Selected region of $A^2\Sigma^+ \leftarrow X^2\Pi(0,0)$ band at 2000K

1. Introduction

- Steps in analysis to obtain spectral absorption coefficient

1. Identify/calculate energy levels of upper + lower states
2. Establish allowed transitions
3. Introduce “transition notation”
4. Identify/characterize oscillator strengths using Hönl-London factors
5. Calculate Boltzmann fraction
6. Calculate lineshape function
7. Calculate absorption coefficient

2. Energy levels

- Term energies

Angular momentum energy (nuclei + electrons)

$$E(n,v,J) = T_e(n) + G(v) + F(J)$$

elec. q. no.
vib. q. no.
ang. mom. q. no.

Electronic energy

Vibrational energy

- Separation of terms: Born-Oppenheimer approximation
- $G(v) = \omega_e(v + 1/2) - \omega_e x_e(v + 1/2)^2$
- Sources of T_e, ω_e, $\omega_e x_e$ ➡ Herzberg
- Overall system : $A^2\Sigma^+ \leftarrow X^2\Pi$

in [cm^{-1}]

$A^2\Sigma^+$	T_e	ω_e	$\omega_e x_e$	$X^2\Pi$	T_e	ω_e	$\omega_e x_e$
	32682.0	3184.28	97.84		0.0	3735.21	82.21

Let's first look at the upper state ➡ Hund's case b!

2. Energy levels

- Hund's case b (Λ=0, S≠0) – more standard, especially for hydrides

Recall:

- Σ, Ω not rigorously defined
- N = angular momentum without spin
- S = 1/2-integer values
- J = N+S, N+S-1, …, |N-S|
- i = 1, 2, …

$F_i(N)$ = rotational term energy

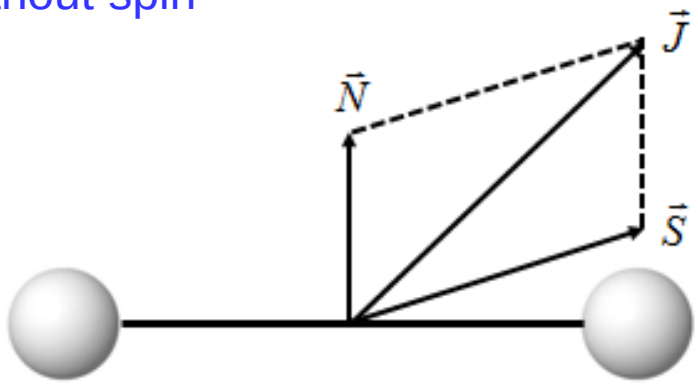

Now, specifically, for OH?

2. Energy levels

- The upper state is $A^2\Sigma^+$

For OH:

- $\Lambda = 0$, $\therefore$ Σ not defined ➡ use Hund's case b
- $N = 0, 1, 2, \ldots$
- $S = 1/2$
- $J = N \pm 1/2$
- F_1 denotes $J = N + 1/2$

  F_2 denotes $J = N - 1/2$

  Common to write either $F_1(N)$ or $F_1(J)$

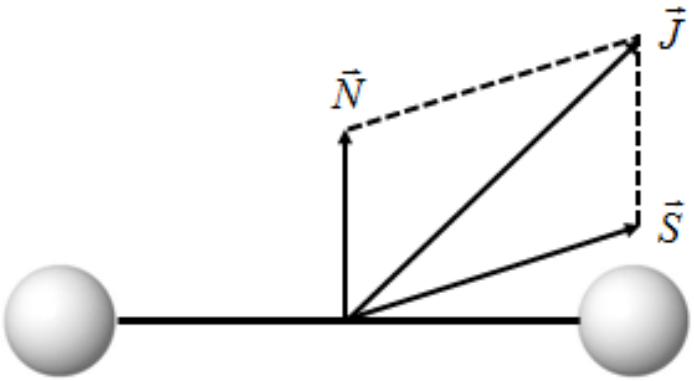

2. Energy levels

- The upper state: $A^2\Sigma^+$
  - $$F_1(N) = B_v N(N+1) - D_v[N(N+1)]^2 + \gamma_v N$$
    $$F_2(N) = B_v N(N+1) - D_v[N(N+1)]^2 - \gamma_v (N+1)$$
    $$\left(\text{splitting constant } \gamma_v \approx 0.1\text{cm}^{-1} \text{ for OH } A^2\Sigma^+\right)$$
    for pure case b
  - ∴ the spin-splitting is $\gamma_v(2N+1)$ ➡ function of v; increases with N

$\gamma_v(2N+1) \sim 0.1(5) \sim 0.5\text{cm}^{-1}$ for N_2
Compare with $\Delta\nu_D(1800\text{K}) = 0.23\text{cm}^{-1}$

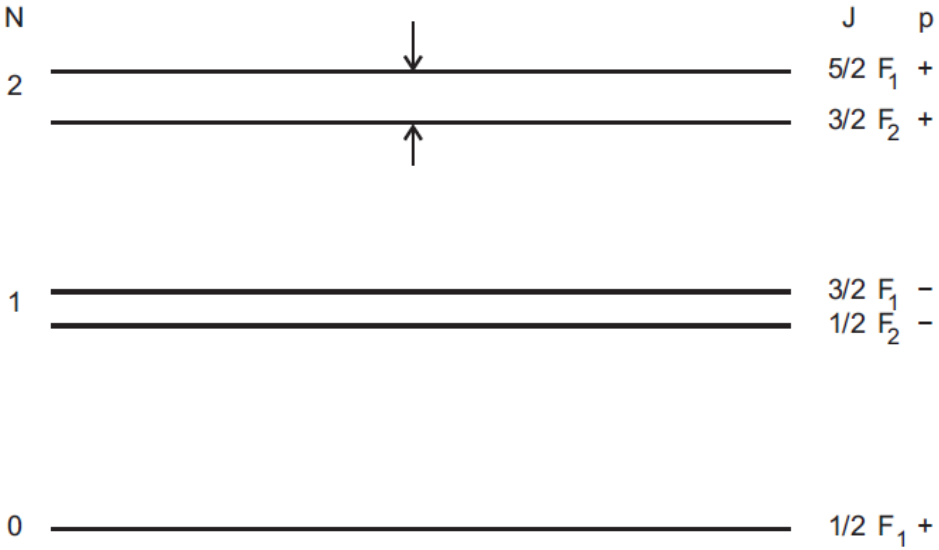

Notes:

- Progression for $A^2\Sigma^+$
- "+" denotes positive "parity" for even N [wave function symmetry]
- Importance? Selection rules require parity change in transition

2. Energy levels

- The ground state: $X^2\Pi$ (Λ=1, S=1/2)

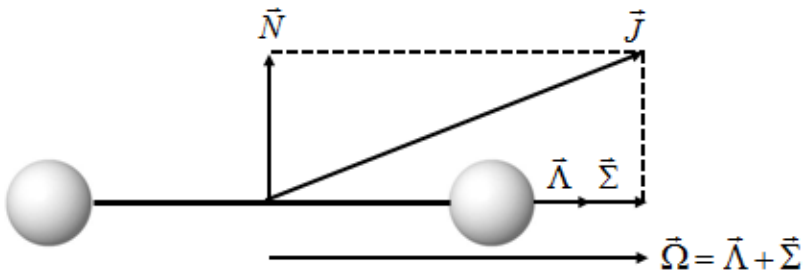

Hund's case ***a***
$\Lambda \neq 0$, $S \neq 0$, Σ defined

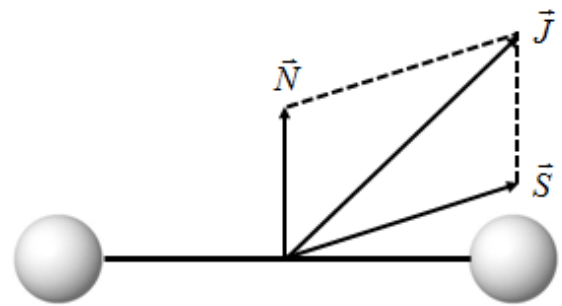

Hund's case ***b***
$\Lambda = 0$, $S \neq 0$, Σ not defined

✐ Note:

1. Rules less strong for hydrides
2. OH behaves like Hund's a @ <u>low</u> N
   like Hund's b @ <u>large</u> N

   ➡ at large N, $\vec{L}$ couples more to N, Λ is less defined, S decouples from A-axis
3. Result? OH $X^2\Pi$ is termed "<u>intermediate case</u>"

2. Energy levels

- The ground state: $X^2\Pi$

Notes:

3. For "intermediate/transition cases"

$$F_1(N) = B_v\left\{(N+1)^2 - \Lambda^2 - \frac{1}{2}\left[4(N+1)^2 + Y_v(Y_v-4)\Lambda^2\right]^{1/2}\right\} - D_v[N(N+1)]^2$$

$$F_2(N) = B_v\left\{N^2 - \Lambda^2 + \frac{1}{2}\left[4N^2 + Y_v(Y_v-4)\Lambda^2\right]^{1/2}\right\} - D_v[N(N+1)]^2$$

where $Y_v \equiv A/B_v$ (< 0 for OH); A is effectively the moment of inertia

Note: $F_1(N) < F_2(N)$

For small N → Behaves like Hund's a, i.e., symmetric top, with spin splitting ΛA

For large N → Behaves like Hund's b, with small (declining) effect from spin

$$F_1 \to B_v\left[(N+1)^2 - \Lambda^2 - (N+1)\right]$$

$$F_2 \to B_v\left[N^2 - \Lambda^2 + N\right]$$

$$\Rightarrow F_1 - F_2 \to B_v\left[(N+1)^2 - N^2 - (2N+1)\right] \to 0$$

2. Energy levels

- The ground state: $X^2\Pi$
  - Notes:
    4. Some similarity to symmetric top

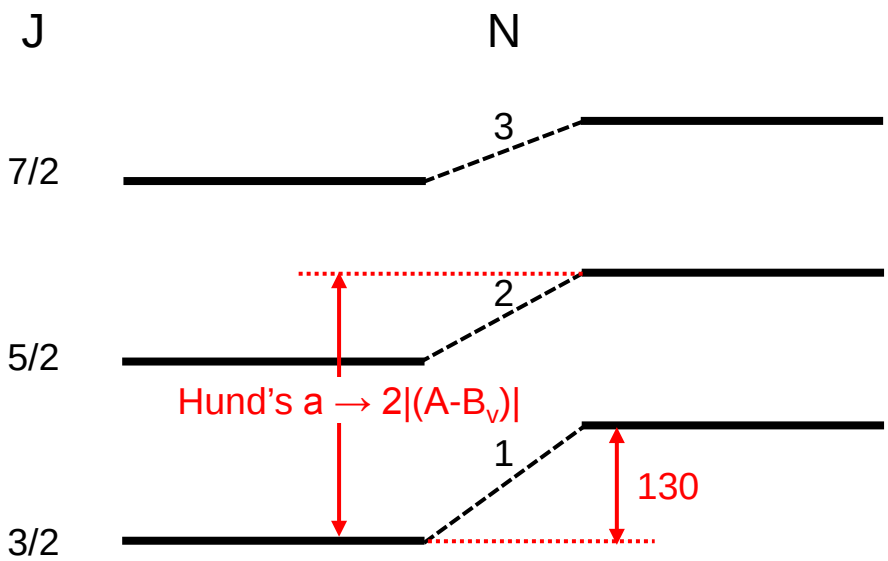

F_1: J = N + 1/2 Ω = 3/2

F_2: J = N – 1/2 Ω = 1/2

Showed earlier that $F_1 < F_2$

$T_e = T_0 + A\Lambda\Sigma$

For OH, A = -140 cm^{-1}

➡ $T_e = T_0 + (-140)(1)(1/2)$, $\Sigma = 1/2$

$+ (-140)(1)(-1/2)$, $\Sigma = -1/2$

➡ ΔT_e = <u>140</u> cm^{-1}

Not too far off the 130 cm^{-1} spacing for minimum J

Recall: Hund's case **a** has constant difference of 2(A-B$_v$) for same J

$$F(J) = BJ(J+1) + (A-B)\Omega^2$$

$$(A–B)\Omega^2 \approx -158.5\Omega^2$$

(A for OH~ -140, B ~ 18.5), Ω = 3/2, 1/2

➡ Ω = 3/2 state lower by <u>316</u> cm^{-1}

Actual spacing is only 188 cm^{-1}, reflects that <u>hydrides quickly go to Hund's case **b**</u>

2. Energy levels

- The ground state: $X^2\Pi$
  - Notes:
    5. Role of Λ-doubling

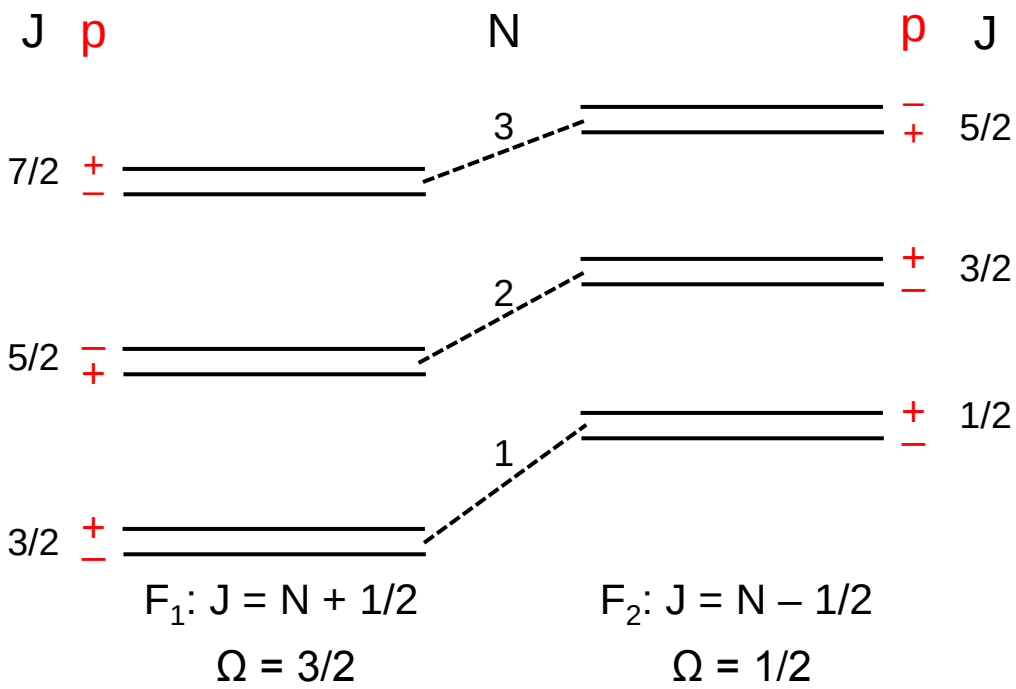

$$\left.\begin{aligned} F_{ic} &= F_i(J) + \delta_c J(J+1) \\ F_{id} &= F_i(J) + \delta_d J(J+1) \end{aligned}\right\} F_{id} < F_{ic}$$

- $F_{ic}(J) - F_{id}(J) \approx 0.04\ cm^{-1}$ for typical J in OH
- c and d have different parity (p)
- Splitting decreases with increasing N

Showed earlier that $F_1 < F_2$

Now let's proceed to draw transitions, but first let's give a primer on transition notation.

3. Allowed radiative transitions

- Transition notations

  Full description: $A^2\Sigma^+$ (v')←$X^2\Pi$ (v") ${}^{Y}X_{\alpha\beta}$(N" or J")

$$\boxed{{}^{Y}X_{\alpha\beta}\left(N''\text{ or }J''\right)}$$

where Y – ΔN (O, P, Q, R, S for ΔN = -2 to +2)

X – ΔJ (P, Q, R for ΔJ = -1, 0, +1)

α = i in F_i'; i.e., 1 for F_1, 2 for F_2

β = i in F_i''; i.e., 1 for F_1, 2 for F_2

Notes:

Strongest trans. e.g., $R_1(7)$ or R_17

1. Y suppressed when ΔN = ΔJ
2. β suppressed when α = β
3. Both N" and J" are used

Example: ${}^{S}R_{21}$:

ΔJ = +1, ΔN = +2

F' = F_2(N')

F" = F_1(N")

- General selection rules
  - Parity must change + → – or – → +
  - ΔJ = 0, ±1
  - No Q (J = 0) transitions, J = 0 → J = 0 not allowed

3. Allowed radiative transitions

- Allowed transitions

Allowed rotational transitions from N"=13 in the $A^2\Sigma^+ \leftarrow X^2\Pi$ system

State or level

a specific v",J",N",and Λ-coupling

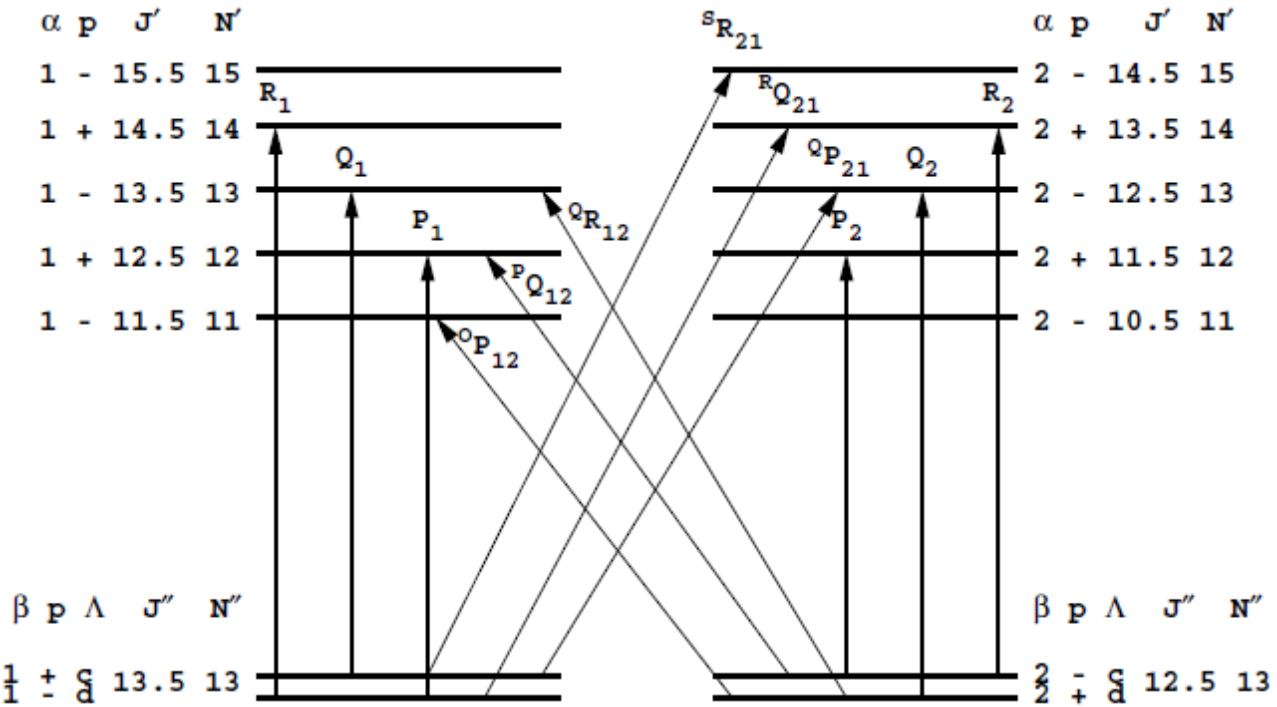

$F_{1c}(13)$, $F_{1d}(13)$ } $F_1(13)$

- 12 bands possible (3 originating from each *lambda-doubled*, *spin-split* X state)
- Main branches: α = β; Cross-branches: α ≠ β
- Cross-branches weaken as N increases

3. Allowed radiative transitions

- Allowed transitions

Allowed rotational transitions from N"=13 in the $A^2\Sigma^+ \leftarrow X^2\Pi$ system

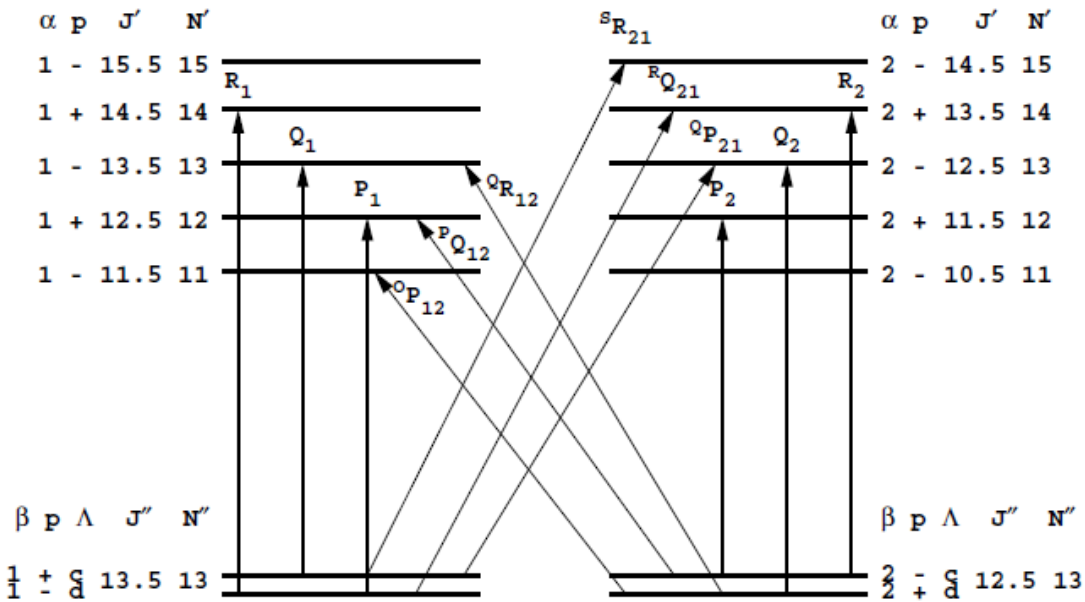

Notes:

- A given J" (or N") has12 branches (6 are strong; ΔJ = ΔN)
- + ↔ – rule on parity
- F_{1c}–F_{1d} ≈ 0.04N(N+1) for OH ➡ for N~10, Λ-doubling is ~ 4cm^{-1}, giving clear separation
- If upper state has Λ-doubling, we get twice as many lines!

3. Allowed radiative transitions

- Allowed transitions

Allowed rotational transitions from N"=13 in the $A^2\Sigma^+ \leftarrow X^2\Sigma^+$ system

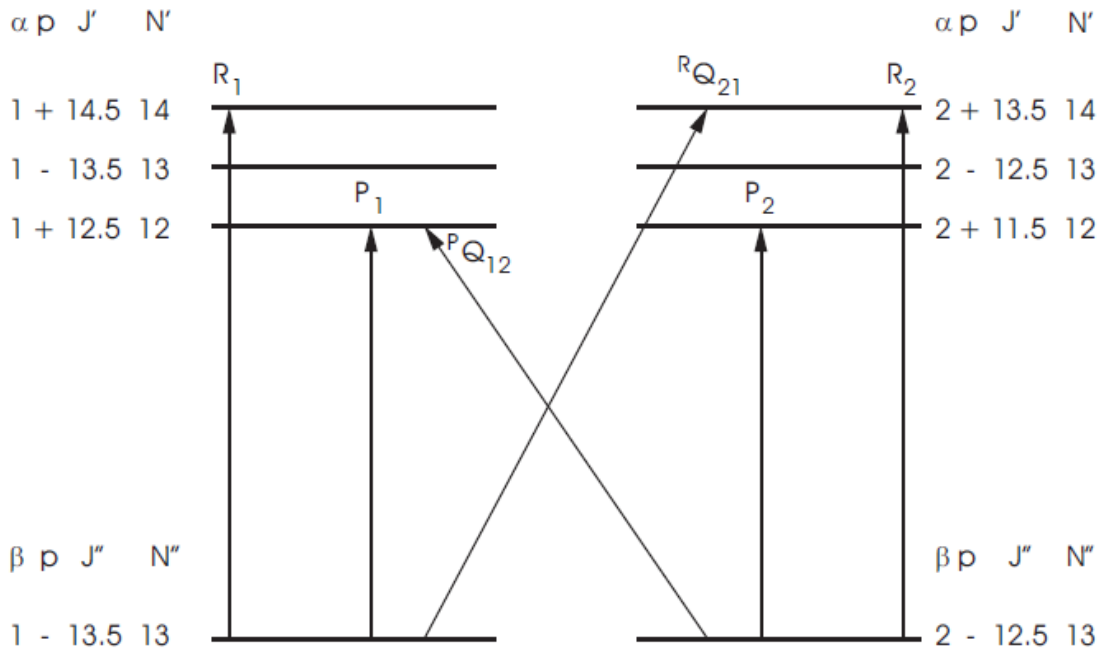

- Note:
  1. The effect of the parity selection rule in reducing the number of allowed main branches to 4
  2. The simplification when Λ=0 in lower state, i.e., no Λ-doubling

4. Working example - OH

- Complete steps to calculate absorption coefficient

1. Identify/characterize oscillator strengths using Hönl-London factors
2. Calculate Boltzmann fraction
3. Calculate lineshape function (narrow-band vs broad-band)
4. Calculate absorption coefficient

Absorption coefficient

#/cm^3 of species (OH), $= \frac{p_A}{kT}$

#/cm^3 in state 1, $= N_a \frac{N_1}{N_a}$ ← Fractional pop. in state 1

$$k_\nu, \mathrm{cm}^{-1} = \left[\frac{\pi e^2}{m_e c}\right] N_1 f_{12} \left(1 - \exp^{-\frac{h\nu}{kT}}\right) \phi(\nu - \nu_0)$$

0.0265 cm^2/s

ϕ[s] = (1/c) ϕ[cm]

To do: evaluate f_{12}, N_1/N_a

Step 4 Step 5

4.1. Oscillator strengths

- Absorption oscillator strength

elec. osc. strength F-C factor H-L factor

$$f_{(n'',v'',\Sigma'',J'',\Lambda''),(n',v',\Sigma',J',\Lambda')} = f_{n''n'} q_{v''v'} \frac{S_{J''J'}}{2J''+1}$$

elec. vib. spin ang. mom. Λ-doubling

or in shorthand notation $f_{J''J'} = \underbrace{f_{n''n'} q_{v''v'}}_{= f_{v''v'}} \frac{S_{J''J'}}{2J''+1}$

$= f_{v''v'}$ = band oscillator strength

For OH $A^2\Sigma^+$–$X^2\Pi$

(v',v")	$f_{v'v''}$
(0,0)	0.00096
(1,0)	0.00028

Notes: $q_{v''v'}$ and $S_{J''J'}$ are normalized

- $\sum_{v'} q_{v''v'} = 1$
- $\sum_{J'} S_{J''J'} = (2J''+1)\underbrace{(2S+1)\delta}_{g''_{el}=4 \text{ for } X^2\Pi}$

1 for Λ = 0 (Σ state), 2 otherwise

this sum includes the S values for all states with J"

4.1. Oscillator strengths

- *Is $S_{J''J'} = S_{J'J''}$?* ➡ Yes, for our normalization scheme!
  - From $g_1 f_{12} = g_2 f_{21}$, and recognizing that 2J+1 is the ultimate (non removable) degeneracy at the <u>state</u> level, we can write, for a specific transition between single states

$$\cancel{(2J''+1)} \cdot f_{el}'' \cdot q_{v''v'} \cdot \frac{S_{J''J'}}{\cancel{2J''+1}} = \cancel{(2J'+1)} \cdot f_{el}' \cdot q_{v'v''} \cdot \frac{S_{J'J''}}{\cancel{2J'+1}}$$

    In this way, there are no remaining electronic degeneracy and we require, for detailed balance, that $f_{el}'' = f_{el}', q_{v''v'} = q_{v'v''}$ and $S_{J''J'} = S_{J'J''}$

- *Do we always enforce $\sum_{J'} S_{J''J'} = (2J''+1)$ for a state?* ➡ No!
  - But note we do enforce $\sum_{J'} S_{J''J'} = (2J''+1)(2S+1)\delta$ (14.17)

    and $\sum_{J''} S_{J''J'} = (2J'+1)(2S+1)\delta$ (14.19)

    where, for OH $A^2\Sigma \leftarrow X^2\Pi$, (2S+1) = 2 and δ = 2.

- *When is there a problem?*
  - Everything is okay for Σ-Σ and Π-Π, where there are equal "elec. degeneracies", i,e., $g''_{el} = g'_{el}$. But for Σ-Π (as in OH), we have an issue. In the $X^2\Pi$ state, $g_{el} = 4$ (2 for spin and 2 for Λ-doubling), meaning each J is split into 4 <u>states</u>. Inspection of our H-L tables for $S_{J''J'}$ for OH $A^2\Sigma \leftarrow X^2\Pi$ (absorption) confirms $\Sigma S_{J''J'}$ from each state is 2J''+1. All is well. But, in the upper state, $^2\Sigma$, we have a degeneracy g'_{el} of 2 (for spin), not 4, and now we will find that the sum of $\sum_{J''} S_{J'J''}$ is twice 2J'+1 for a single J' when we use the H-L values for $S_{J''J'}$ for $S_{J'J''}$. However, as there are 2 states with J', the overall sum $\sum_{J''} S_{J'J''} = (2J'+1)4$ as required by (14.19)

4.1. Oscillator strengths

- Absorption oscillator strength for f_{00} in OH $A^2\Sigma^+$–$X^2\Pi$

Source	f_{00}
Oldenberg, et al. (1938)	0.00095 ± 0.00014
Dyne (1958)	0.00054 ± 0.0001
Carrington (1959)	0.00107 ± 0.00043
Lapp (1961)	0.00100 ± 0.0006
Bennett, et al. (1963)	0.00078 ± 0.00008
Golden, et al. (1963)	0.00071 ± 0.00011
Engleman, et al. (1973)	0.00096
Bennett, et al. (1964)	0.0008 ± 0.00008
Anketell, et al. (1967)	0.00148 ± 0.00013

4.1. Oscillator strengths

- Absorption oscillator strength

Transition	$S_{J''J'}/(2J''+1)$	$\Sigma F_1(J)$	$\Sigma F_2(J)$	$\Sigma[F_1(J)+F_2(J)]$
$Q_{12}(0.5)$	0.667	0	2	2
$Q_2(0.5)$	0.667			
$R_{12}(0.5)$	0.333			
$R_2(0.5)$	0.333			
$P_1(1.5)$	0.588	2	2	4
$P_{12}(1.5)$	0.078			
$P_{21}(1.5)$	0.392			
$P_2(1.5)$	0.275			
$Q_1(1.5)$	0.562			
$Q_{12}(1.5)$	0.372			
$Q_{21}(1.5)$	0.246			
$Q_2(1.5)$	0.678			
$R_1(1.5)$	0.165			
$R_{12}(1.5)$	0.235			
$R_{21}(1.5)$	0.047			
$R_2(1.5)$	0.353			
$P_1(2.5)$	0.530	2	2	4
$P_{12}(2.5)$	0.070			
$P_{21}(2.5)$	0.242			
$P_2(2.5)$	0.358			
$Q_1(2.5)$	0.708			
$Q_{12}(2.5)$	0.263			
$Q_{21}(2.5)$	0.214			
$Q_2(2.5)$	0.757			
$R_1(2.5)$	0.256			
$R_{12}(2.5)$	0.173			
$R_{21}(2.5)$	0.050			
$R_2(2.5)$	0.379			

Transition	$S_{J''J'}/(2J''+1)$	$\Sigma F_1(J)$	$\Sigma F_2(J)$	$\Sigma[F_1(J)+F_2(J)]$
$P_1(3.5)$	0.515	2	2	4
$P_{12}(3.5)$	0.056			
$P_{21}(3.5)$	0.167			
$P_2(3.5)$	0.405			
$Q_1(3.5)$	0.790			
$Q_{12}(3.5)$	0.195			
$Q_{21}(3.5)$	0.170			
$Q_2(3.5)$	0.814			
$R_1(3.5)$	0.316			
$R_{12}(3.5)$	0.131			
$R_{21}(3.5)$	0.044			
$R_2(3.5)$	0.402			
$P_1(9.5)$	0.511	2	2	4
$P_{12}(9.5)$	0.016			
$P_{21}(9.5)$	0.038			
$P_2(9.5)$	0.488			
$Q_1(9.5)$	0.947			
$Q_{12}(9.5)$	0.050			
$Q_{21}(9.5)$	0.048			
$Q_2(9.5)$	0.950			
$R_1(9.5)$	0.441			
$R_{12}(9.5)$	0.035			
$R_{21}(9.5)$	0.014			
$R_2(9.5)$	0.462			

Hönl-London factors for selected OH transitions

4.2. Boltzmann fraction

1. We seek the fraction of molecules in a single state for which

$$\sum_{J'} S_{J''J'} = 2J''+1$$

2. In general,

$$N_i / N = g_i e^{-\varepsilon_i / kT} / Q$$

$$Q = Q_e \cdot Q_v \cdot Q_r$$

3. Electronic mode

$$g_e = (2S+1)\phi \leftarrow \begin{cases} \phi = 1, \Lambda = 0 \\ \phi = 2, \Lambda \neq 0 \end{cases}$$

$$\Rightarrow \left.\begin{array}{ll} g_e = 4 & {}^2\Pi \\ g_e = 2 & {}^2\Sigma \end{array}\right\} \text{OH}$$

# of rot. levels produced by spin splitting & Λ-doubling = 4 for $^2\Pi$

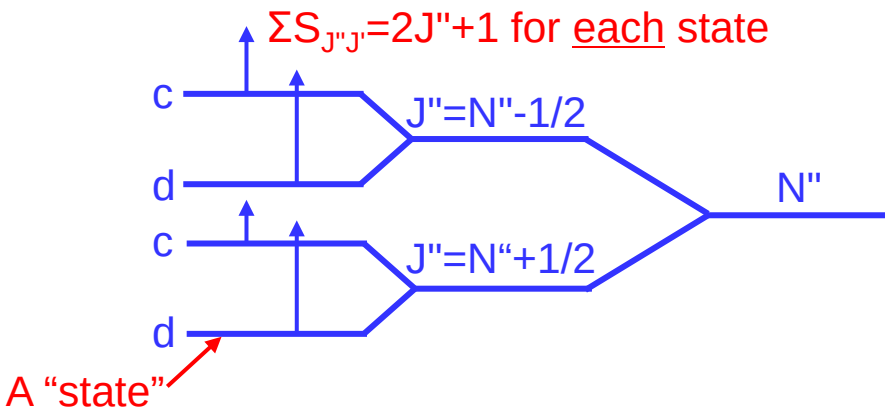

Elec. level

the sum of this over all levels is 1

$$\frac{N(n)}{N} = (2S+1)\phi \exp(-hcT_e(n)/kT)/Q_e$$

$$Q_e = \sum_n (2S+1)\phi \exp(-hcT_e(n)/kT)$$

Note:

hund's (a) includes $A\Omega^2$

4.2. Boltzmann fraction

4. Vibrational mode

$$\frac{N(n,v)}{N(n)} = \exp(-hcG(v)/kT)/Q_v$$

$$Q_v = \sum_v \exp(-hcG(v)/kT)$$

Again, each of these →1 when summed

5. Rotational mode (hund's (b))

- $$\frac{N(n,v,N)}{N(n,v)} = (2N+1)\exp(-hcF(N)/kT)/Q_r$$

$$\theta_r = hcB_v/k$$

$$Q_r = \sum_{N=\Lambda}^{\infty}(2N+1)\exp(-hcF(N)/kT) \Rightarrow Q_r = \frac{T}{\theta_r} \text{ for T} >> \theta_r$$

✎ Note: don't use F_1+F_2(N) here; until we add spin splitting

Now what about fraction of those with N in a given J?

- $$\frac{N(n,v,N,J)}{N(n,v,N)} = \frac{(2J+1)}{(2N+1)(2S+1)}$$

Since # of states in N is (2N+1)(2S+1)ϕ, while # of states in J is (2J+1) ϕ

≈ ½ for OH as expected

- $$\frac{N(n,v,N,J,p)}{N(n,v,N,J)} = \frac{1}{\phi}$$

(fraction with spectral parity)

4.2. Boltzmann fraction

6. Combining

$$\frac{N(n,v,N,J,p)}{N} = \frac{N_1}{N}$$ (i.e., the Boltzmann fraction in <u>state</u> 1)

$$= \frac{N(n)}{N}\frac{N(n,v)}{N(n)}\frac{N(n,v,N)}{N(n,v)}\frac{N(n,v,N,J)}{N(n,v,N)}\frac{N(n,v,N,J,p)}{N(n,v,N,J)}$$

$$= \frac{(2J+1)\exp\left(-\frac{hc}{kT}\left[T_e(n)+G(v)+F_i(N)\right]\right)}{Q_e Q_v Q_r}$$

Proper F_i now!

Note:

1. The fraction in a given state is 1/4 of that given by rigid rotor!
2. Always know $\Sigma(N_i/N) = 1$, both in total and for each mode separately.

We have 1 loose end to deal with:

<u>narrow-band</u> and <u>broadband</u> absorption measurement.

4.3. Narrow-band vs broad-band absorption measurement

- Narrow-band absorption

  Measured quantity

$$T_\nu = (I/I_0)_\nu = \exp(-S_{12}\phi_\nu L) \quad \text{with} \quad S_{12} = \left[\frac{\pi e^2}{m_e c}\right] N_1 f_{12}\left(1-\exp^{-\frac{h\nu}{kT}}\right)$$

Oscillator strength for transition

$$\left(\frac{N_1}{N_l}\right)\left(N_l = \text{tot. no. dens. of } l = \frac{p_l}{kT}\right)$$

Boltzmann fraction of species l = $F_{v'',J'',\ldots}(T)$

thus, if T_ν (e.g. T_{ν_0}) is <u>measured</u>, and

if L, p, 2γ, T, f_{12} are <u>known</u>

$$= \sum_{\substack{i \\ \text{bd. species}}} 2\gamma_i X_i$$

then can solve for N_l ← Quantity usually sought

4.3. Narrow-band vs broad-band absorption measurement

Let's look at the classical (old-time) approach, pre 1975

- Broadband absorption

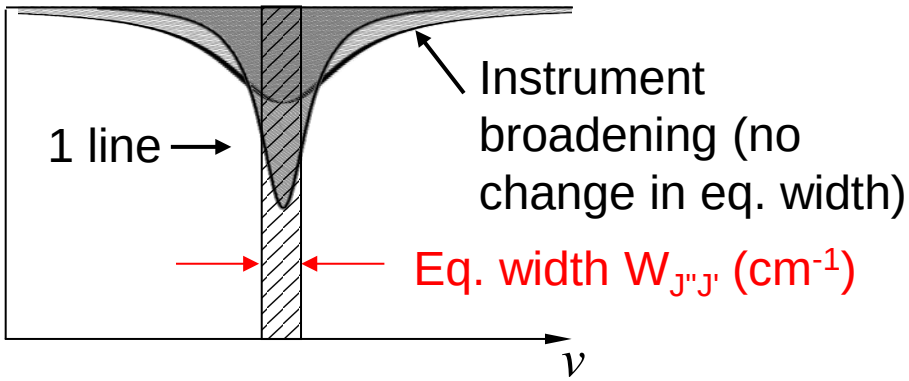

Integrated area is called: integrated absorbance, or eq. width

(for 1 line from 1 state)

$$W_{line} = W_{J''J'} = \int A_{\bar{\nu}} d\bar{\nu} = \int \left(1 - T_{\bar{\nu}}\right) d\bar{\nu}$$

$$= \int_{line} \left\{1 - \exp\left(-K_{J''J'} \phi(\bar{\nu}) L\right)\right\} d\bar{\nu}$$

$$K_{J''J'} = S_{J''J'} P_i$$

Transform variables

$$\bar{\nu} = \frac{\Delta \bar{\nu}_D}{2\sqrt{\ln 2}} x$$

$$W_{J''J'} = \frac{\Delta \bar{\nu}_D}{\sqrt{\ln 2}} \int_0^{\infty} \left\{1 - \exp\left[-K_{J''J'} L \frac{2\sqrt{\ln 2}}{\sqrt{\pi} \Delta \bar{\nu}_D} V(x, a)\right]\right\} dx$$

4.3. Narrow-band vs broad-band absorption measurement

Let's look at the classical (old-time) approach, pre 1975

- Broadband absorption ➡ Requires use of "curves of growth"

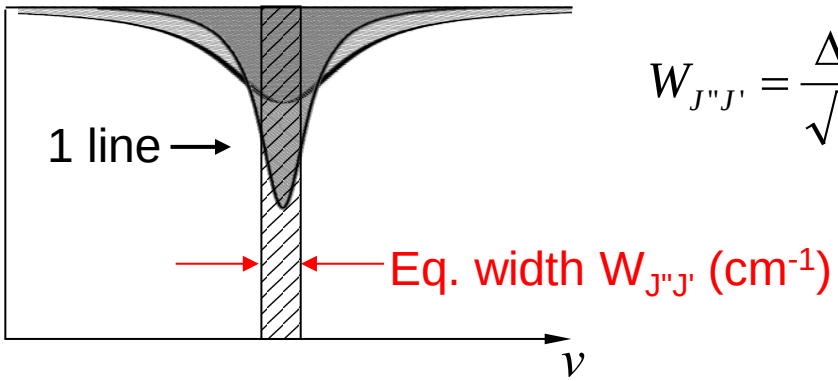

$$W_{J''J'} = \frac{\Delta\bar{\nu}_D}{\sqrt{\ln 2}}\int_0^\infty \left\{1-\exp\left[-K_{J''J'}L\frac{2\sqrt{\ln 2}}{\sqrt{\pi}\Delta\bar{\nu}_D}V(x,a)\right]\right\}dx$$

- Procedure: measure $W_{J''J'}$, calculate $\Delta\nu_D$ and a, infer $K_{J''J'}$, convert $K_{J''J'}$ to $N_{species}$
- Note:
  1. Simple interpretation only in optically thin limit,

$$W_{J''J'} = \int\left[1-\left(1-K_{J''J'}\phi(\bar{\nu})L\right)\right]d\bar{\nu}$$

$$W_{J''J'} = K_{J''J'}L = \frac{\pi e^2}{mc^2}N_1 f_{12}L$$

  2. Measured eq. width is indep. of instrument broadening!
  3. **Before lasers, use of absorption spectroscopy for species measurements require use of Curves of Growth!**

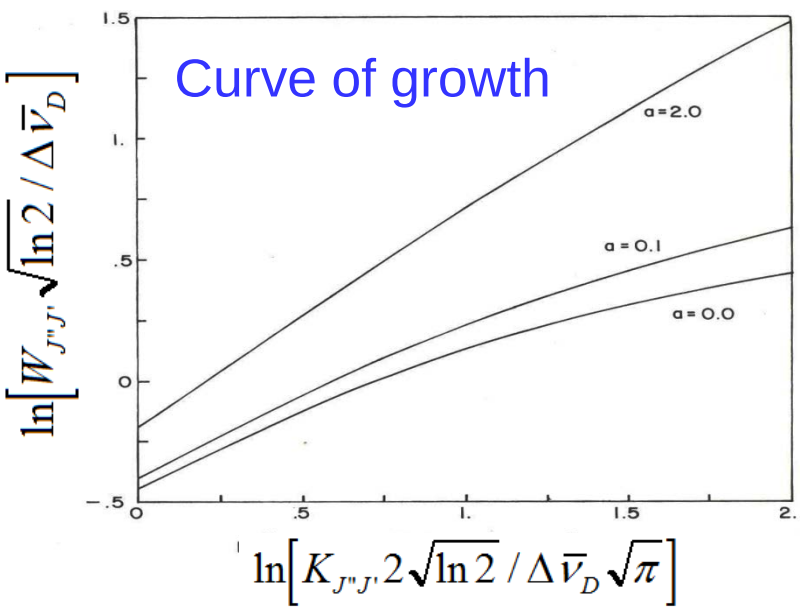

4.4. Example calculation (narrow-band)

- Consider spectral absorption coefficient of the $(0,0)Q_1(9)$ line in the OH $A^2\Sigma^+ – X^2\Pi$ system, at line center.
  - λ~309.6nm, ν~32300cm^{-1}, T = 2000K, $\Delta\nu_C$ = 0.05cm^{-1}

Express k_ν as a function of OH partial pressure

$$k_\nu\left[\mathrm{cm}^{-1}\right] = 2.651\times10^{-2}\,\frac{\mathrm{cm}^2}{\mathrm{s}}\,\frac{P_a}{kT}\,\frac{N_{(n,v,\Sigma,J,\Lambda)''}}{N_a}\,f_{J''J'}\,\phi(\nu_0)$$

❸ ❶ ❷

$$N_a = P_a / kT$$

❶ Oscillator strength (using tables)

$$f_{Q_1(9)} = f_{v''v'}\frac{S_{J''J'}}{2J''+1} = 0.00096\times0.947 = 9.09\times10^{-4}$$

❷ Lineshape factor (narrow-band)

$$\left.\begin{aligned}\Delta\bar{\nu}_D(2000\mathrm{K}) &= 0.25\mathrm{cm}^{-1}\\ \Delta\bar{\nu}_C(2000\mathrm{K}) &= 0.05\mathrm{cm}^{-1}\end{aligned}\right\} a = 0.17 \Rightarrow \phi(\nu_0) = 3.13\mathrm{cm}\ \text{ or }\ 1.04\times10^{-10}\mathrm{s}$$

4.4. Example calculation (narrow-band)

- Consider spectral absorption coefficient of the (0,0)Q_1(9) line in the OH $A^2\Sigma^+$–$X^2\Pi$ system, at line center.
  - λ~309.6nm, ν~32300cm^{-1}, T = 2000K, $\Delta\nu_C$ = 0.05cm^{-1}

Express k_ν as a function of OH partial pressure

$$k_\nu\left[\mathrm{cm}^{-1}\right] = 2.651\times10^{-2}\,\frac{\mathrm{cm}^2}{\mathrm{s}}\,\frac{P_a}{kT}\,\frac{N_{(n,v,\Sigma,J,\Lambda)''}}{N_a}\,f_{J''J'}\,\phi(\nu_0) \qquad N_a = P_a/kT$$

❸ ❶ ❷

❸ Population fraction in the absorbing state

$$\frac{N_{f_{1c}(0.5)}}{N_a} = \frac{\exp\left[-hcT_e(0)/kT\right]}{Q_e}\cdot\frac{\exp\left[-hcG(0)/kT\right]}{Q_v}\cdot\frac{(2J''+1)\exp\left[-hcF_1(9.5)/kT\right]}{Q_r}$$

$$= \frac{\exp(0)}{4}\cdot\frac{\exp\left[-2660\mathrm{K}/T\right]}{0.287}\cdot\frac{20\exp\left[-2313\mathrm{K}/T\right]}{T/26.66\mathrm{K}}$$

$$= \frac{1}{4}\cdot\frac{0.264}{0.287}\cdot\frac{6.29}{75.0}$$

$$= 0.25\cdot 0.920\cdot 0.0839$$

$$= 0.0193$$

4.4. Example calculation (narrow-band)

- Consider spectral absorption coefficient of the $(0,0)Q_1(9)$ line in the OH $A^2\Sigma^+$–$X^2\Pi$ system, at line center.
  - λ~309.6nm, ν~32300cm^{-1}, T = 2000K, $\Delta\nu_C$ = 0.05cm^{-1}

Express k_ν as a function of OH partial pressure

$$k_\nu\left[\mathrm{cm}^{-1}\right] = 2.651\times10^{-2}\,\frac{\mathrm{cm}^2}{\mathrm{s}}\,\frac{P_a}{kT}\,\frac{N_{(n,v,\Sigma,J,\Lambda)''}}{N_a}\,f_{J''J'}\,\phi(\nu_0) \qquad N_a = P_a/kT$$

❸ ❶ ❷

$$\Rightarrow\; k_\nu\left[\mathrm{cm}^{-1}\right] = \left(2.651\times10^{-2}\,\frac{\mathrm{cm}^2}{\mathrm{s}}\right)\left(P_a[\mathrm{atm}]\right)\left(3.66\times10^{18}\,\frac{\mathrm{cm}^{-3}}{\mathrm{atm}}\right)(1.93\%)\left(9.09\times10^{-4}\right)\left(1.04\times10^{-10}\,\mathrm{s}\right)$$

$$= 177\,\frac{\mathrm{cm}^{-1}}{\mathrm{atm}}\left(P_a[\mathrm{atm}]\right)$$

Beer's Law $I_\nu = I_\nu^0 \exp(-k_\nu L)$

$\Rightarrow$ <u>59%</u> absorption

for L = 5cm, X_{OH} = 1000ppm, T = 2000K, P = 1atm

4.4. Example calculation (narrow-band)

- Selected region of OH $A^2\Sigma^+ \leftarrow X^2\Pi$ (0,0) band at 2000K

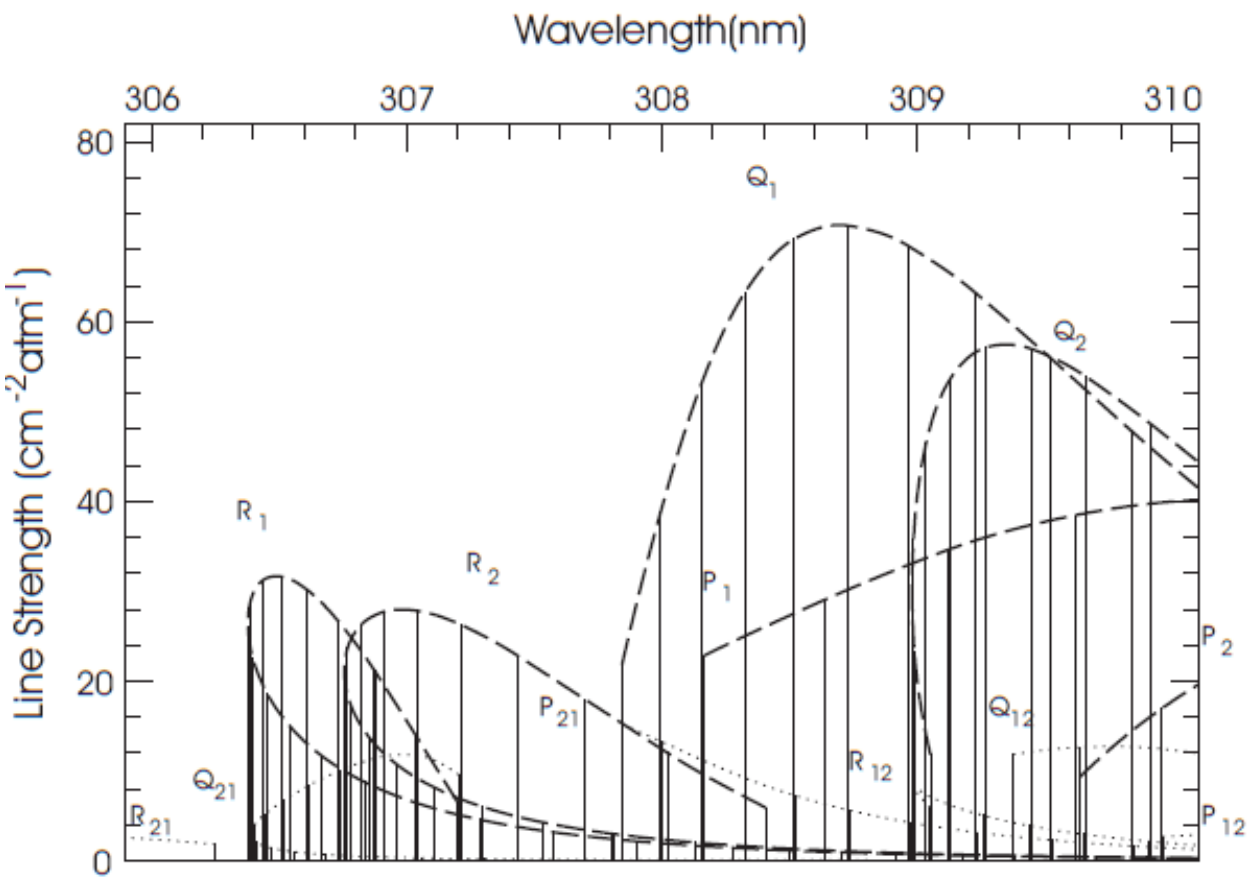

Notes:

- Lines belonging to a specific branch are connected with dashed or dotted curve
- Thicker dashed lines – main branches; thin dotted lines – cross branches
- Bandhead in R branches if $B_{v'}<B_{v''}$; Bandhead in P branches if $B_{v'}>B_{v''}$
- Note bandhead in ${}^{R}Q_{21}$ branch

Next:
TDLAS, Lasers and Fibers

- Fundamentals
- Applications to Aeropropulsion

Quantitative Laser Diagnostics for Combustion Chemistry and Propulsion

Lecture 9: Tunable Diode Laser Absorption (TDLAS)

1. History and vision – for aeropropulsion
2. Absorption fundamentals
3. Absorption sensor strategies
4. Wavelength access – lasers/detectors
5. Example applications – combustion
6. Example applications - aerospace
7. Future trends for aerospace

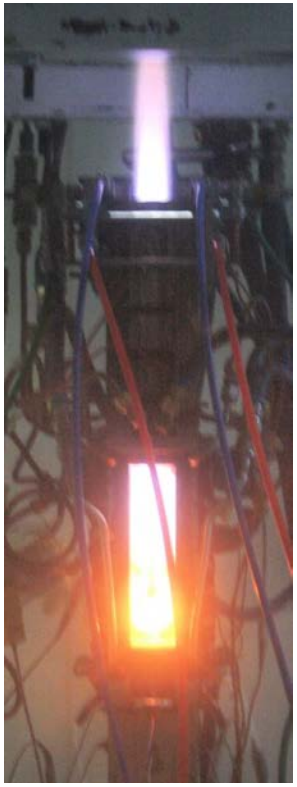

Direct-connect scramjet combustor
at UVa flow facility

1. The History of TDL Absorption for Aeropropulsion: 35 Years: From the Laboratory to Flight

1977 – TDL absorption in shock tube flows and flames

1989 – Mass flux sensor using O_2 absorption

1993 – Multiplexed measurements of H_2O, T and momentum flux

1998 – Combustion control (lab flames, incinerator)

2001 – Multi-species in flames: CO, CO_2, NH_3, H_2O

1996-present – Applications to flow facility characterization: arcjets, hypersonic flow tunnels, gas turbine engine sector rigs…

1998-present – Applications for engine tests: scramjet combustors, commercial aircraft engines, ic-engines, pulse detonation engines, gas turbines, augmentors…

2012 – TDL absorption in scramjet flight tests

T/species in Shocktube

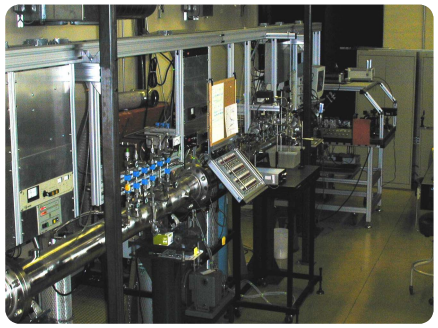

Hanson, *Appl Opt* (1977)

SCRAMJET @ WPAFB

Rieker, *Proc Comb Inst* (2009)

Facility @ CALSPAN

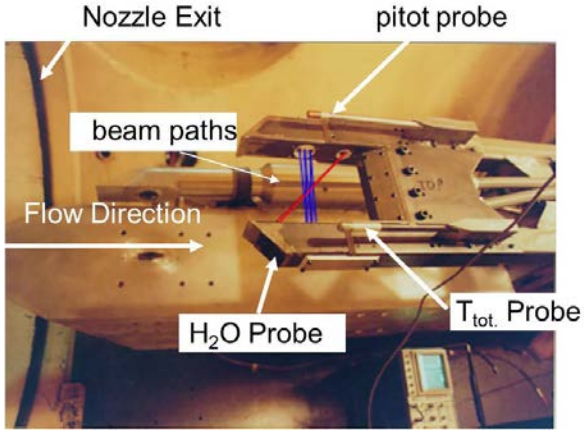

1. Vision for TDLAS Sensors for Aeropropulsion

– Diode laser absorption sensors offer prospects for time-resolved, multi-parameter, multi-location sensing for performance testing, model validation, feedback control

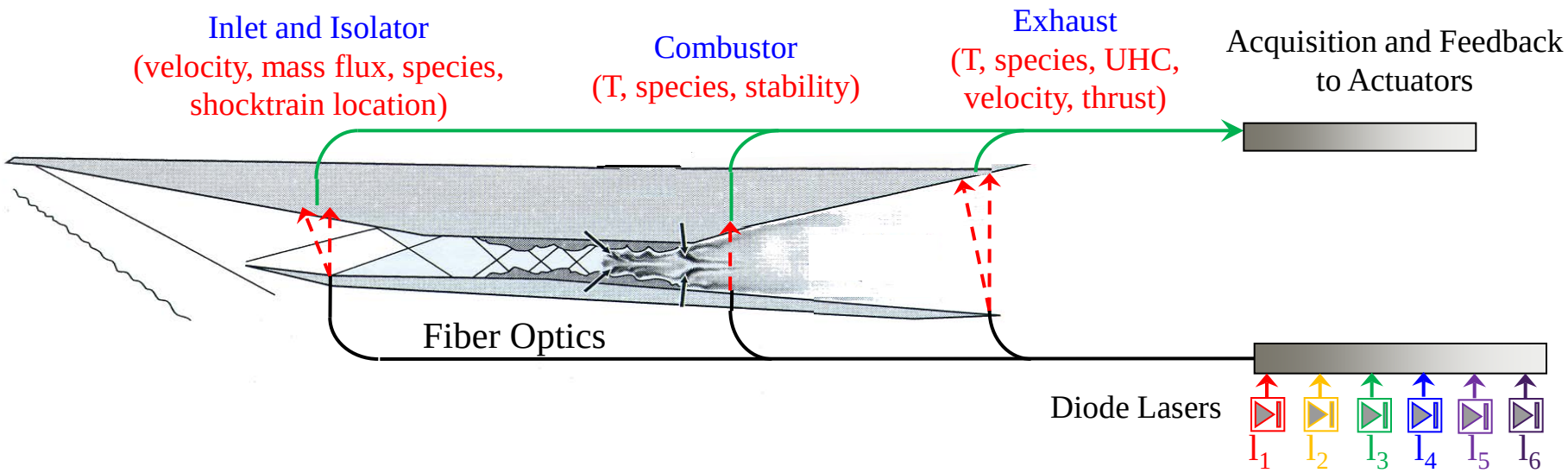

- Sensors developed for T, V, H_2O, CO_2, O_2, & other species
- Prototypes tested and validated at Stanford
- Several successful demonstrations in ground test facilities
- Opportunities emerging for use in flight

Now for some absorption fundamentals

2. Absorption Fundamentals: The Basics

Absorption of monochromatic light

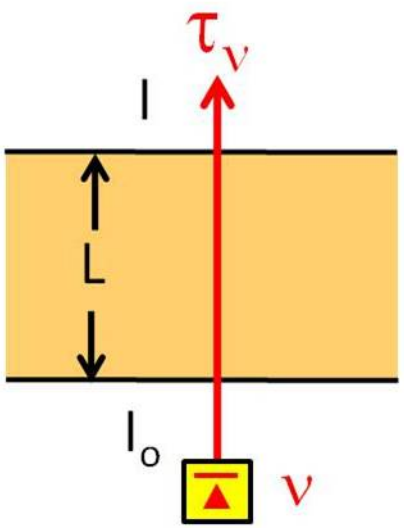

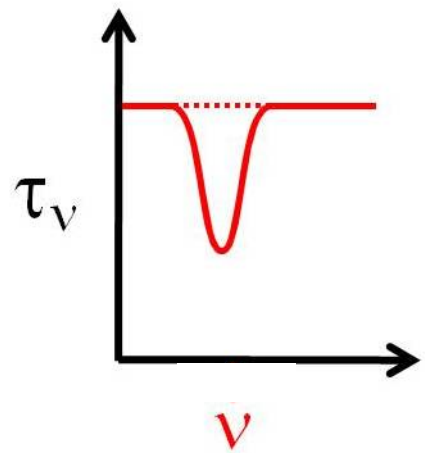

- **Scanned-wavelength *line-of-sight* direct absorption**
  - **Beer-Lambert relation** $\tau_\nu \equiv \frac{I_t}{I_o} = \exp(\underbrace{-k_\nu \cdot L}_{\text{absorbance}}) = \exp(-n_i \cdot \sigma_\nu \cdot L)$
  - **Spectral absorption coefficient** $k_\nu = S(T) \cdot \Phi(T, P, \chi_i) \cdot \chi_i \cdot P$

2. Absorption Fundamentals: The Basics

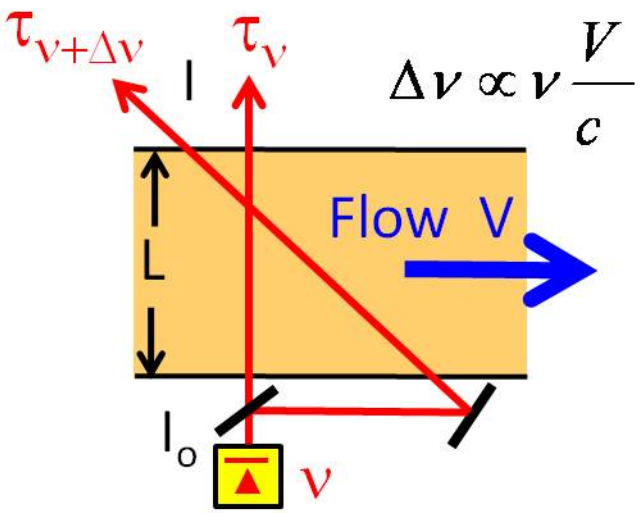

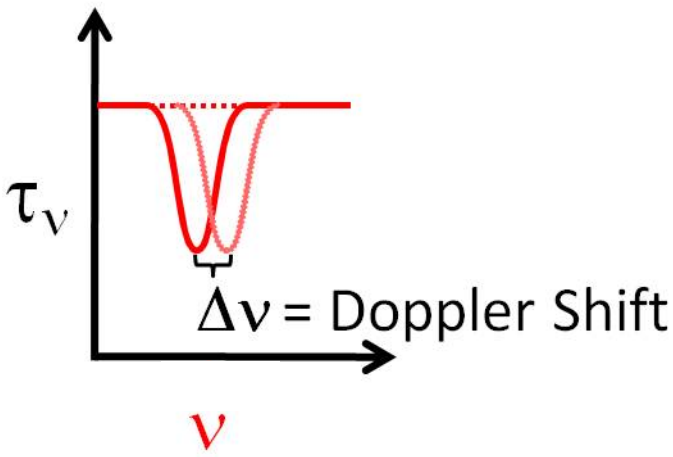

- **Shifts & shape of Φ contain information (T,V,P,χ_i)**

2. Absorption Fundamentals: The Basics

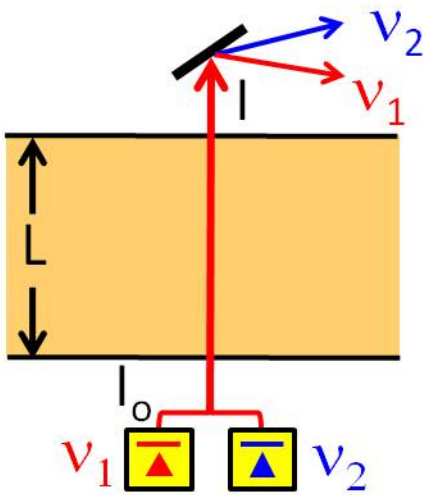

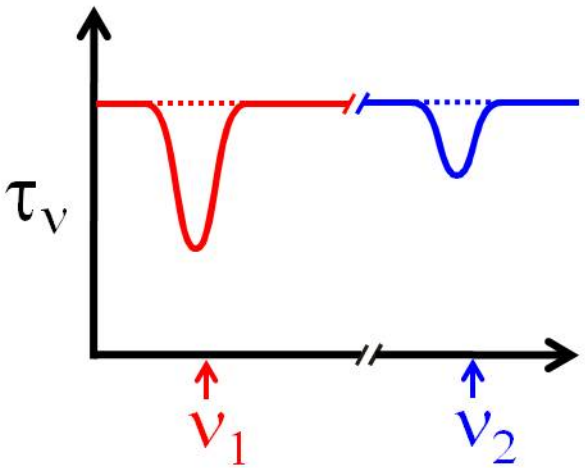

- **T from ratio of absorption at two wavelengths**

2. Absorption Fundamentals: Summary

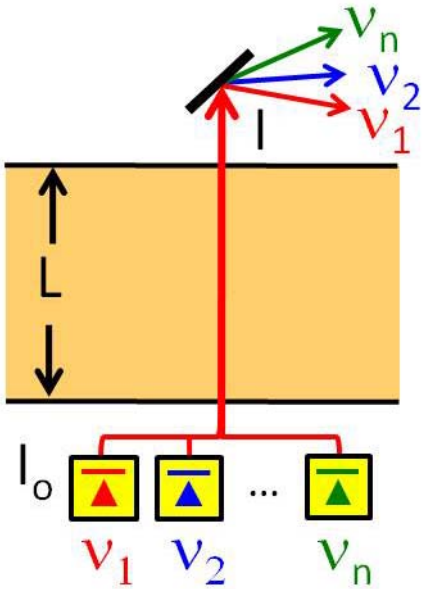

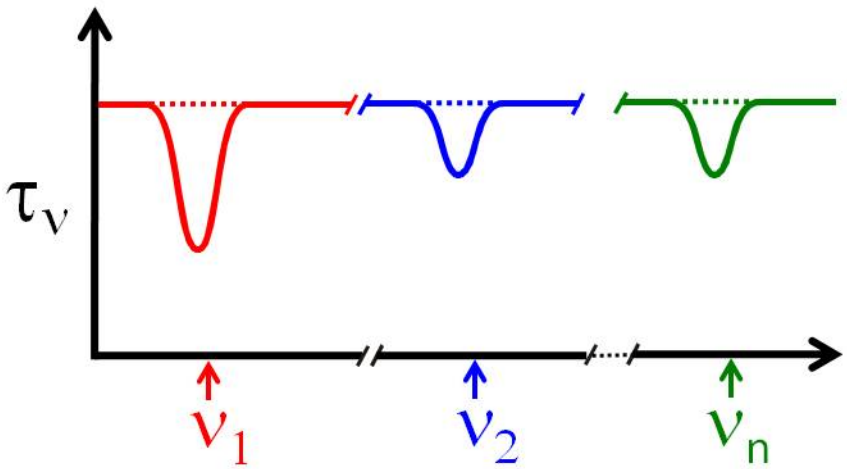

- **Wavelength multiplexing is also effective**
  - **To monitor multiple parameters or species**
  - **To assess non-uniformity along line-of-sight**

Two primary strategies for absorption measurements

3. Absorption Sensor Strategies:

Direct Absorption (DA) & Wavelength Modulation Spectroscopy (WMS)

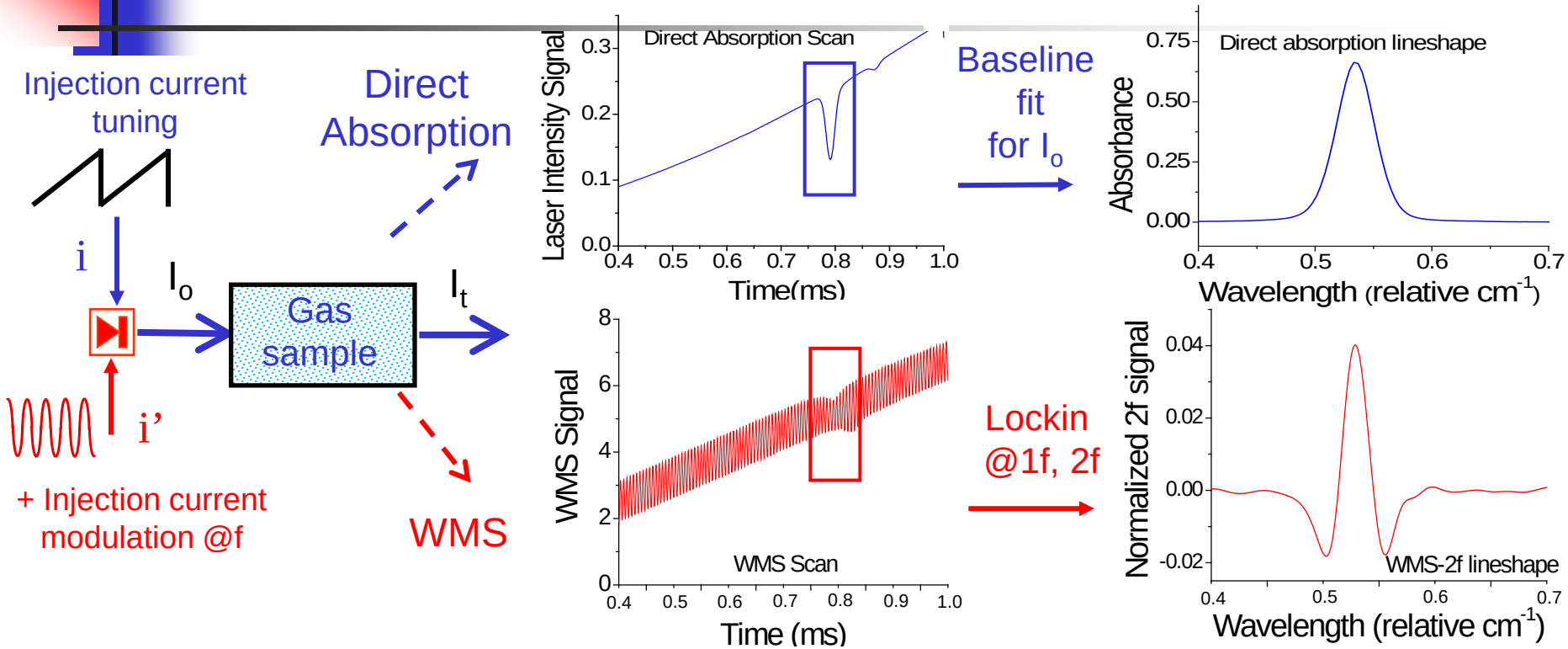

- **Direct absorption: Simple, if absorption is strong enough**
- **WMS: More sensitive especially for small signals (near zero baseline)**
  - **WMS with TDLs improves noise rejection**
  - ***Normalized WMS, e.g. 2f/1f* cancels scattering losses!**

3. Absorption Sensor Strategies:

WMS-2f/1f Accounts for Non-Absorption Losses

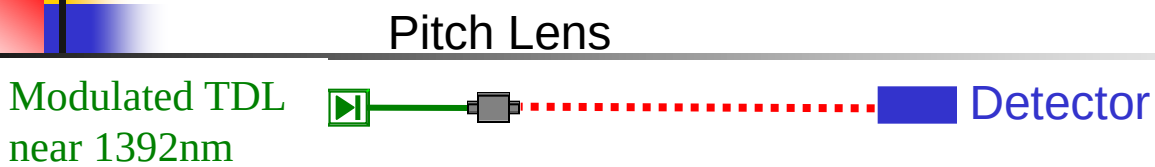

- Fixed λ WMS-*2f/1f*
- Ambient H_2O (T=296 K, 60% RH)
- L=29.5 cm, ~6% absorbance)

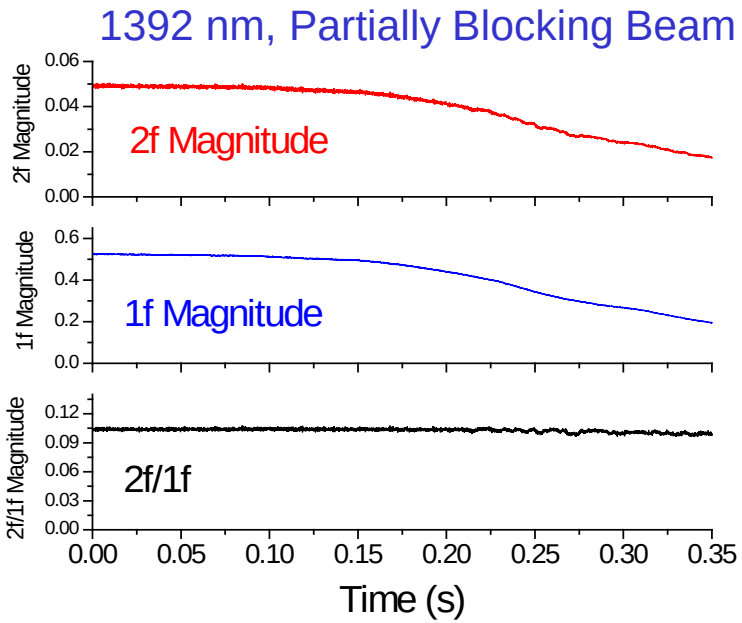

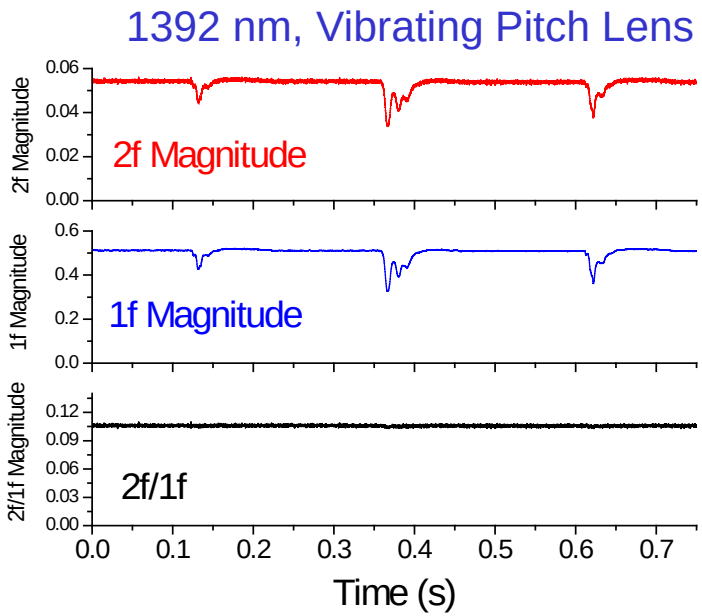

- **Demonstrate normalized WMS-*2f/1f* in laboratory air**
  - **2f/1f unchanged when beam attenuated (e.g., scattering losses)**
  - **2f/1f unchanged when optical alignment is spoiled by vibration**

WMS-*2f/1f* signals free of window fouling or particulate scattering

What species/wavelengths can we access?

4. Wavelength Access: A Wide Range of Combustion Species/Applications using Wavelengths in the IR

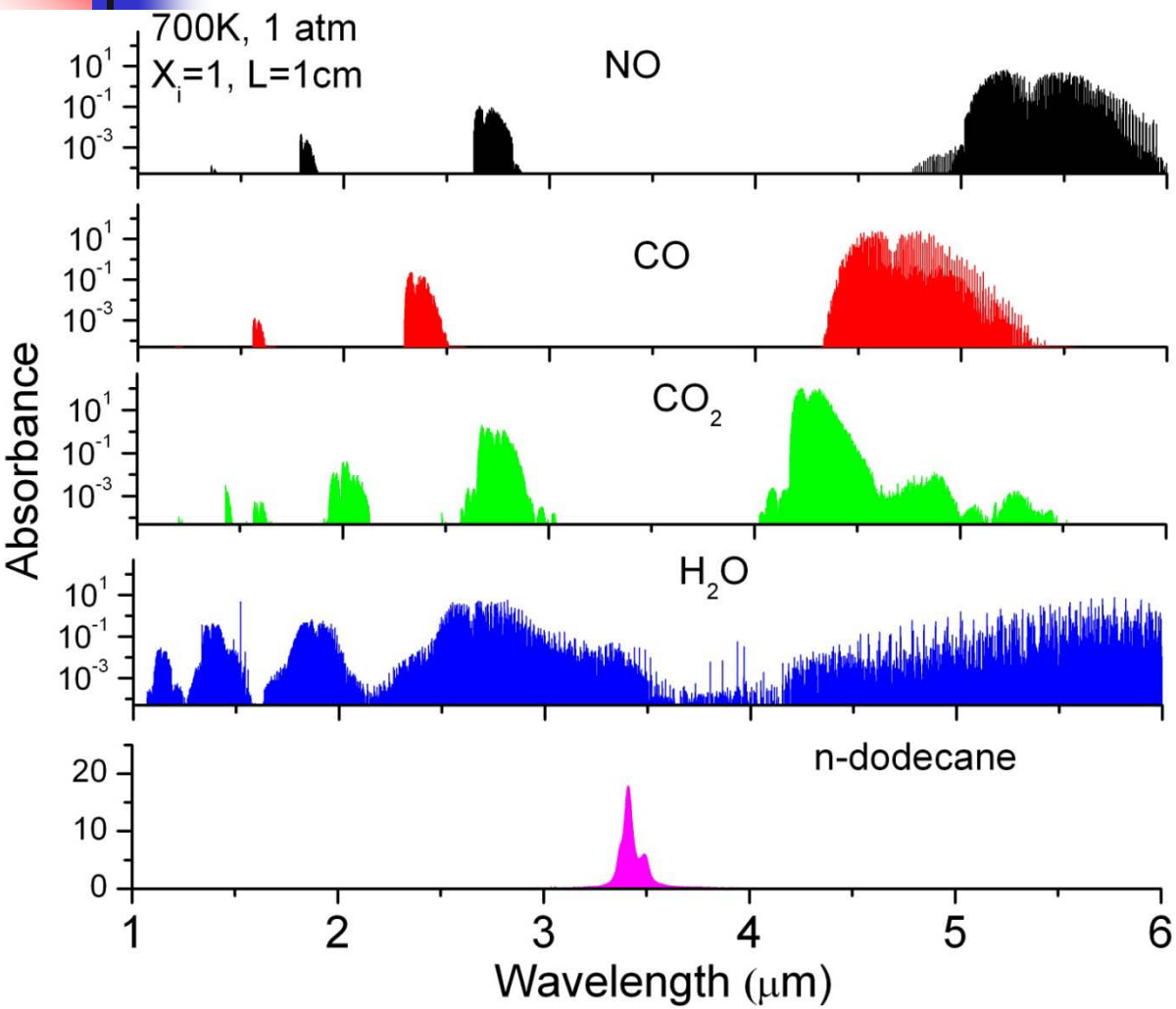

- Small species such as NO, CO, CO_2, and H_2O have discrete rotational transitions in the vibrational bands
- Larger molecules, e.g., hydrocarbon fuels, have blended features
- Different strategies used to monitor discrete lines or blended absorption features

4. Wavelength Access:
TDLs Access Visible to Mid-IR

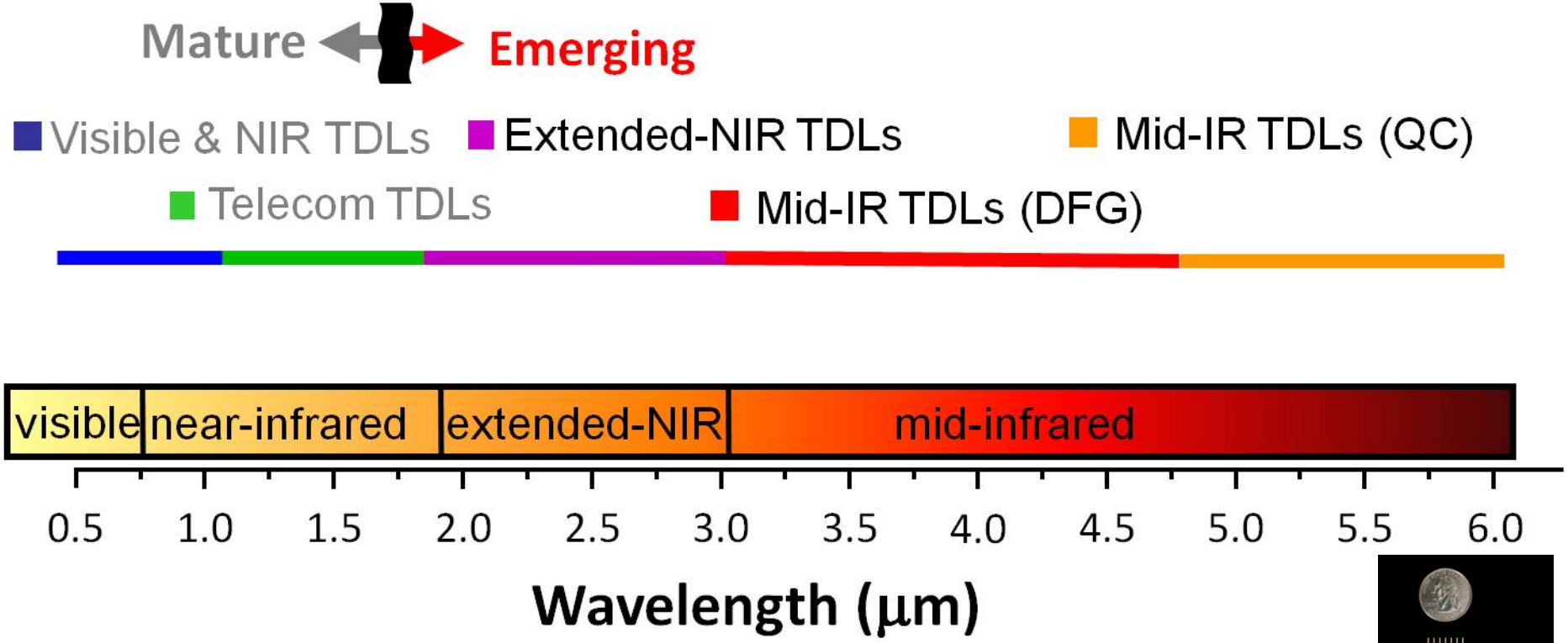

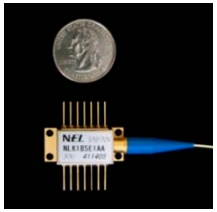

- Allows access to many atoms and molecules
- Visible and telecom TDLs can be fiber-coupled
- TDLs at wavelengths > telecom are emerging rapidly

Now lets consider hardware: lasers and detectors

4. Wavelength Access - Lasers

- Sources – Semiconductor lasers
  - Available from the near UV (375 nm) to the far-IR (~ 11 μm)
    - Power: ~ 1 to 500 mW
    - Low power restricts their application to absorption experiments
  - Near-IR lasers are compact, rugged, and fiber-coupled
  - DFB lasers can be rapidly tuned over several wavenumbers by changing the injection current or laser temperature
    - External cavity diode lasers can be tuned more than 100 cm^{-1}

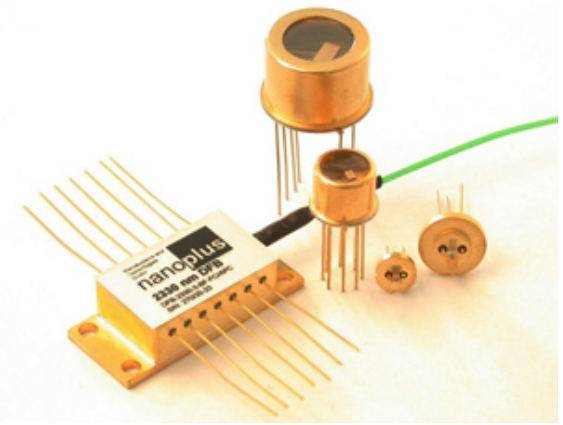

Diode lasers, near- to extended-near-IR
($1000 - $6000)
Fiber-coupled up to 2.3μm

QC lasers, mid-IR (~$40,000)

4. Wavelength Access - Detectors

- Detectors – Photodiode/Photovoltaic detectors
  - A photodiode is a semiconductor that generates voltage or current when light is incident on it
  - Like photoconductors, they have a minimum photon energy associated with the bandgap energy of the semiconductor
  - Source of noise: Johnson noise (not shot-noise limited)
  - A variation is avalanche photodiode, signal (volts) = constant x intensity

Detector material	λ [μm]
Si	0.2 – 1.1
Ge	0.4 – 1.8
InAs	1.0 – 3.8
InSb	1.0 – 7.0
InSb (77K)	1.0 – 5.6
HgCdTe (77K)	1.0 – 25.0

4. Wavelength Access - Detectors

- Detectors – Select a detector
  - **Criteria**: wavelength, time response, noise, simplicity, cost …

Wavelength

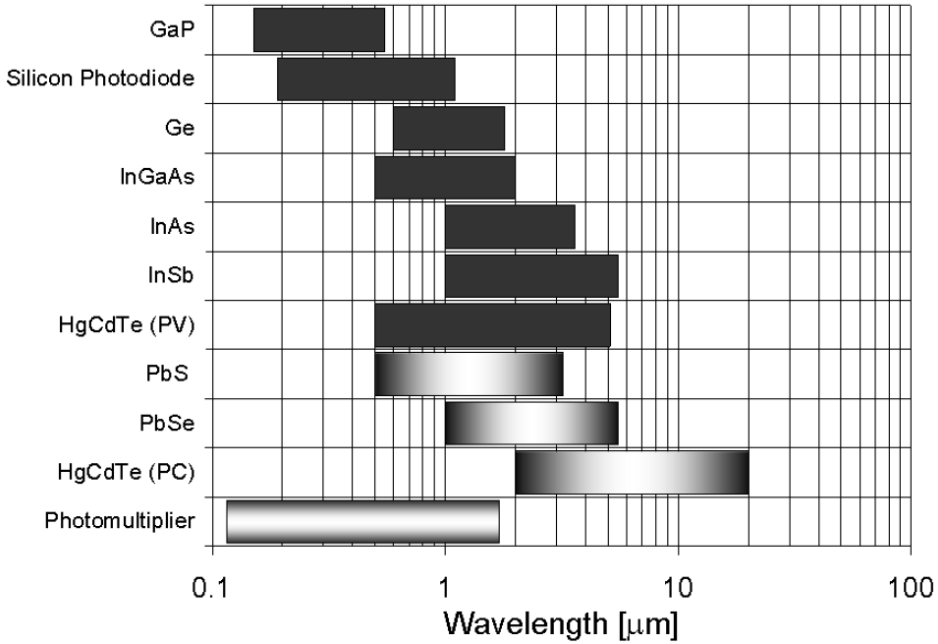

Bandwidth

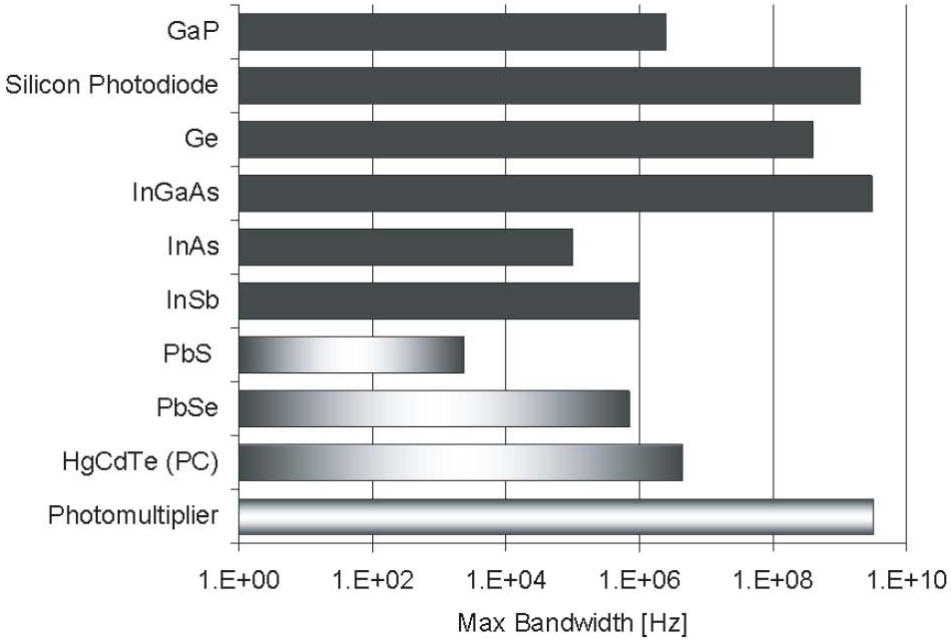

- Frequency bandwidth is important for time-resolved measurements
- Bandwidth depends on the detector area, material, temperature, and pre-amplifier gain

4. Wavelength Access - Detectors

- Detectors – <u>Select a detector</u>
  - Detector noise is characterized by the detectivity, ***D****

$$D^* = \frac{\sqrt{A_{\text{Detector}}\Delta f}}{\text{NEP}}$$

    - Δf = bandwidth
    - NEP = noise equivalent power: the amount of the optical power required to equal the magnitude of the detector noise
    - D* is improved at lower temperatures (cooling)

  - The signal-to-noise ratio (SNR) for a measurement dominated by the detector noise can be calculated using:

$$\text{SNR} = \frac{P_{\text{incident}}}{\text{NEP}} = \frac{P_{\text{incident}} D^*}{\sqrt{A_{\text{Detector}}\Delta f}}$$

  - Cost and complexity are also important considerations
  - Spatially uniform responsivity is also important
    - Smaller and cooled detectors are more uniform

5. Example TDL Applications – Combustion

1. Extended NIR provides stronger CO_2 absorption
2. Exploit strong CO_2 absorption near 2.7μm for precision T
3. Exploit 1f-normalized WMS-2f for T with aerosol present

5.1 CO_2, T Sensor Using Extended-NIR

Extended NIR Enables Large Increase in Sensitivity

- Access to CO_2 enabled by new DFB lasers for λ >2.5 μm
- The band strength near 2.7 μm is orders of magnitude stronger than NIR

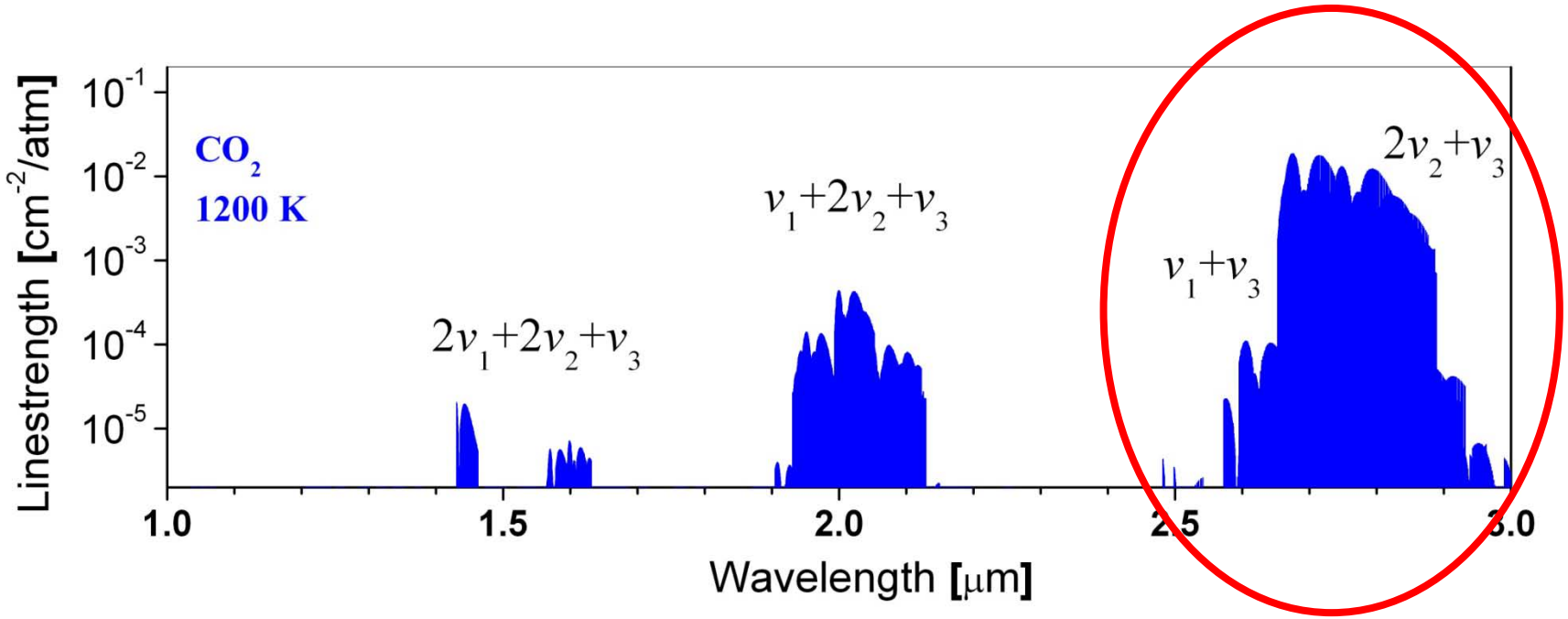

- **Many candidate transitions for optimum line pair (depending on T)**

Next: Line selection in $2\nu_2+\nu_3$ band

5.1 Extended-NIR Sensor for CO_2, T

Strategy: Sense T by ratio of absorption by two CO_2 transitions

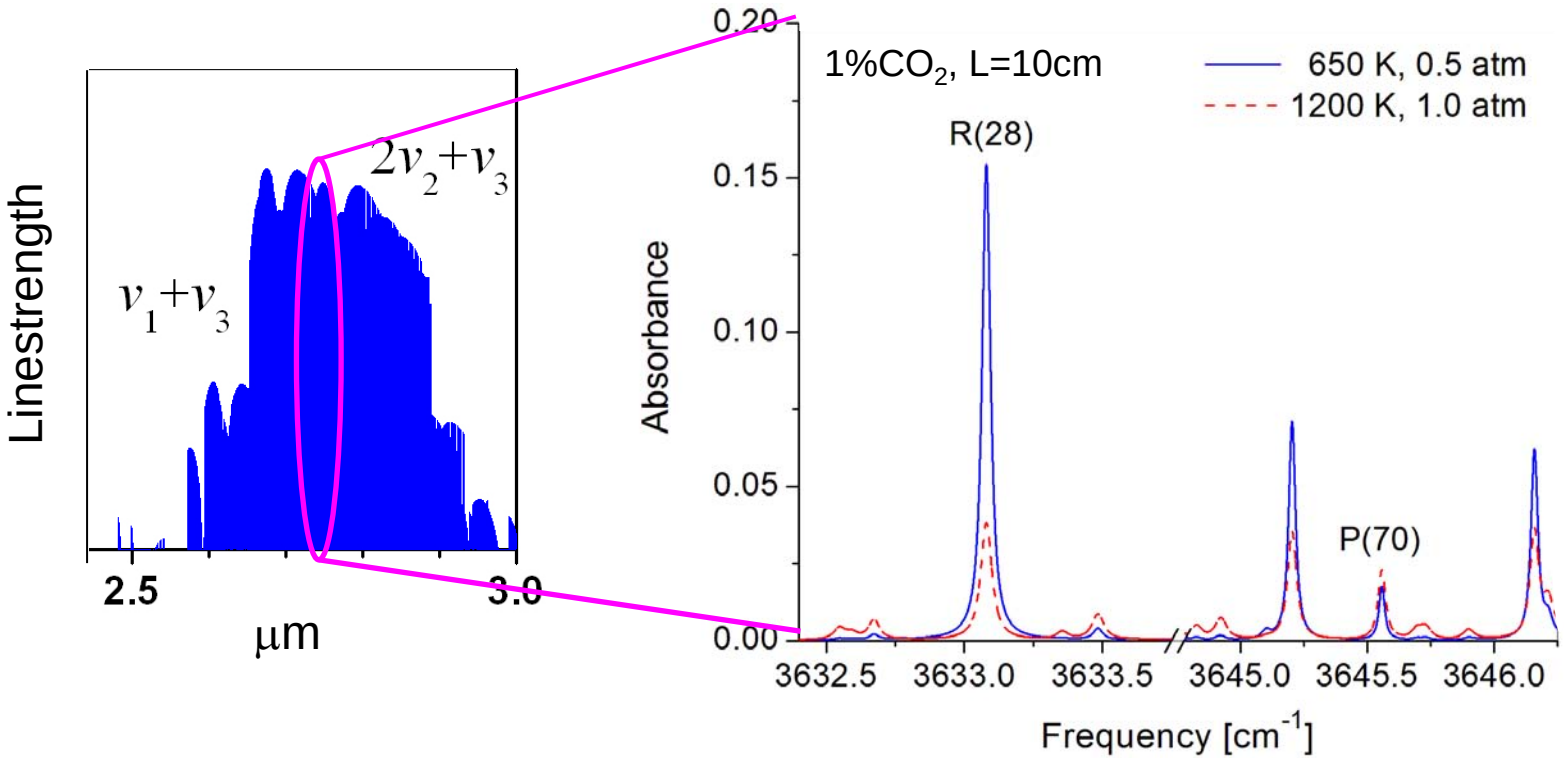

- A near optimum line pair R(28) and P(70) selected
  - Strong, isolated from H_2O, wide separation in E”

Validate in shock tube to demonstrate achievable precision

5.2 Shock-Tube Validation of Extended NIR CO_2, T Sensor

Precision Time-Resolved T from WMS-2f/1f of CO_2

Validate fast, sensitive strategy for CO_2, T using a shock tube

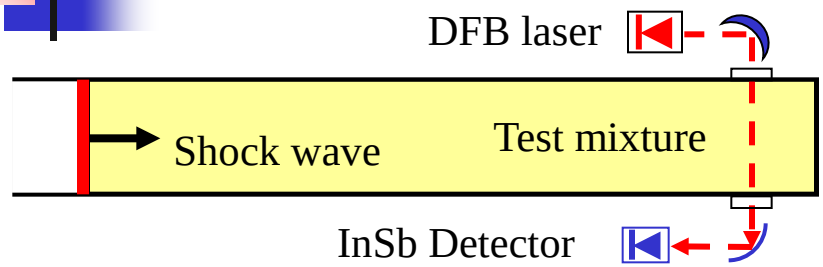

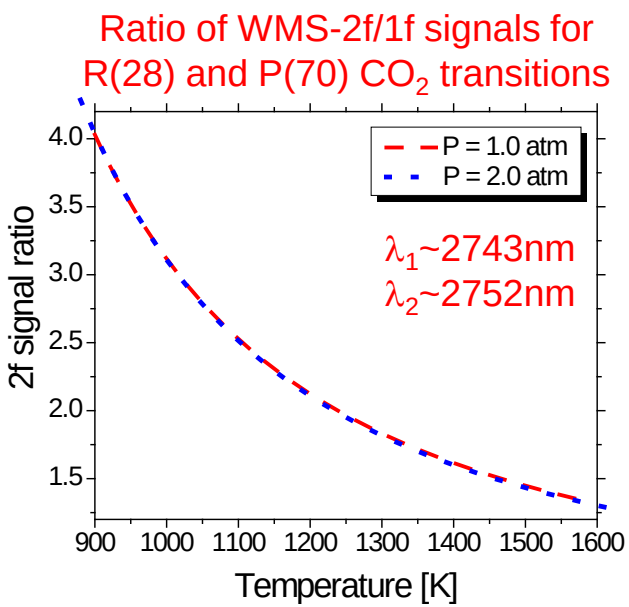

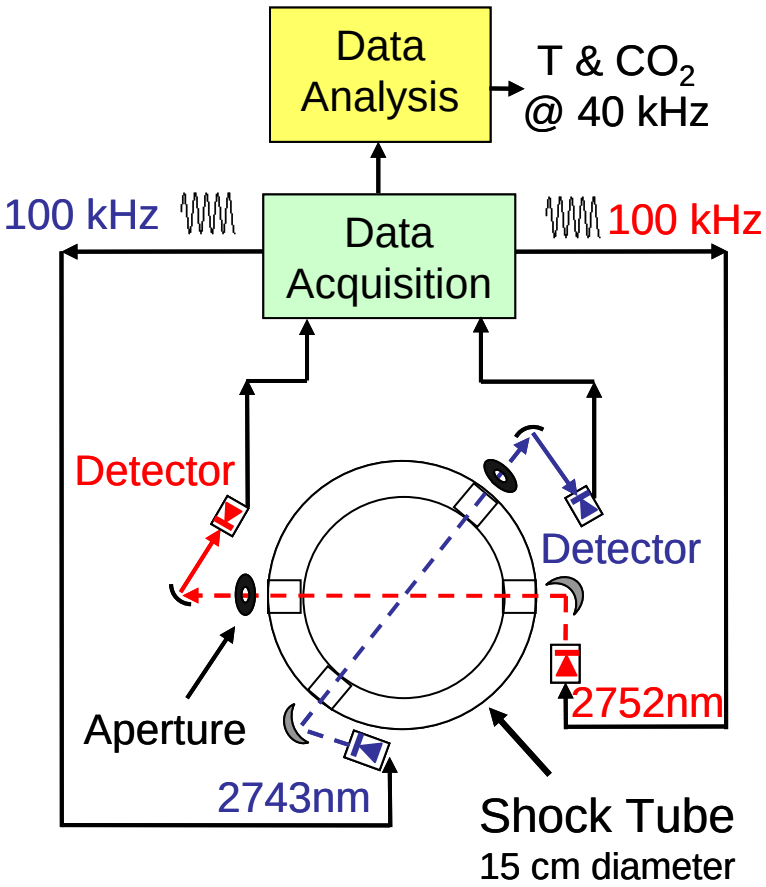

- **Ratio of WMS-2f signals sensitive to temperature**

Next: Measured accuracy and precision

5.2 Shock-Tube Validation of Extended NIR CO_2, T Sensor

Temperature vs Time in Shock-Heated Ar/CO_2 Mixtures

Accuracy

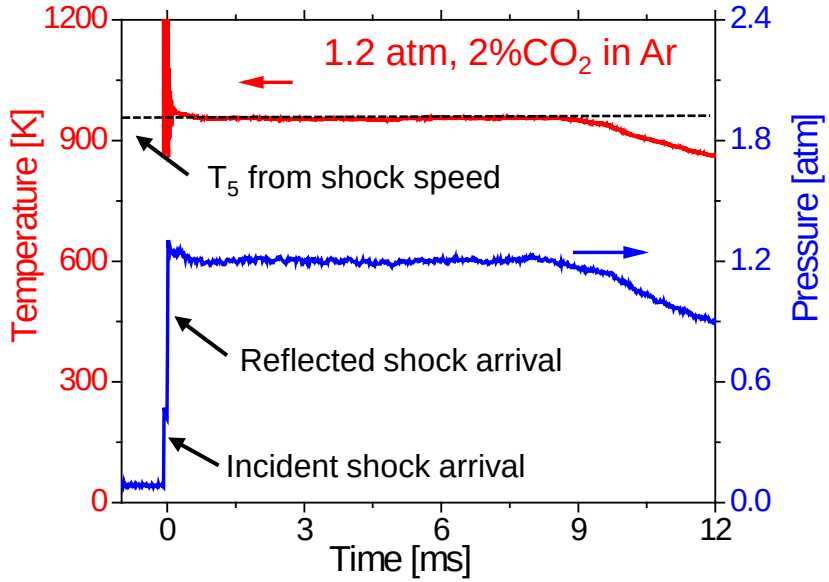

Precision

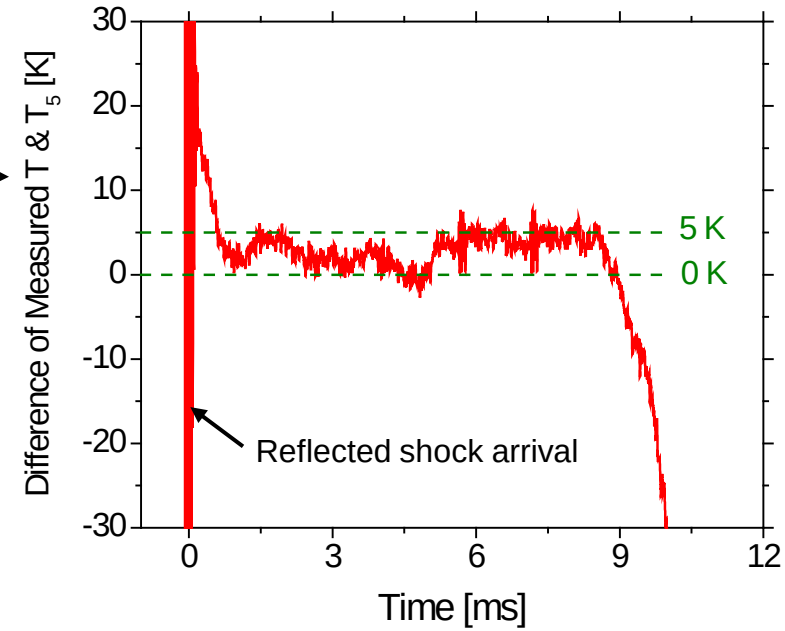

- **Temperature data agree with T_5 determined from ideal shock relations**
- **Temperature precision of ±3 K demonstrated!**
- **Unique capability for real-time monitoring of T in reactive flows**

Next: High potential for multi-phase flows, e.g., droplet evaporation

5.3 1f-Normalized WMS-2f for CO_2 with Scattering

Validate in Aerosol-Laden Gases

- Aerosol shock tube experiment: 2% CO_2 /Ar in n-dodecane aerosol
  - *L*=10 cm, P_2=0.5 atm; P_5=1.5 atm

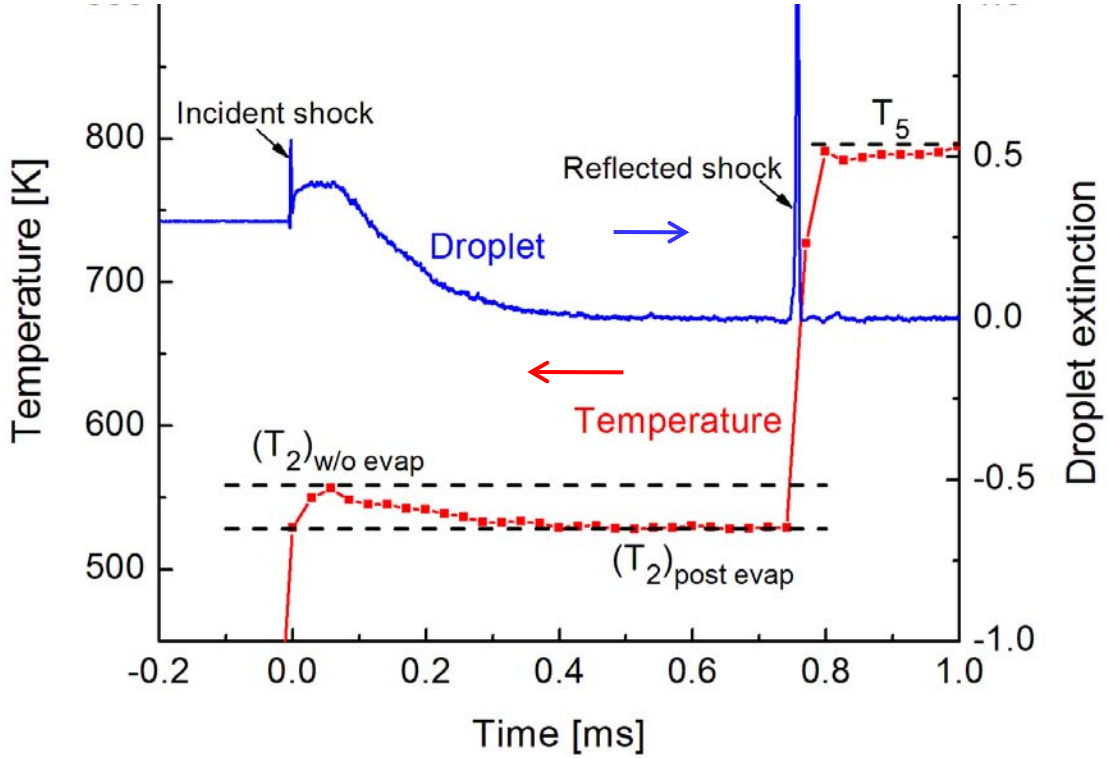

- **2f/1f TDL sensor successfully measures T in presence of aerosol!**

Next example: Detection of gasoline in IC-engines

6. Example TDL Applications - Aerospace

1. Subsonic velocity in a laboratory wind tunnel @SU – ambient H_2O
2. Supersonic velocity in a test facility @NASA – H_2O from vitiation
3. Supersonic combustion @UVa
   - Exploit mid-IR absorption for strong signals
   - H_2O, CO, and CO_2 measurements to compare with CFD
   - Scramjet unstart monitor

6.1 Subsonic Velocity @ SU:
TDLAS Sensors in Wind Tunnel

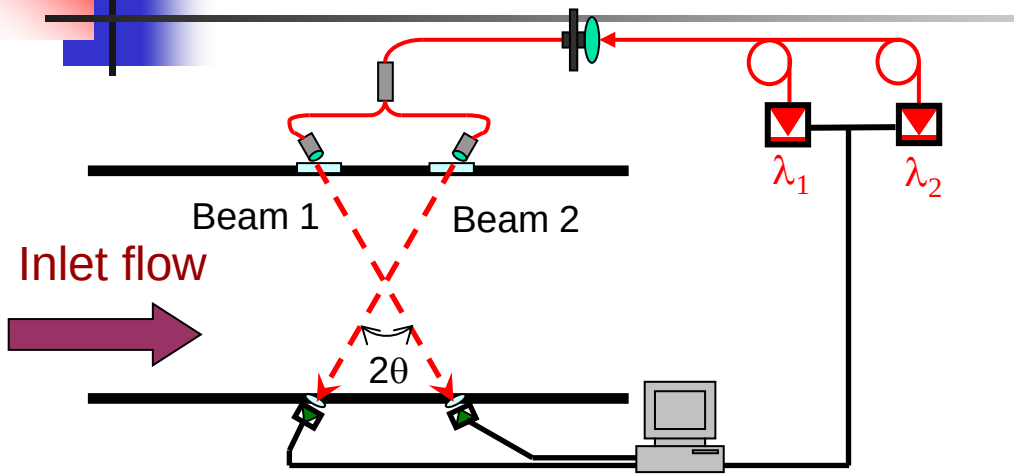

$$\frac{\Delta\nu}{\nu_0} = \frac{2V}{c}\sin\theta$$

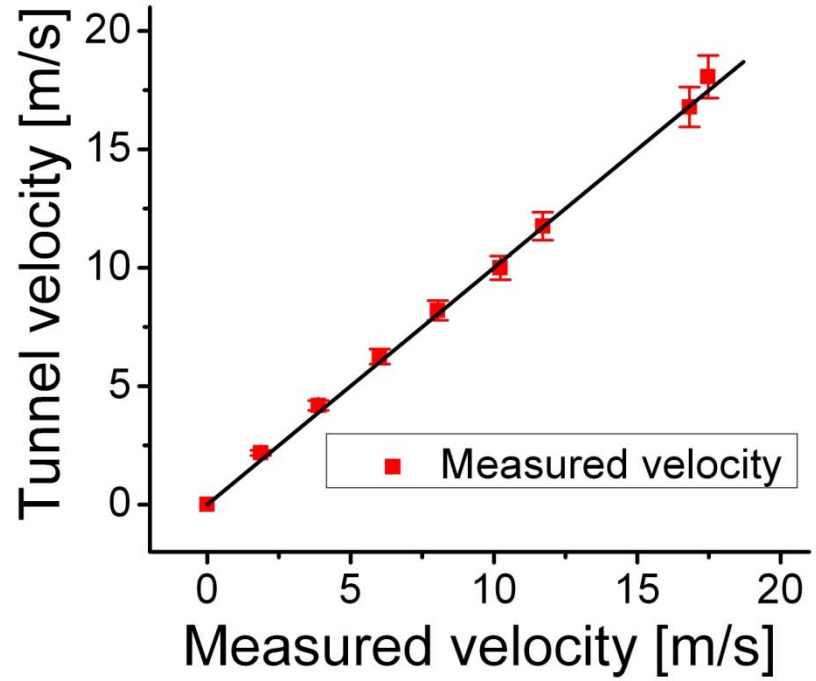

- TDL sensor of mass flux based on H_2O absorption
- Velocity from Doppler shift of absorption wavelength
- Validate sensor in subsonic wind tunnel w/ ambient H_2O @ Stanford
- 0.5 m/s precision for V in uniform subsonic flow

Next: Test in supersonic-flow facilities at NASA Langley

23

6.2 Supersonic Velocity@NASA Langley via TDLAS: Direct-Connect Supersonic Combustion Test Facility

Vitiated inlet air

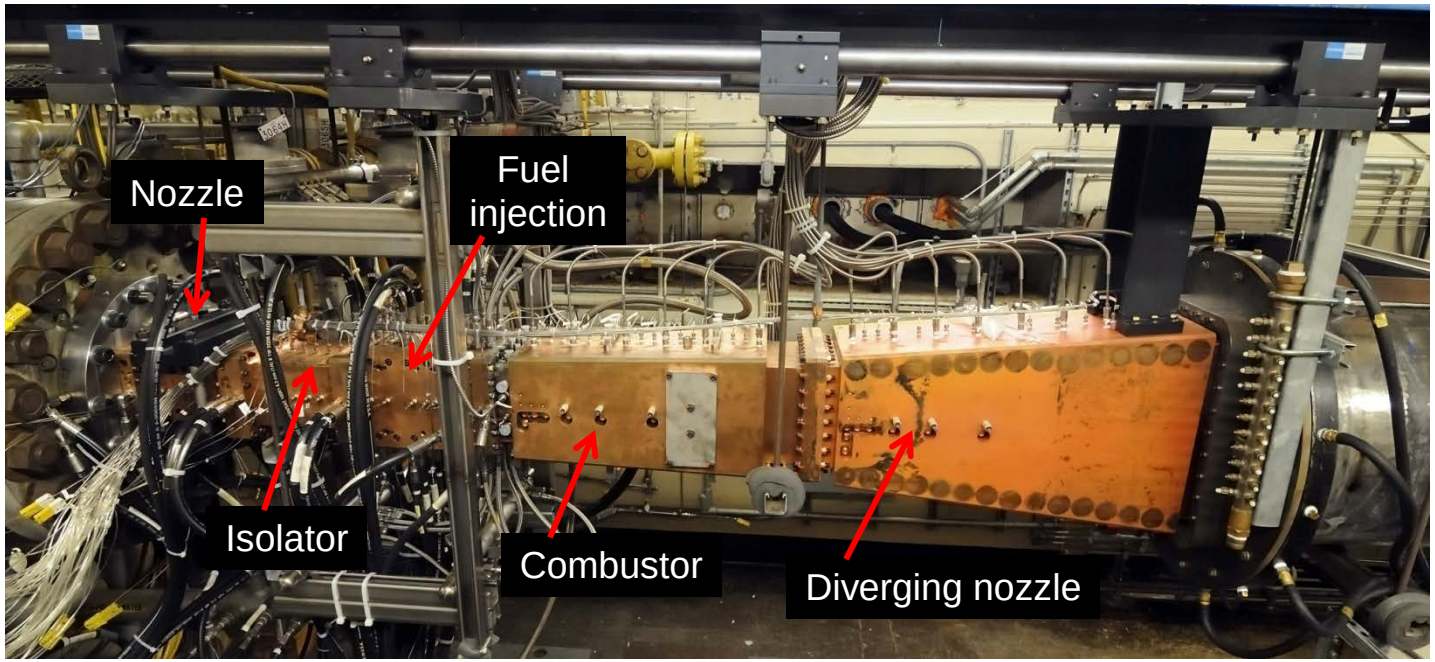

DCSCTF: Simulates atmospheric supersonic and hypersonic flight conditions

- M=2.65 nozzle with T_{static}~ 990K and P_{static}~ 0.7 atm; simulates M=5 flight
  - Add optical access to isolator
  - Measure V, T, mass flux

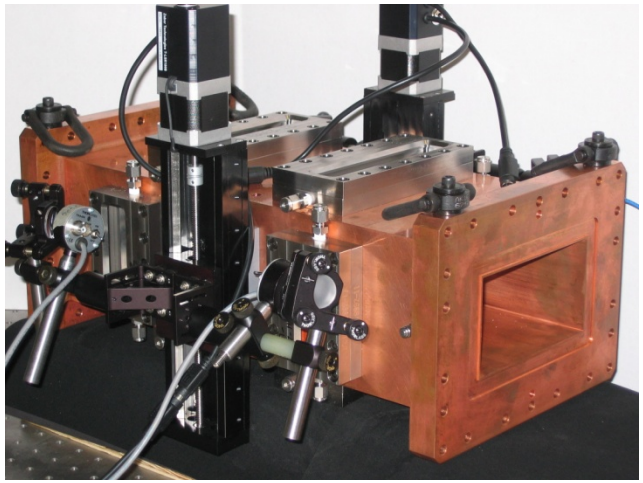

6.2 Supersonic Velocity @NASA via TDLAS

Supersonic test facility at NASA Langley (2009)

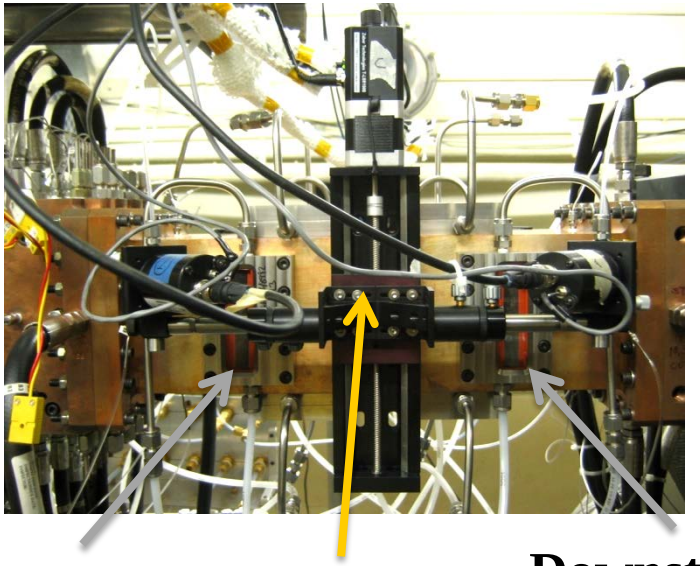

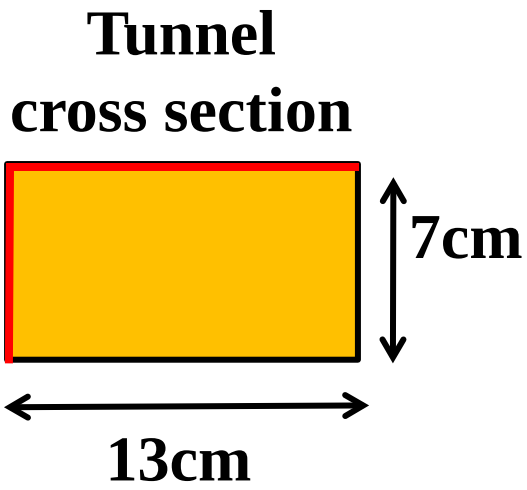

- Sensor translates to probe vertical and horizontal planes

6.2 Supersonic Velocity @NASA via TDLAS

Supersonic test facility at NASA Langley (2009)

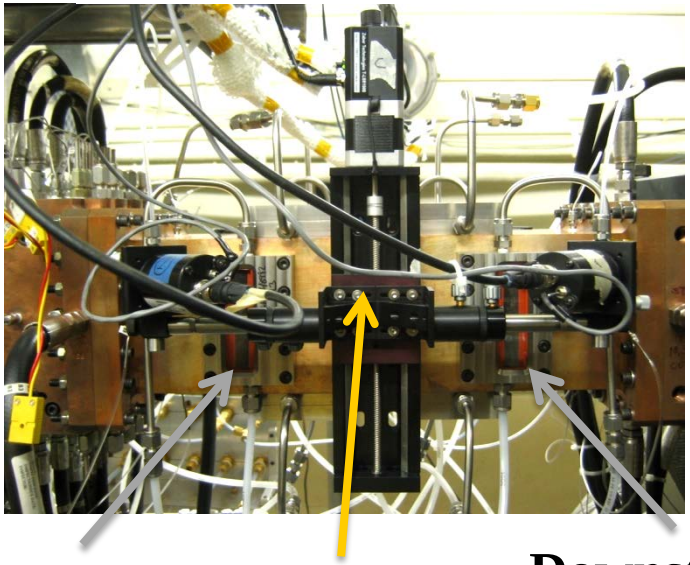

Vertical Scan

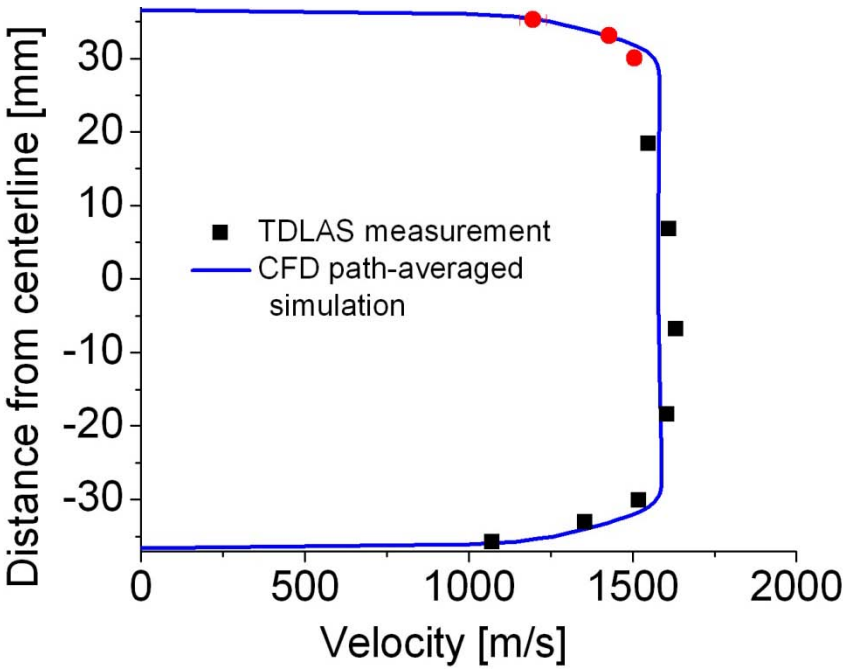

- **Sensor translates to probe vertical and horizontal planes**

Chang et al., AIAA, 2011

6.2 Supersonic Velocity @NASA via TDLAS

Supersonic test facility at NASA Langley (2009)

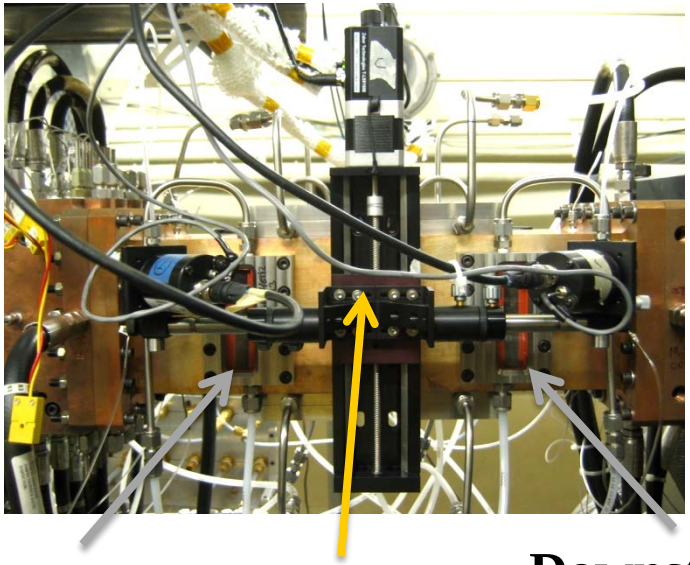

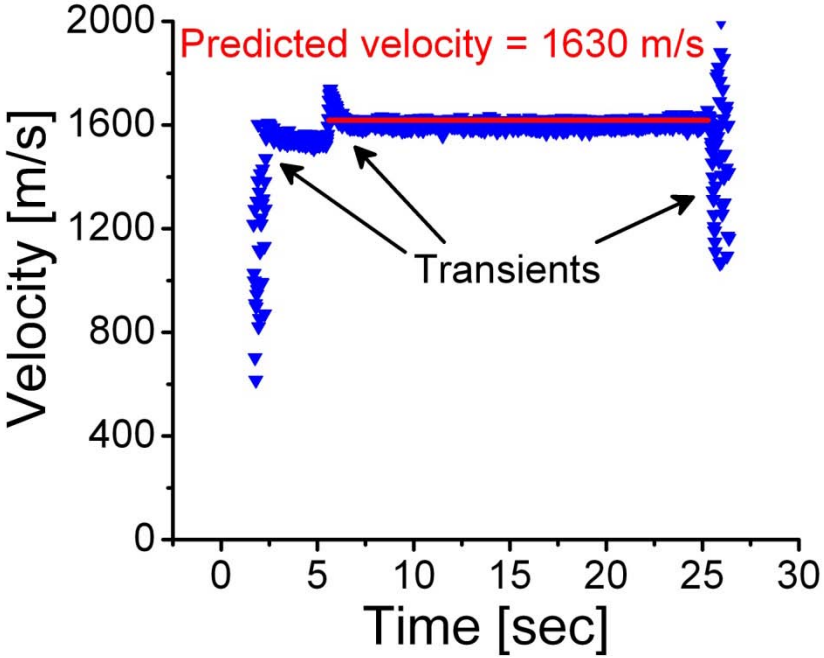

- **Sensor translates to probe vertical and horizontal planes**
- **Fast sensor captures start-up transients in V and T**

Next: A supersonic combusting flow @ UVa

Chang et al., AIAA, 2011

6.3 Mid-IR absorption sensing in scramjet flows

Goal: Spatially-resolved CO, CO_2 and H_2O in supersonic combustion

Mach 5 flight condition
Mach 2 in combustor
C_2H_4/Air, $\phi \approx 0.15$

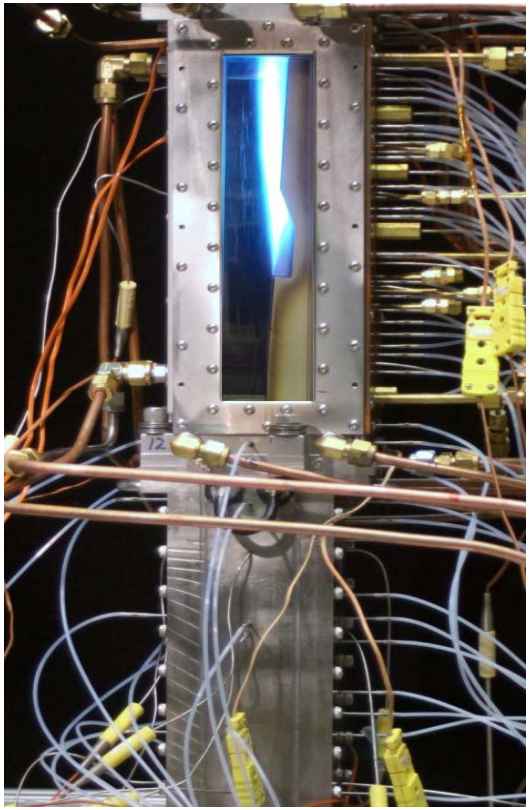

UVa Supersonic Combustion Facility
Charlottesville, VA

6.3 Mid-IR absorption sensing in scramjet flows

Optical Setup: Translating LOS

Four lasers
Two for H_2O and T
One for CO and one for CO_2

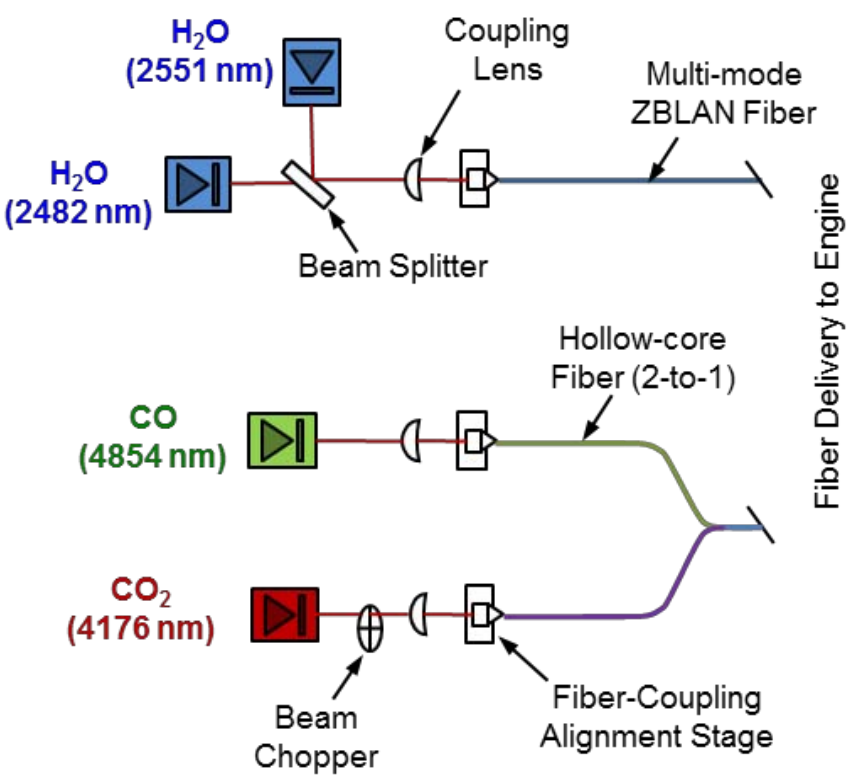

SIDE VIEW
Supersonic flow path

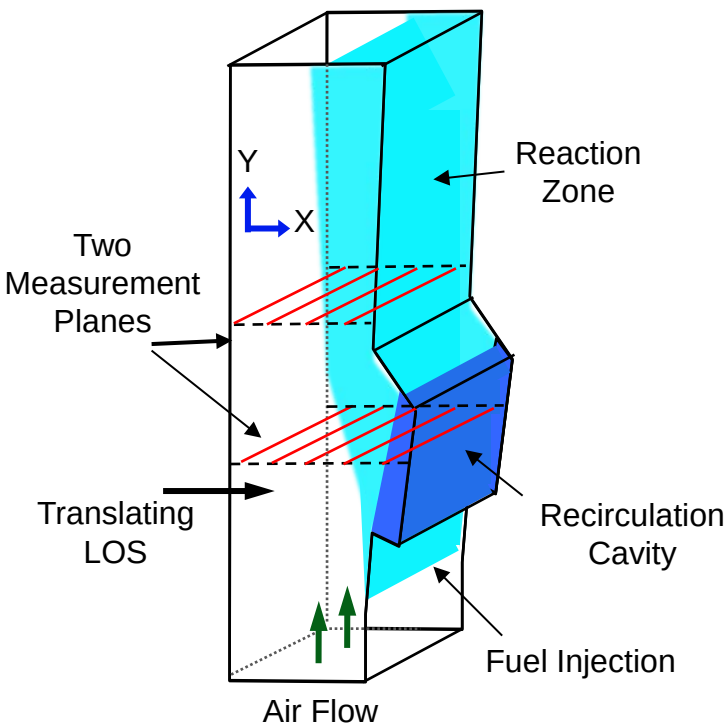

- **First use of fiber-coupled Mid-IR for aero-applications**

6.3 Mid-IR absorption sensing in scramjet flows

Time-resolved CO and T Measurements

UVa Combustor

C_2H_4 + Air: $\phi \approx 0.15$

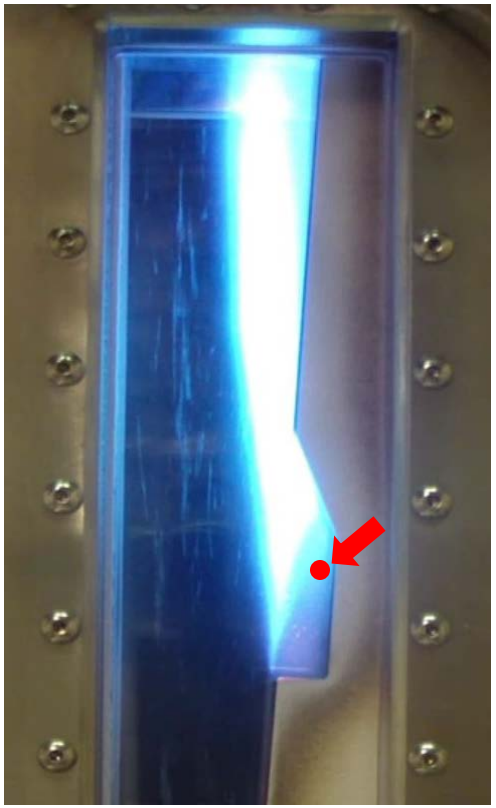

Two-line CO T measurement @ 6 kHz

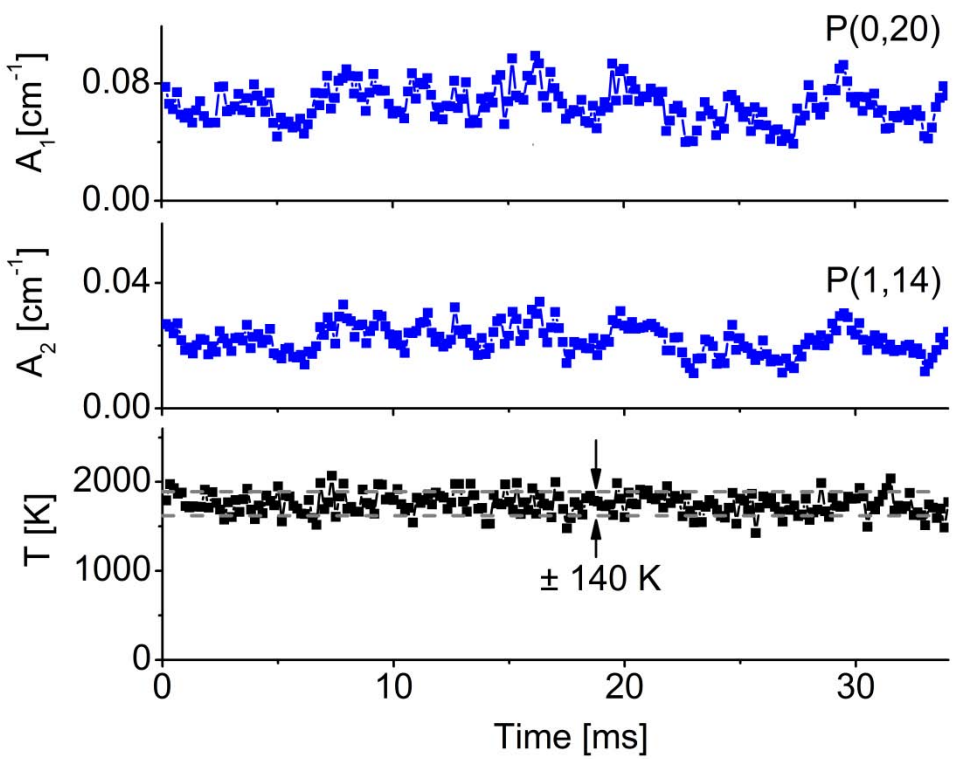

- **TDL sensor captures flow fluctuations**

6.3 Mid-IR absorption sensing in scramjet flows

Comparison of TDL Data with CFD (NCSU)

UVa Combustor

C_2H_4 + Air: $\phi \approx 0.15$

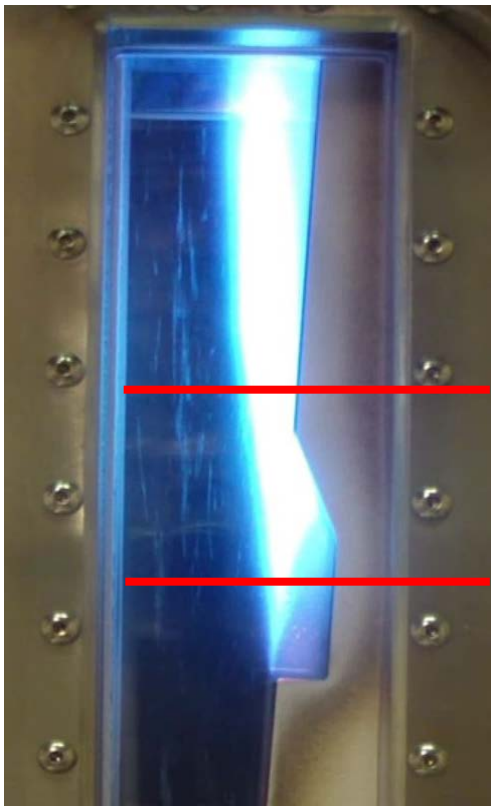

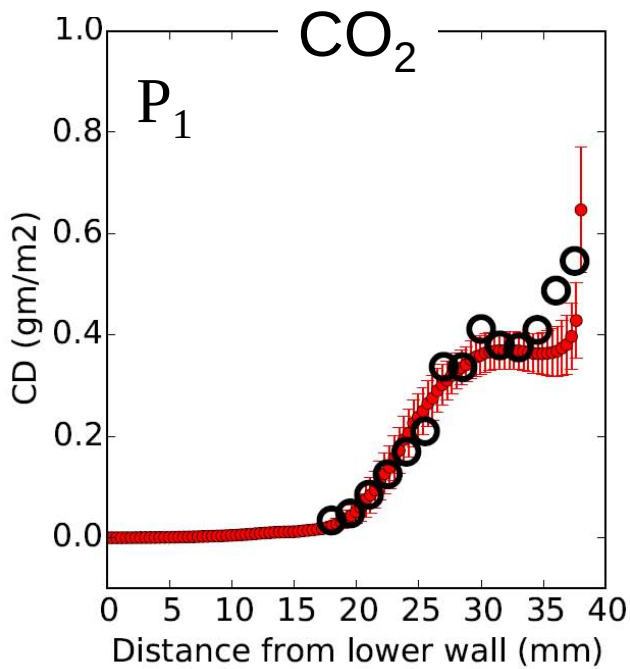

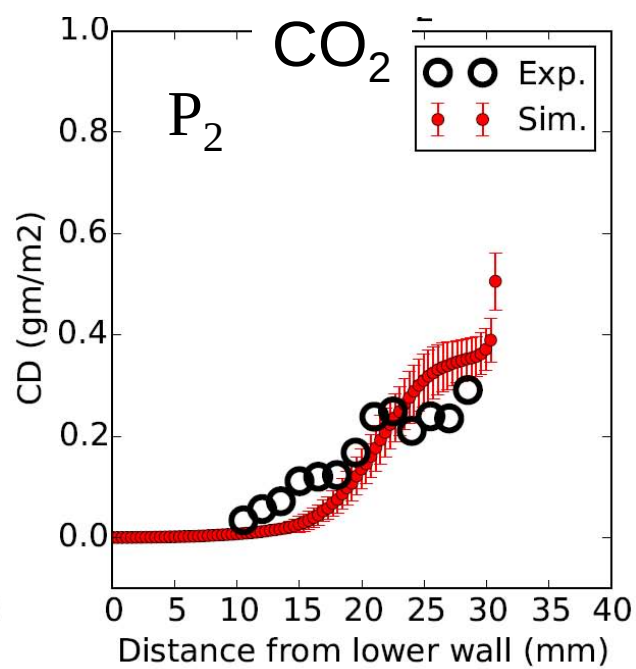

Measured and CFD CO_2 in good agreement

6.3 Mid-IR absorption sensing in scramjet flows

Comparison of TDL Data with CFD (NCSU)

UVa Combustor

C_2H_4 + Air: $\phi \approx 0.15$

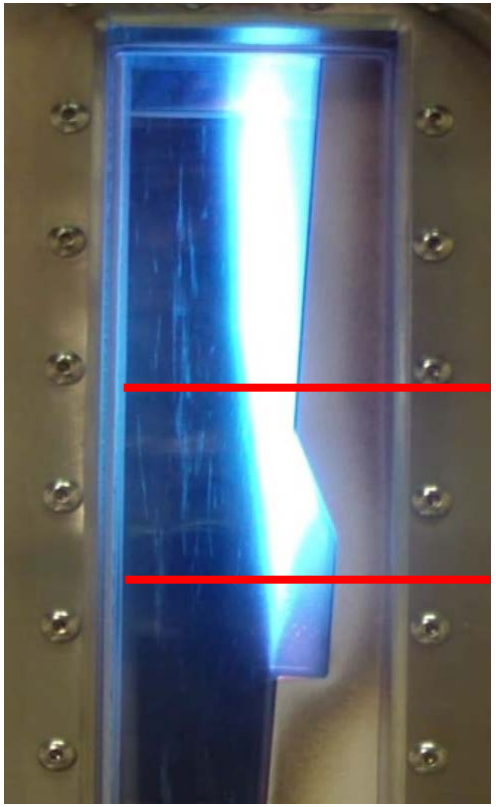

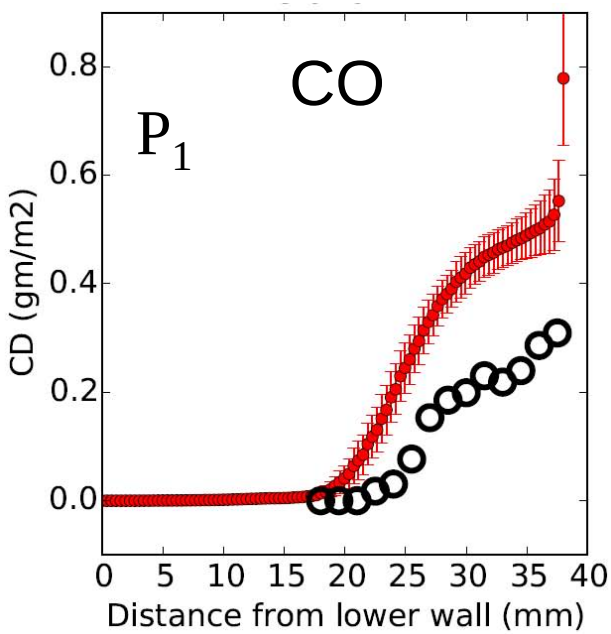

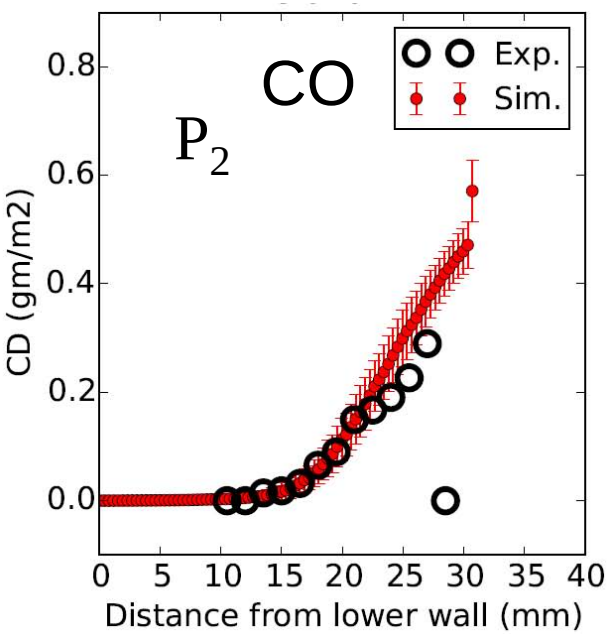

CFD overpredicts CO in cavity

6.4 Scramjet Unstart Monitor

Example: Fluctuations in T Uniformity via TDLAS

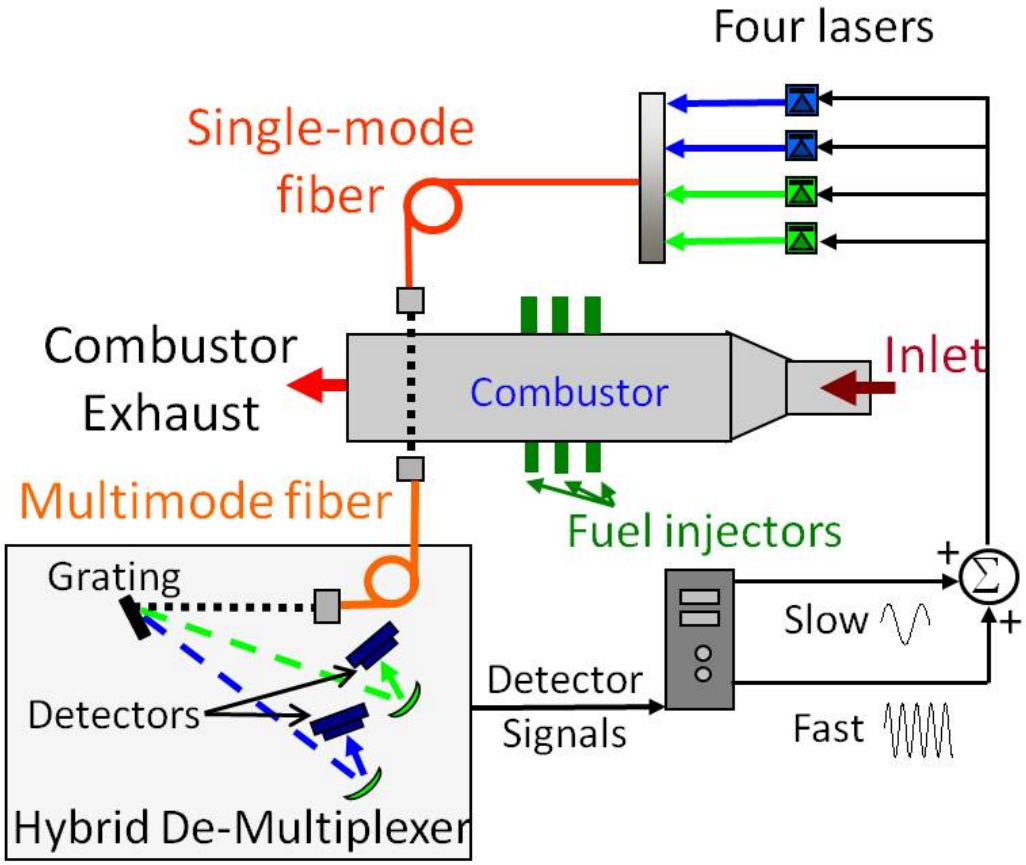

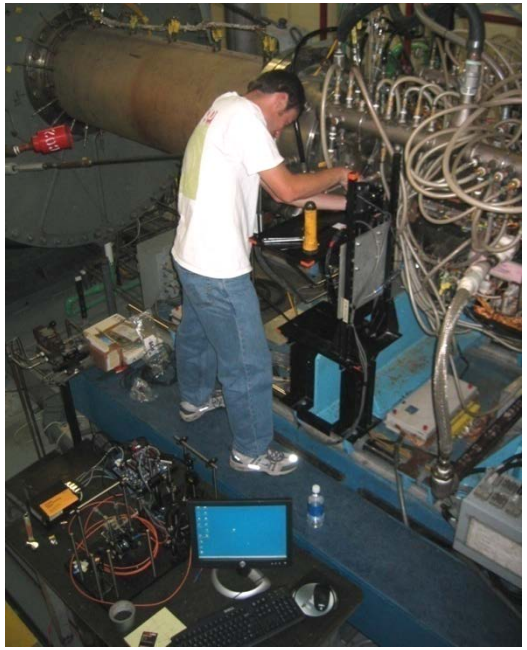

2007

- **Simultaneous measurements on 4 H_2O lines**
  - **Two lines for T_{low} and two lines for T_{high}**

6.4 Scramjet Unstart Monitor

Sensor Monitors Time-Resolved T_{low} vs T_{high}

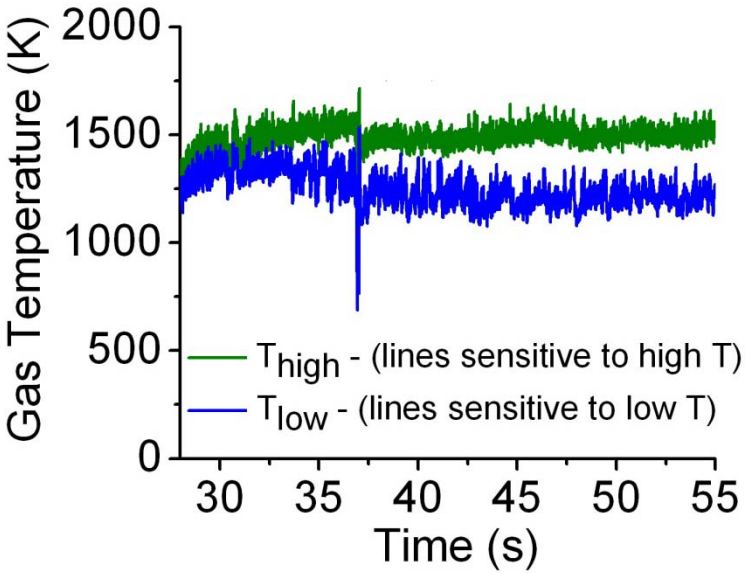

Running FFT of T_{low} & T_{high}

Ratio low-frequencies

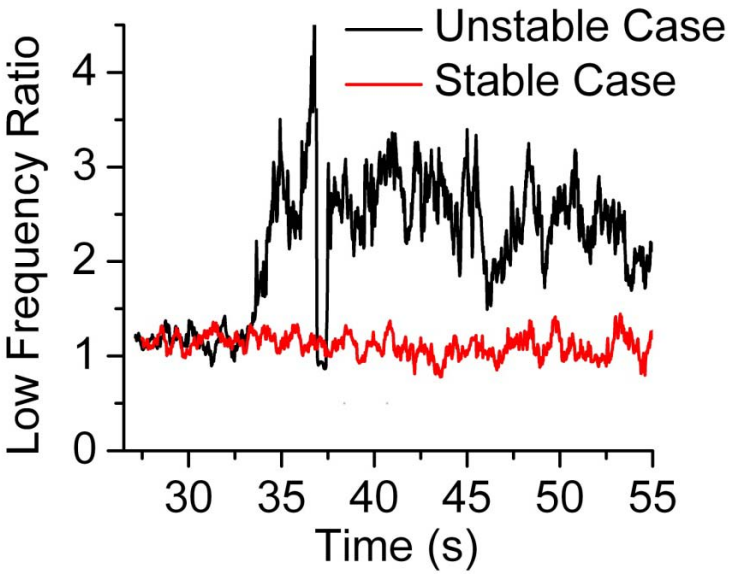

- **$T_{low} \neq T_{high}$ indicates temperature is not uniform**
- **Low-frequency fluctuations anticipate inlet unstart**
- **Fluctuation sensing : A new paradigm for control!**

Rieker et al., Proc Comb Inst, 2008

7. Future trends for TDLs Sensing

- Portable TDL-based aerospace sensors useful for T, V, species and mass flux over wide range of conditions, facilities
- Robust TDL-based sensors for long term monitoring of energy systems

- Current and future topics:
  - Characterization/maintenance/control of facilities/emissions
  - Emerging applications in flight systems
  - Extension to UV and mid-IR to access new species

    → CO, CO_2, HC's, radicals, NO, NO_2
  - Research in advanced energy and propulsion concepts

Next Lecture

TDLAS Applications to Energy Conversion

1. Fuel in IC engines – fuel and T
2. H_2O and T in slagging coal gasifier
3. H_2O in NCCC coal gasifier
4. NO and CO in coal-fired boiler exhaust

Quantitative Laser Diagnostics for Combustion Chemistry and Propulsion

Lecture 10: TDLAS Applications to Energy Conversion

1. Introduction
2. Fuel in IC engines – fuel and T
   - Absorption cross section vs gasoline blend
3. H_2O and T in slagging coal gasifier
4. H_2O in transfer coal gasifier
5. NO and CO in coal-fired boiler exhaust
6. Future trends – energy conversion

Transport coal gasifier at the National Carbon Capture Center Wilsonville, AL

1. Introduction:
TDLAS is Practical in Harsh Environments

- Utilizes economical, robust and portable TDL light sources and fiber optics
- Can yield multiple properties: species, T, P, V, & m in real-time over wide conditions
  - T to 8000K, P to 50 atm, V to 15km/sec, multiphase flows, overcoming strong emission, scattering, vibration, and electrical interference
- Demonstrated in harsh environments and large-scale systems:
  - Aero-engine inlets, scramjets, pulse detonation engines, IC engines, arcjets, gas turbines, shock tunnels, coal-fired combustors, rocket motors, furnaces….
- Potential use in control of practical energy systems

Coal-fired Utility Boiler

Chao, *Proc Comb Inst*, 2011

IC-Engines @ Nissan

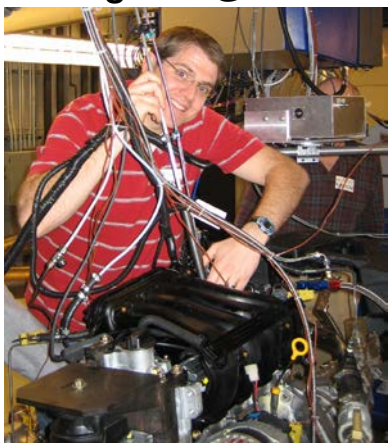

Jeffries, *SAE J. Eng*, 2010

Coal Gasifier @ U of Utah

Jeffries, *Pittsburgh Coal Conf,* 2011

2. Fuel and T Sensing in IC Engines w/ TDLAS

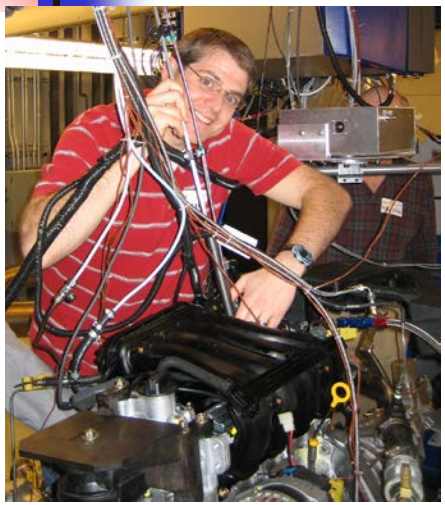

Nissan North America 2007, Fuel & T

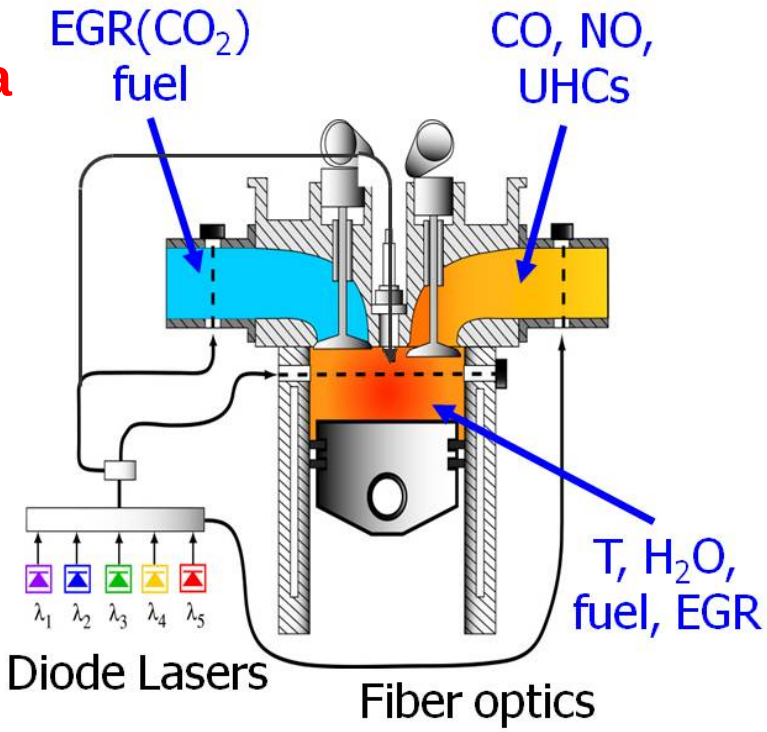

Nissan/PSI/SU Sensor @UC Berkeley, 2005 T & H_2O

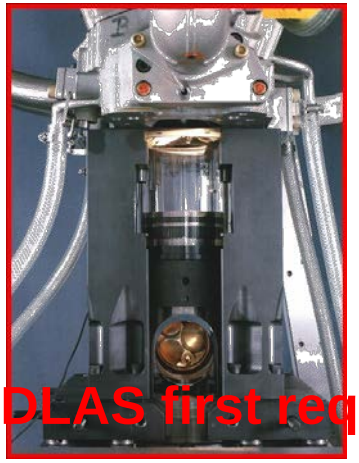

CRF Sandia, 2006 T & H_2O

Quantitative TDLAS first requires cross section data

2. Fuel and T Sensing in IC Engines w/ TDLAS

Gasoline has Unstructured Absorption & Many Blends

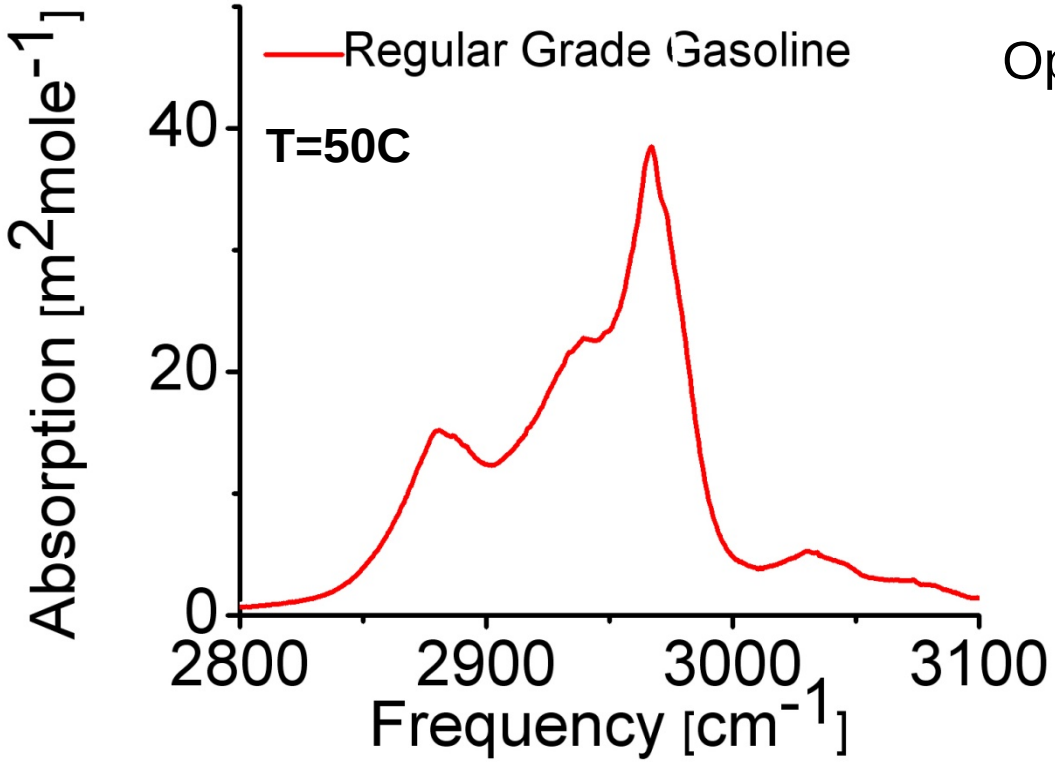

Optical frequency in cm^{-1}
defined: $\nu \equiv 1/\lambda$
where λ is wavelength

- Absorption spectrum measured with FTIR
- Strongest absorption in region of C-H stretching vibration

2. Fuel and T Sensing in IC Engines w/ TDLAS

Gasoline Absorption Varies with Temperature

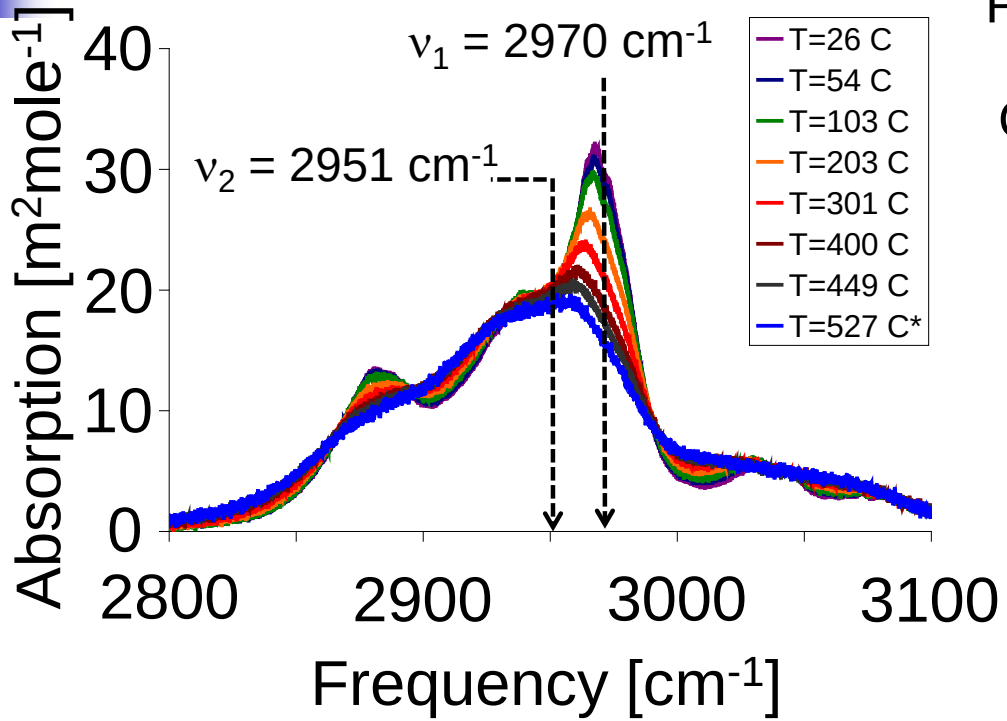

Premium grade gasoline

Optical frequency in cm^{-1}
defined: $\nu \equiv 1/\lambda$
where λ is wavelength

- Absorption cross section versus temperature measured with FTIR
- Strongest absorption in region of C-H stretching vibration
- Pick one laser frequency (ν_1) with large T dependence
- Pick one laser frequency (ν_2) with small T dependence
  - Determine temperature from absorption ratio of selected frequencies

2. Fuel and T Sensing in IC Engines w/ TDLAS

Gasoline Absorption Varies with Blend

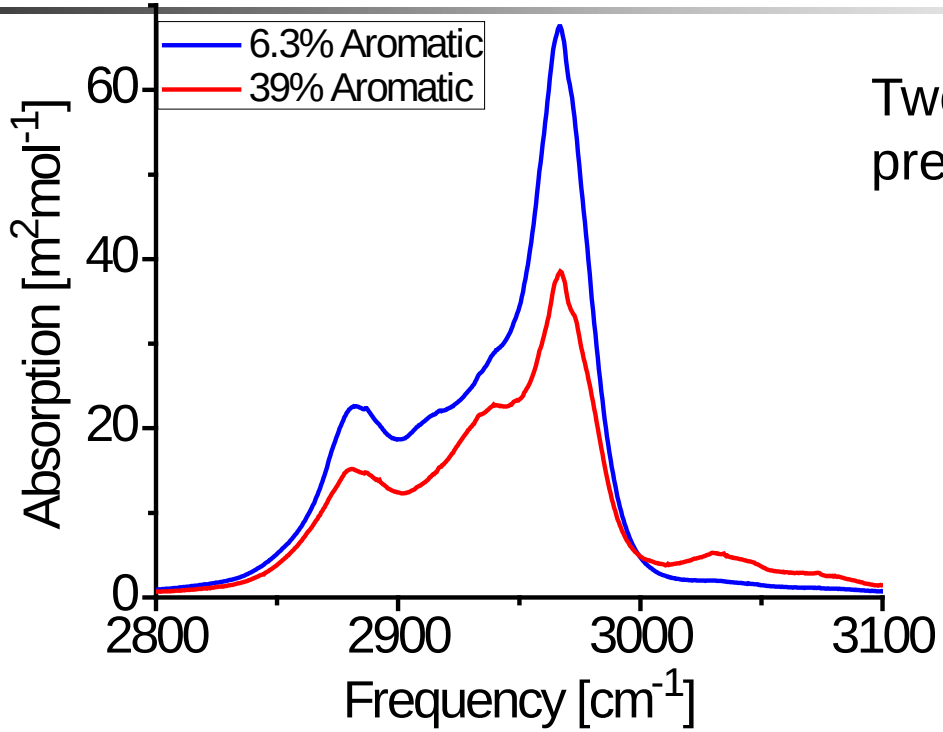

Two different blends of premium grade gasoline

- Measured (FTIR) absorption cross section varies with blend

2. Fuel and T Sensing in IC Engines w/ TDLAS

Stanford Model of Gasoline Absorption Cross Section

$$\bar{\sigma}_{\text{model}}(\lambda,T)=\sum_{j=1}^{5} X_j \sigma_j(\lambda,T)$$

- Gasoline absorption cross section model:
  - Determine composition of gasoline blend by hydrocarbon class
    - Fractions of paraffin, olefin, aromatics, and oxygenate from standard tests (ASTM D1319 & ASTM D4815)
      - Assume oxygenates are ethanol
      - Normal- and iso-paraffin fraction based on fuel grade
  - Determine absorption cross section $\sigma_j(\lambda,T)$ for hydrocarbon class
    - Empirical database (see Klingbeil et al., Fuel **87**(2008)3600)
  - Weighted sum of σ_j by mole fraction X_j of each hydrocarbon class
- Absolute measurements without calibration using this cross section

2. Fuel and T Sensing in IC Engines w/ TDLAS

Cross Section Model Validation Experiments

Gasoline Composition

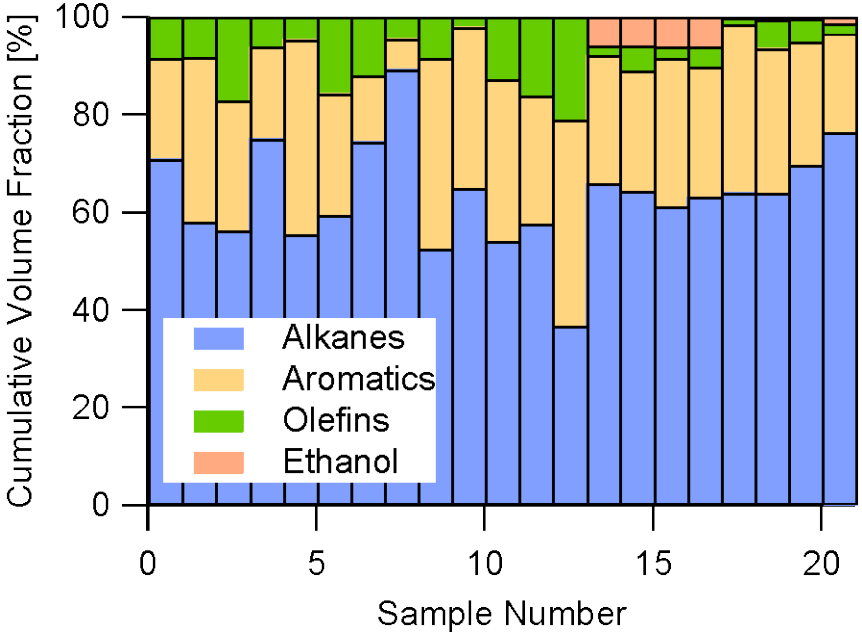

Comparison between model and experiment

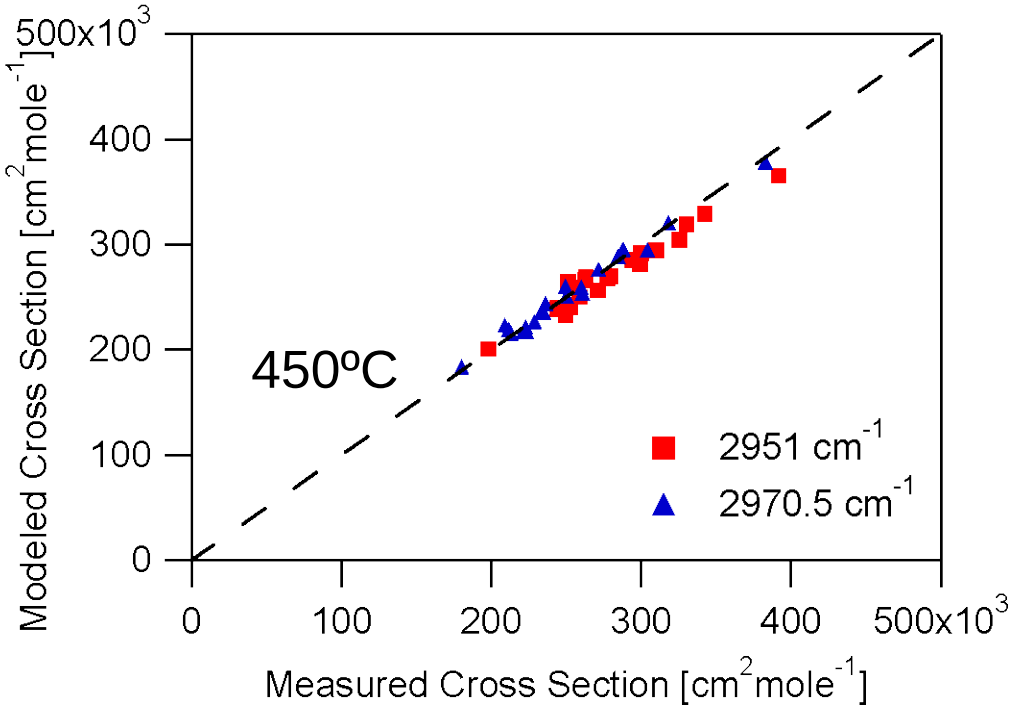

- 21 Gasoline samples measured (sample collection augmented by Chevron)
  - Sample pool covers expected range of gasoline compositions
  - Composition variation in cross section larger than x2 at target ν_1 & ν_2
- FTIR measured cross sections in good agreement with model predictions

2. Fuel and T Sensing in IC Engines w/ TDLAS

Gasoline Sensor Needs 3-Color Laser

Three color laser system

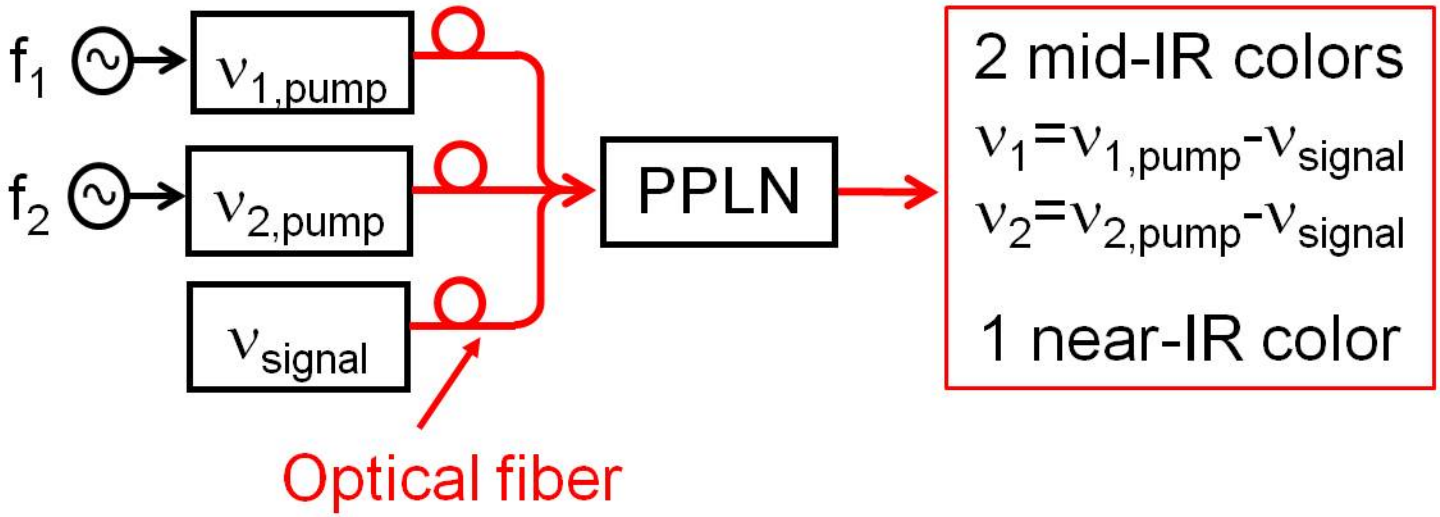

- Difference frequency of two near-IR lasers for mid-IR outputs
  - Third near-IR laser provides two mid-IR outputs
- Two Mid-IR colors for simultaneous fuel and T
- NIR color can be used to identify liquid droplets of fuel

2. Fuel and T Sensing in IC Engines w/ TDLAS

Optical Access Key to In-cylinder Fuel Measurements

SU, Nissan, PSI collaborative project (2003-2008)

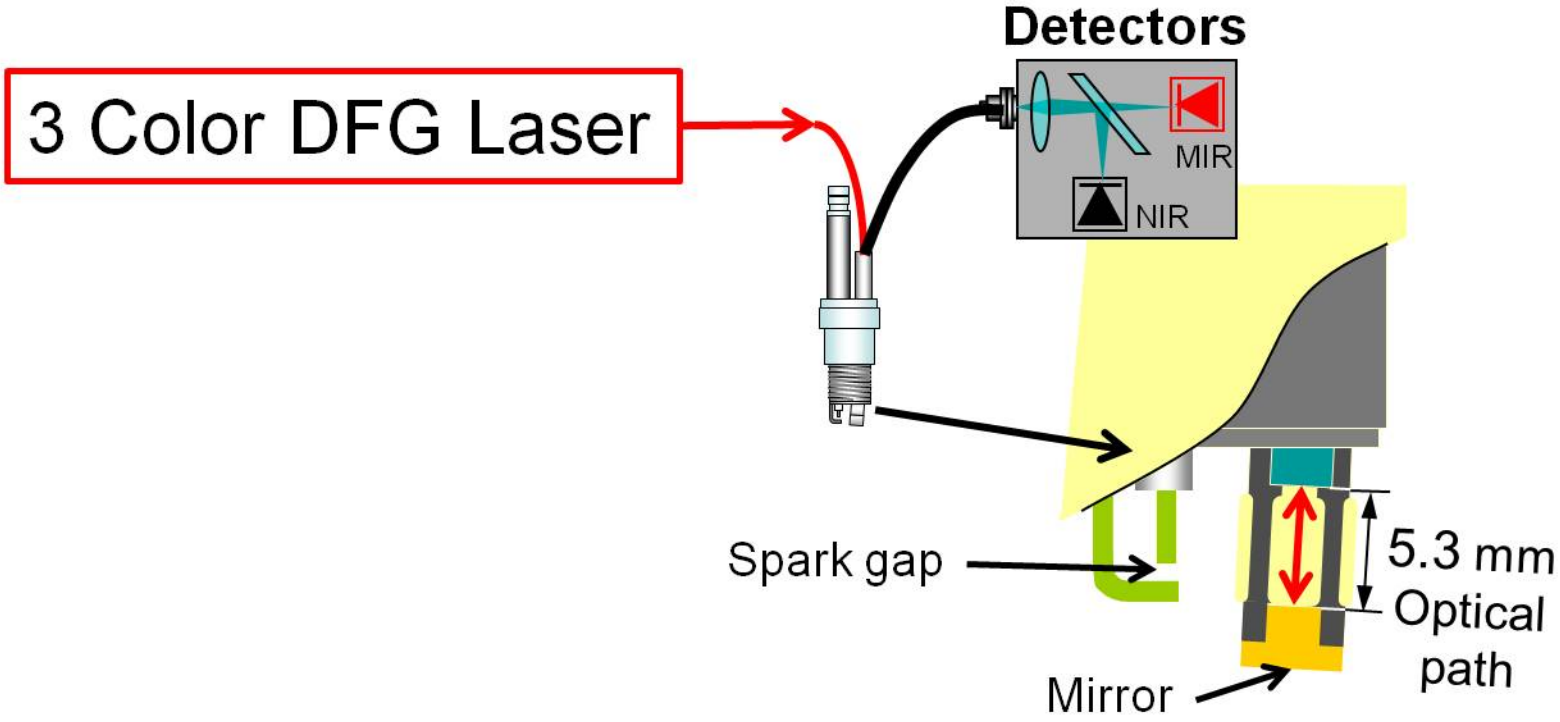

- Measure fuel vs time (CA) close to spark ignition

2. Fuel and T Sensing in IC Engines w/ TDLAS

Crank-Angle-Resolved Gasoline Absorption

- **Single-cycle data from production engine**

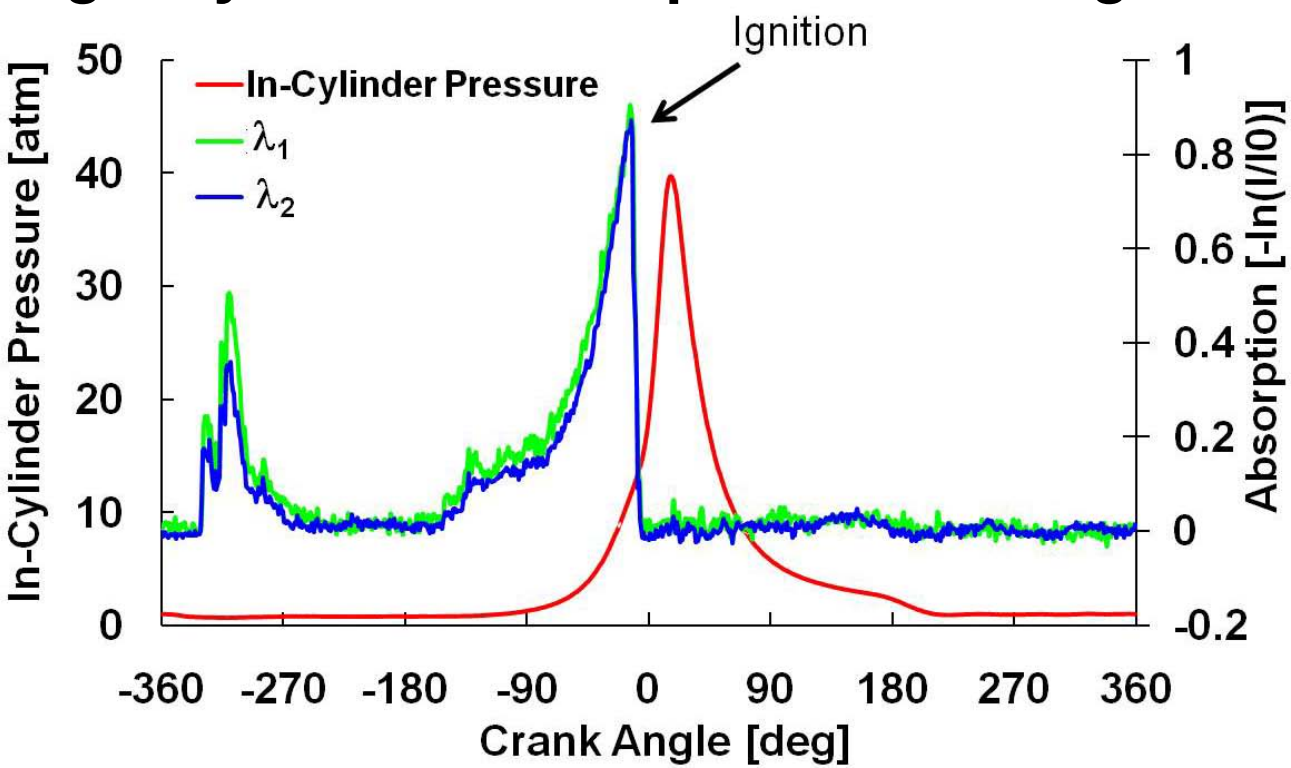

Nissan North America (2007)

- **High-quality, low-noise data for entire cycle**
- **Sensor provides cycle-by-cycle statistics of F/A ratio**
  - **Critical for understanding/controlling UHC emissions**

Jeffries et al., *SAE International Journal of Engines, 2010*

2. Fuel and T Sensing in IC Engines w/ TDLAS

Cold Start Fluctuations Critical for Emissions Control

Peak fuel at ignition for 400 cold start cycles

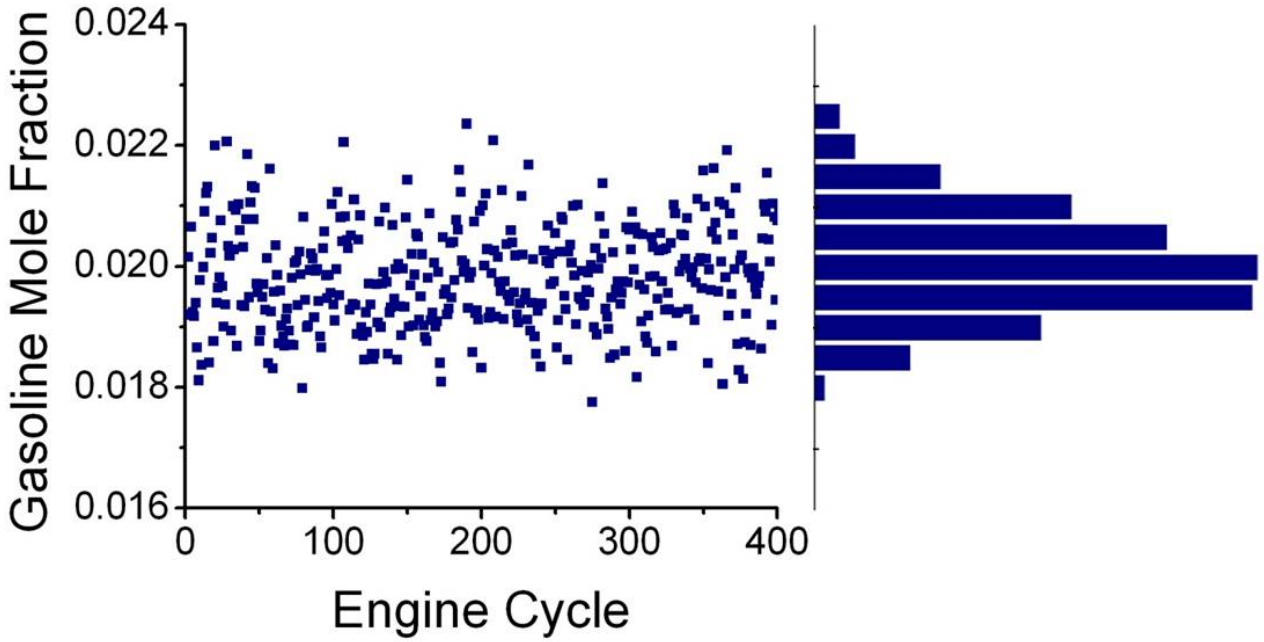

- **High-resolution data quantifies changes in fuel loading**
- **Provides new tool to optimize MPI & DIG engines**

Part 3: Sensors to optimize coal gasification

3. H_2O & T in Slagging Coal Gasifier @ Utah
Vision for TDLAS Sensing in IGCC

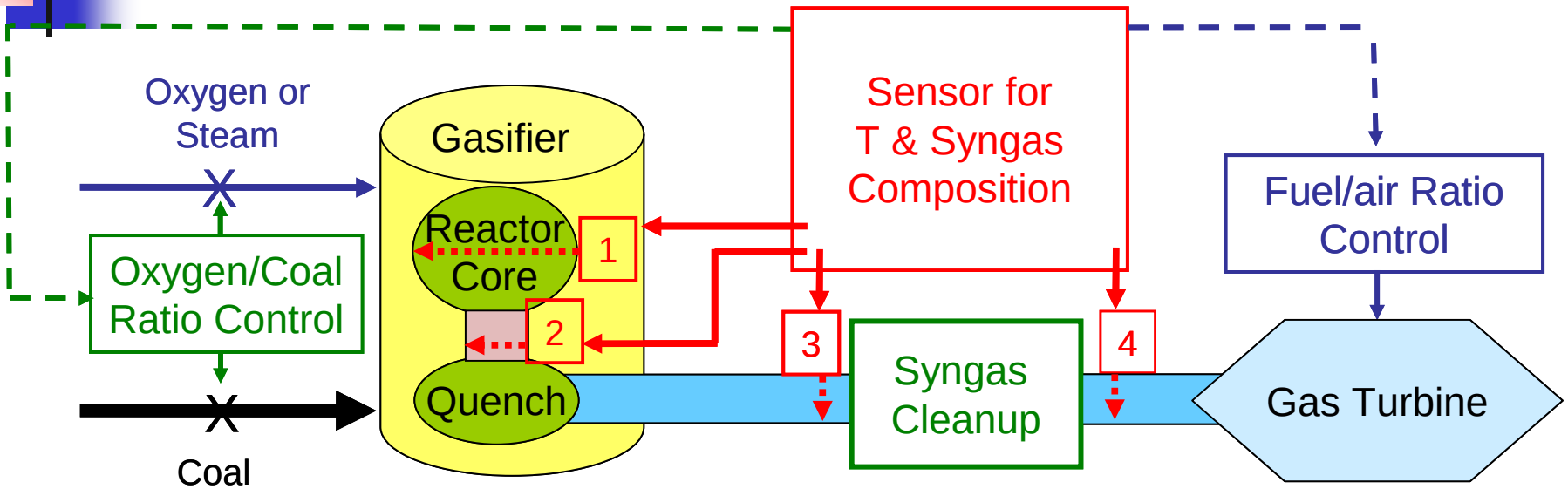

Vision: Sensor for control signals to optimize gasifier output and gas turbine input

- Two flow parameters considered: gas temperature and syngas energy
  - Gas temperature determined by ratio of H_2O measurements
  - For O_2 blown systems CO, CH_4, CO_2, and H_2O provide syngas energy
    - Where H_2 can be determined by gas balance
- Four measurement stations considered: spanning reactor core to products

13

3. H_2O & T in Slagging Coal Gasifier @ Utah

Entrained flow gasifier @ Utah

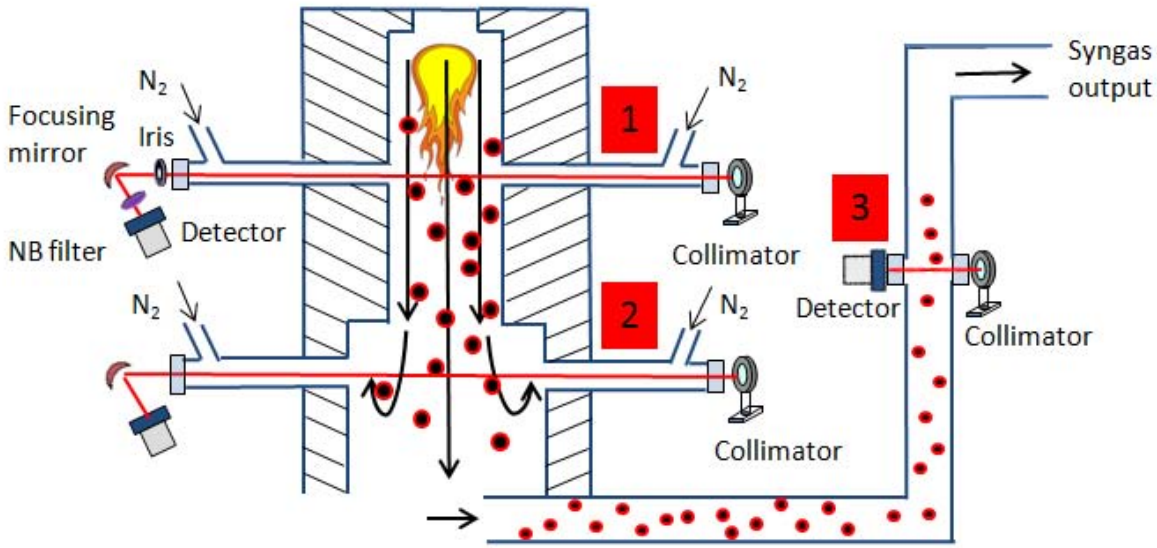

Sensor locations
1: Reactor Core
T: 1300K-1700K
2: Quench
T: 600K-1000K
3: Post-quench
T: 330K-400K

Pressure range investigated:
50psig to 200psig

- **Measurement locations 1 and 2 provide opportunity for control**
  - **Temperature sensing by ratio of H_2O absorption lines**
- **Measurement location 3 monitors syngas heating value**
  - **Monitor CO, H_2O, CO_2, CH_4, and assume balance H_2**

Jeffries et al., *Pittsburgh Coal Conf*, 2011

3. H_2O & T in Slagging Coal Gasifier @ Utah

Challenge: Absorption Broadened by Pressure

- **Practical combustion devices often operate at elevated pressures**

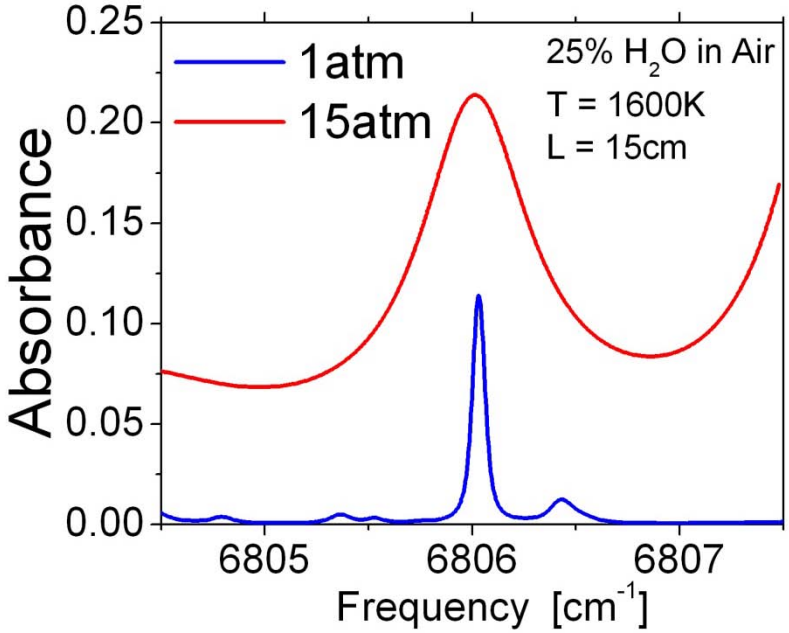

- **Pressure broadening**
  - **Blends nearby transitions**
  - **Eliminates the baseline between transitions**
- **Particulate in the synthesis gas attenuates laser transmission**
- **Solution: 1f-normalized WMS: accounts for varying transmission**

3. H_2O & T in Slagging Coal Gasifier @ Utah
Transmission loss by particulate scattering

Transmission of laser light at non-absorbing wavelength vs reactor pressure at syngas output

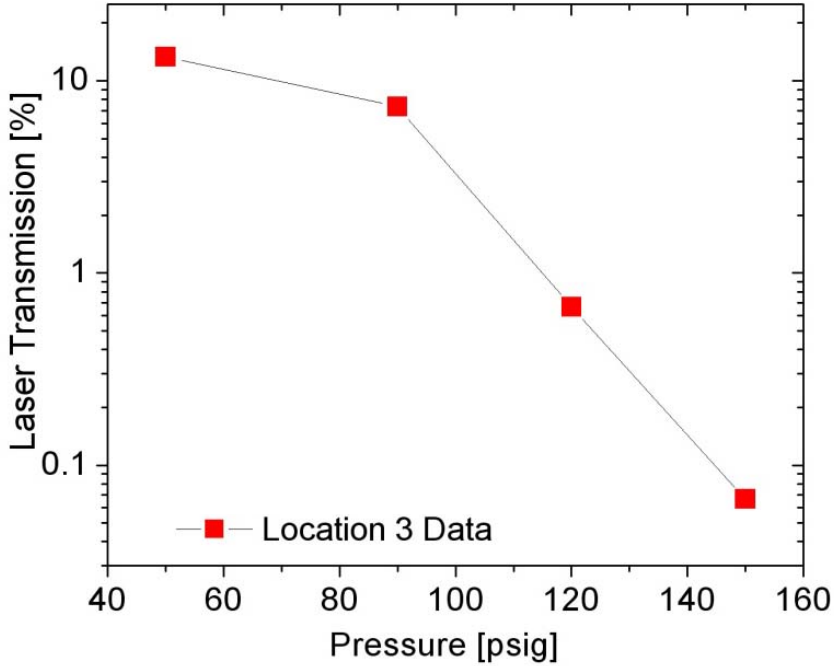

- Reactor loading, throughput, and efficiency increase with pressure
- Particulate loading also increases with pressure
- Scattering losses severely reduce laser transmission

Solution: 1f-normalized wavelength-modulation spectroscopy (WMS *2f/1f*)

3. H_2O & T in Slagging Coal Gasifier @ Utah
TDLAS Temperature in Reactor Core

Two H_2O transitions: 7426cm^{-1}, E”~1300cm^{-1}, f = 13kHz
7466cm^{-1}, E”~2660cm^{-1}, f = 10kHz

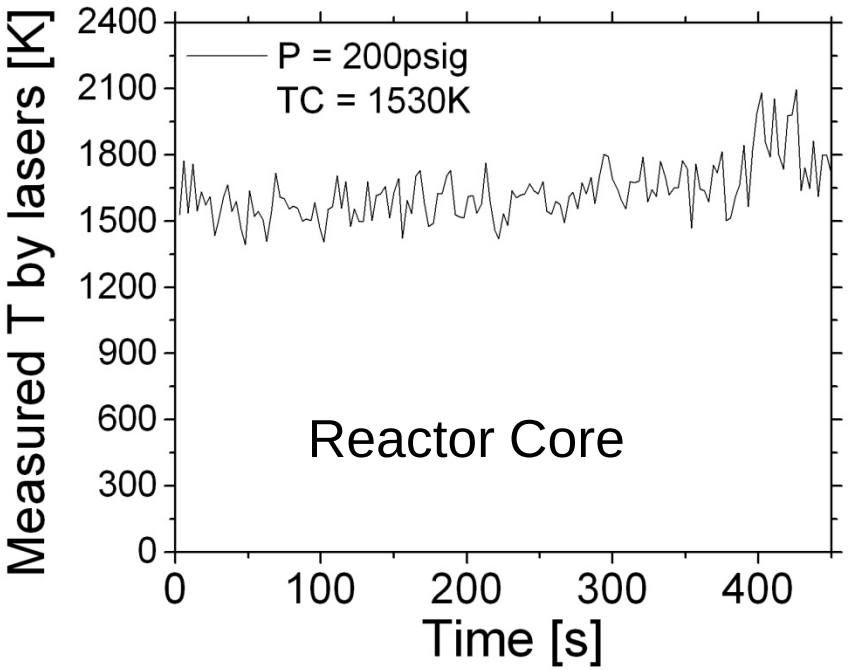

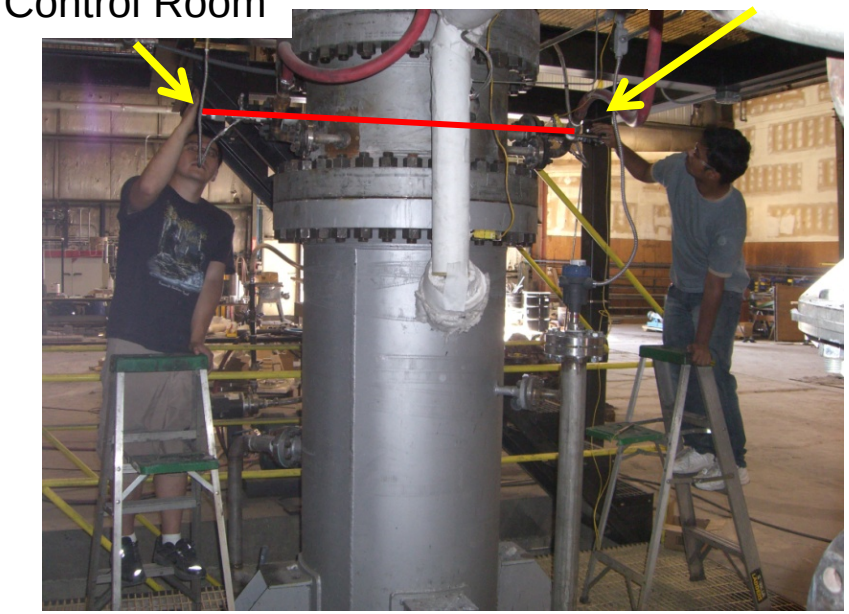

Laser beam alignment @Utah
– no access during experiments

- **Normalization scheme successful with low transmission (< 0.02%)**
- **Fluctuations in T reveal unsteadiness in reactor core**

3. H_2O & T in Slagging Coal Gasifier @ Utah

CO and CO_2 vs Time in Syngas Output

CO measurements

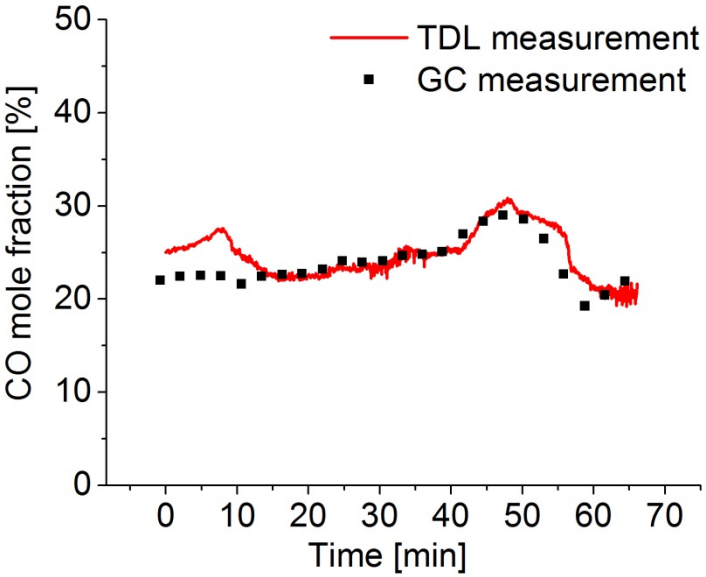

CO_2 measurements

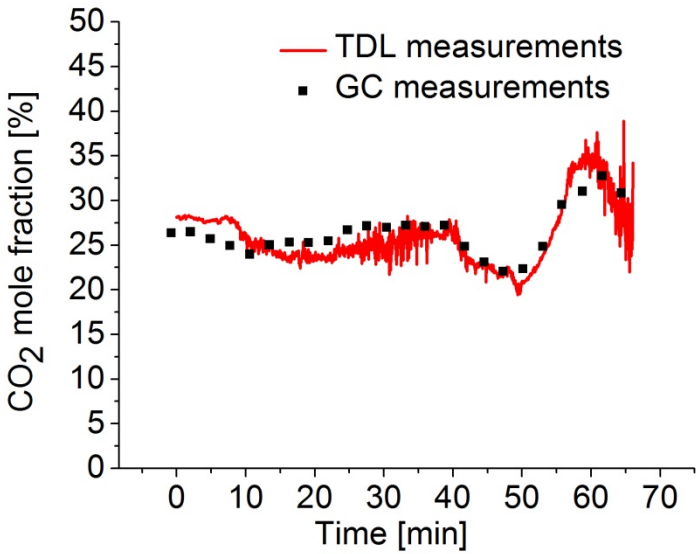

- Monitor composition of syngas output at location 3
  - Simultaneous measurements of CO, CH_4, CO_2, and H_2O
- Coal/O_2 feed rates varied changes CO & CO_2 values during final 30 minutes
- GC data adjusted to account for ~4 min sampling/drying delay
  - TDL data in good agreement with GC

3. H_2O & T in Slagging Coal Gasifier @ Utah

CH_4 and H_2O vs Time in Syngas Output

CH_4 measurements

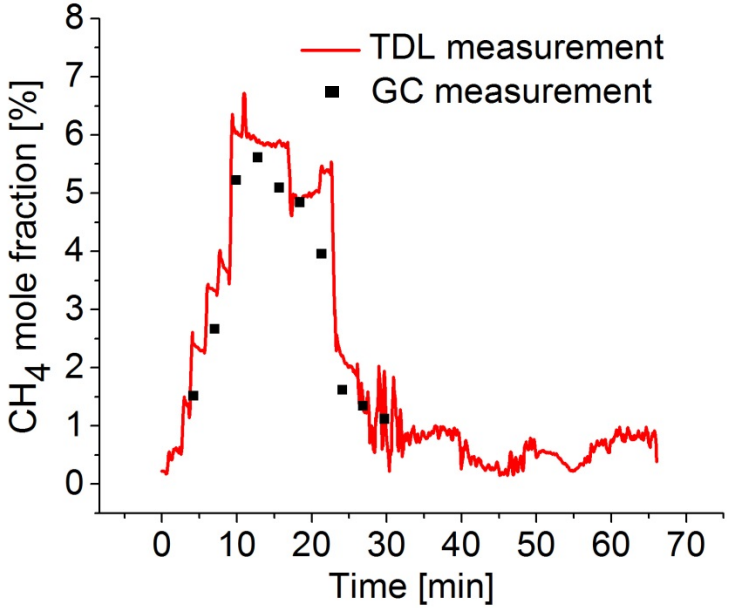

H_2O measurements

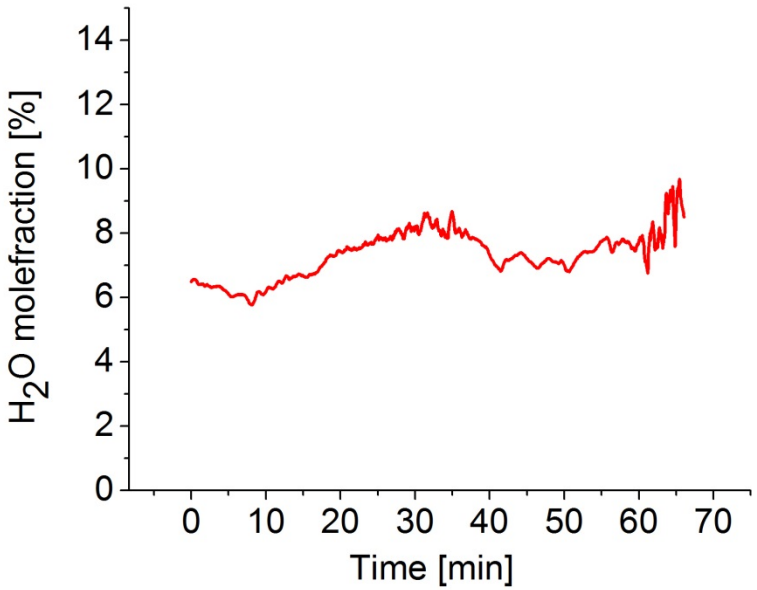

- Monitor composition of syngas output at location 3
  - Simultaneous measurements of CO, CH_4, CO_2, and H_2O
- CH_4 added to syngas to test sensor response during first 30 minutes
- GC data adjusted to account for ~4 min sampling/drying delay
  - TDL data in good agreement with GC

Part 4: Extend to industrial-scale gasifier

4. H_2O in Transfer Coal Gasifier @NCCC
Large-Scale DoE Demonstration Facility

Instrumentation shelter

Note man-sized figure

- NCCC transport gasifier based on a circulating fluidized bed concept

Goal:

Laser absorption *in situ* measurements of moisture and temperature of syngas

4. H_2O in Transfer Coal Gasifier @NCCC

TDL Sensor Located Downstream of PCD

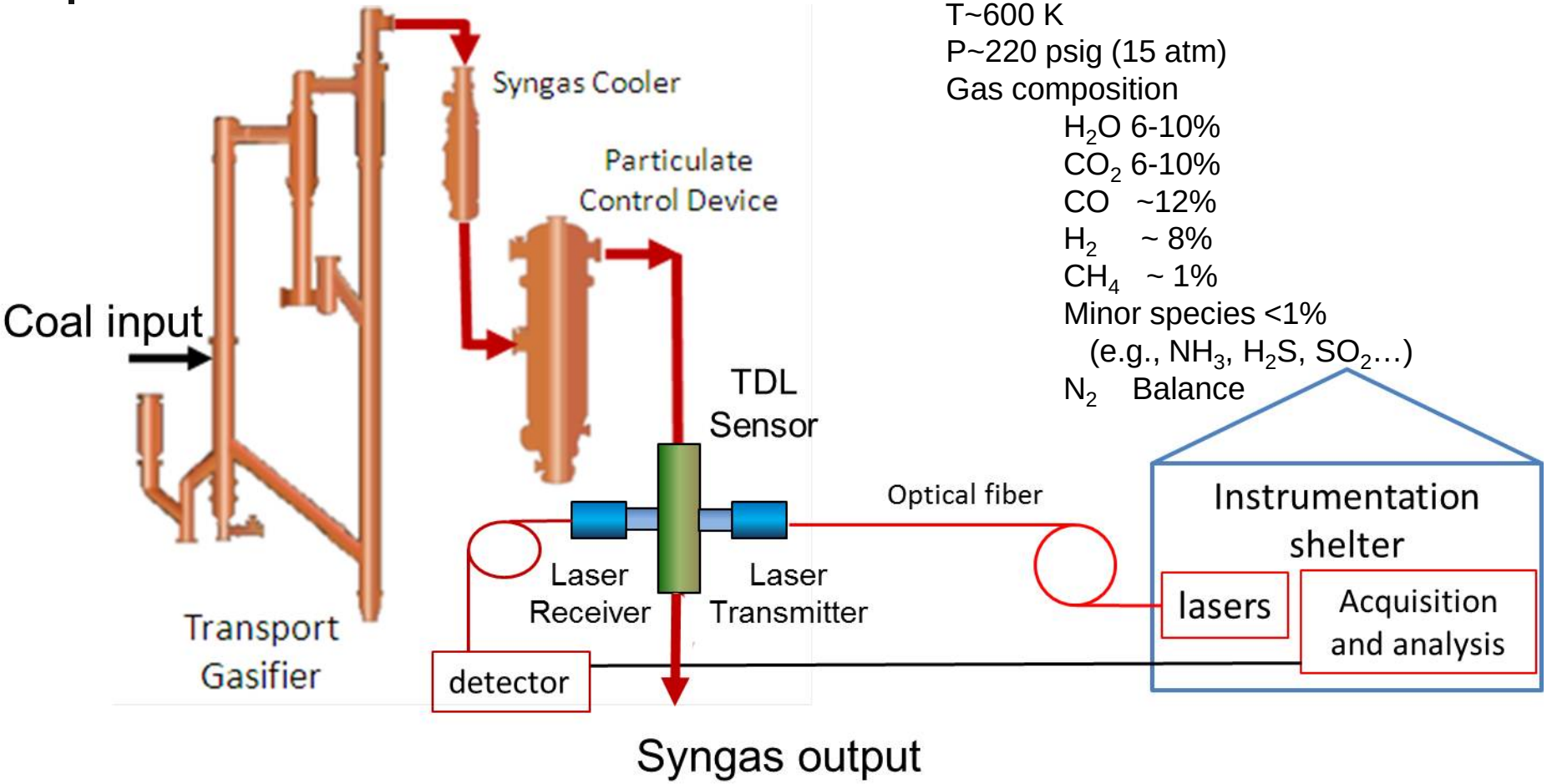

Nominal conditions at TDL sensor

- T~600 K
- P~220 psig (15 atm)
- Gas composition
  - H_2O 6-10%
  - CO_2 6-10%
  - CO ~12%
  - H_2 ~ 8%
  - CH_4 ~ 1%
  - Minor species <1% (e.g., NH_3, H_2S, SO_2…)
  - N_2 Balance

- TDL sensor monitors syngas flow 99 feet downstream of the PCD
- Small (0.01%) transmission due to beam steering & scattering from ash

4. H_2O in Transfer Coal Gasifier @NCCC

Laser Sensor Installed on Syngas Output Flow

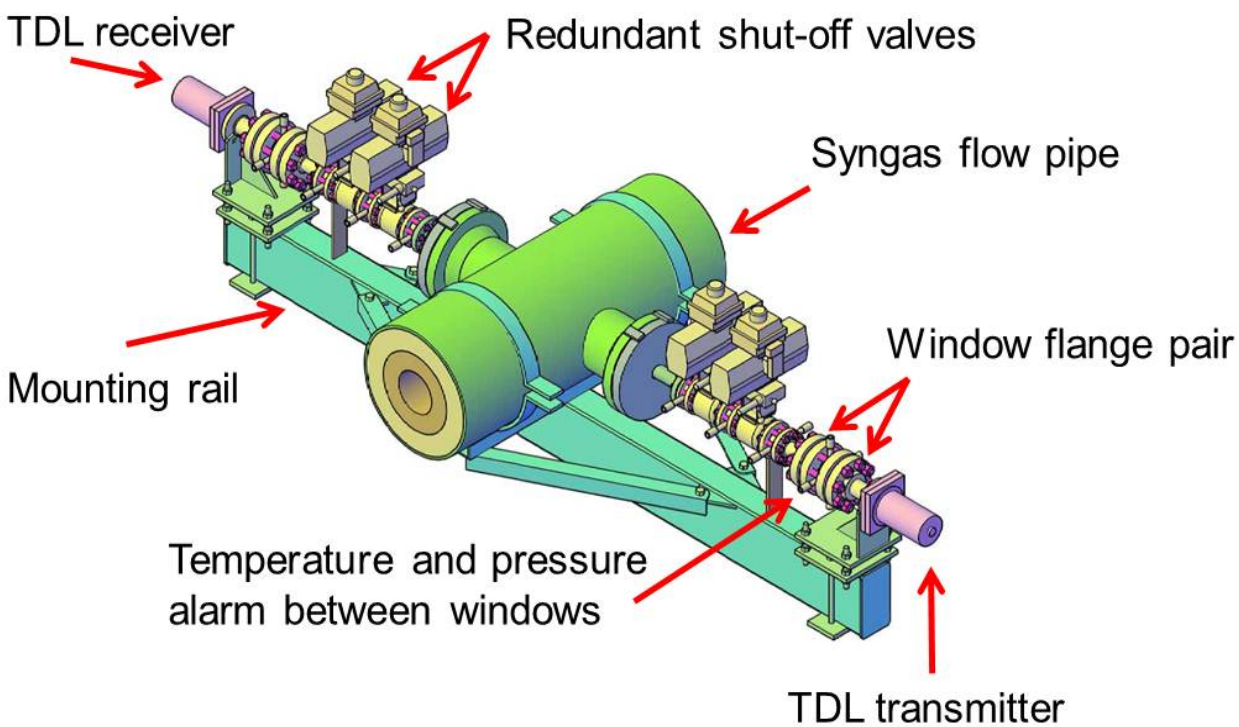

- Safety a paramount element of engineering design
  - Redundant shut-off valves to isolate laser sensor
  - Redundant sapphire windows with P/T failure sensor
- Transmitter and receiver mounted on rail hung from process pipe to minimize thermal motion from process/weather

4. H_2O in Transfer Coal Gasifier @NCCC

Laser Sensor Installed on Syngas Output Flow

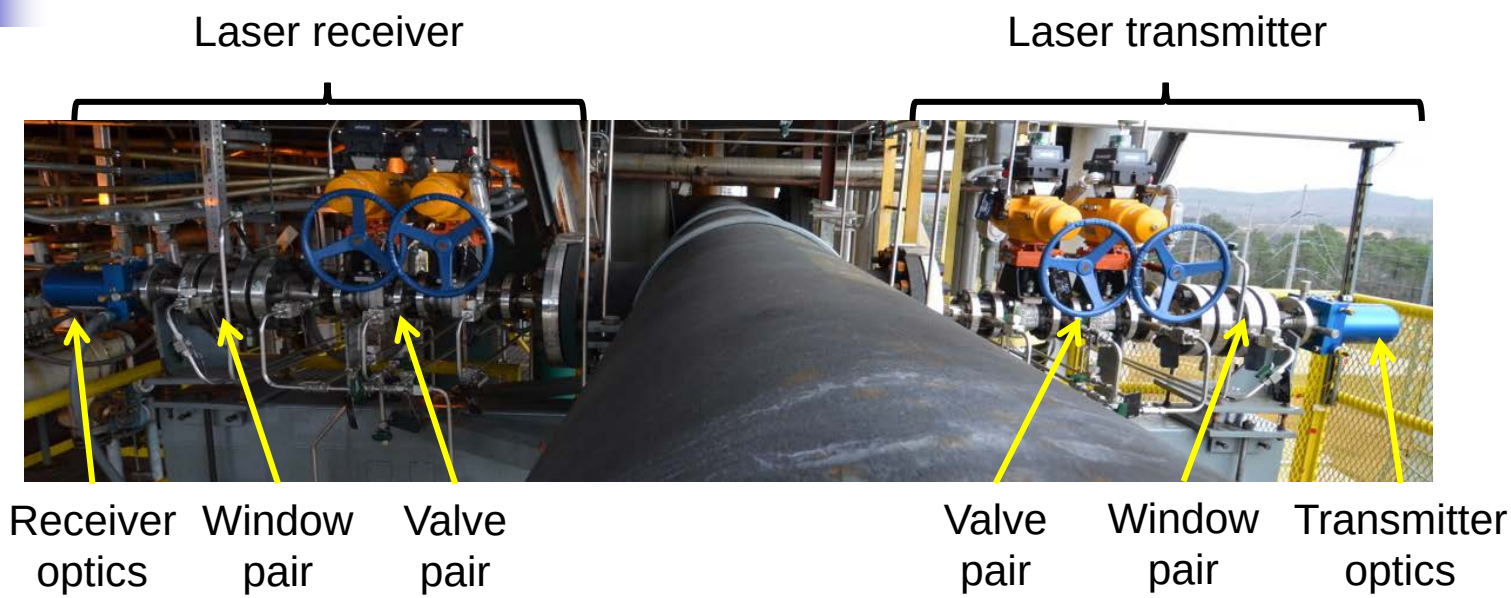

- Photo illustrates the large-scale of this commercial size system

Now let's look at sensor measurements during start-up

4. H_2O in Transfer Coal Gasifier @NCCC

Time-Resolved TDLAS During Gasifier Start-up

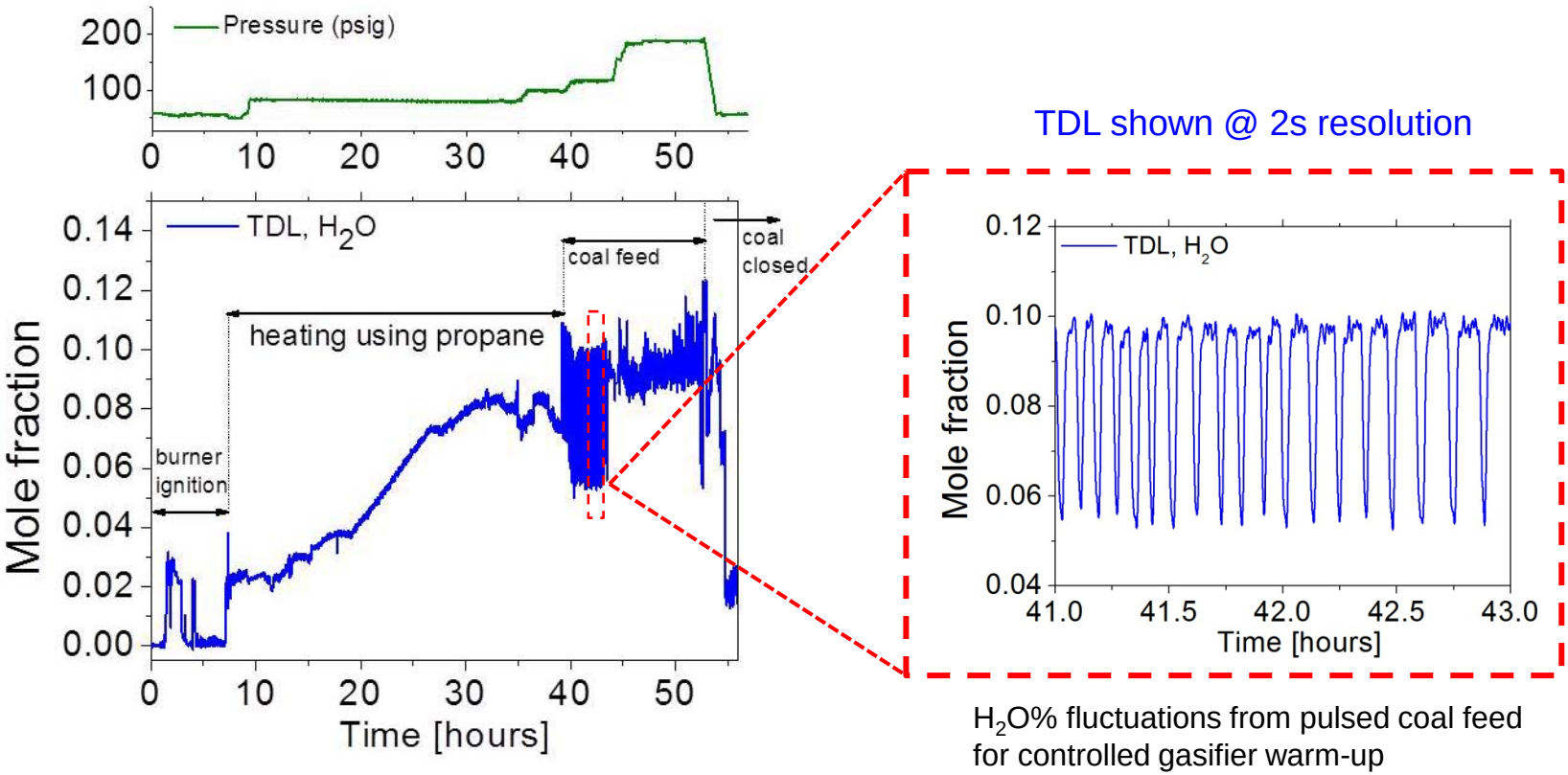

H_2O% fluctuations from pulsed coal feed for controlled gasifier warm-up

- *In situ* measurements of syngas moisture content capture start-up events
  - Propane heater ignition (H_2O combustion products) and warm-up
  - TDLAS of H_2O captures pulsing of coal feeder to control warm-up rate of the rig
  - Transition to gasification
- TDL sensor captures a shut-down at 54 hours

4. H_2O in Transfer Coal Gasifier @NCCC

TDL Sensor Captures Transient in Gasifier Reactor

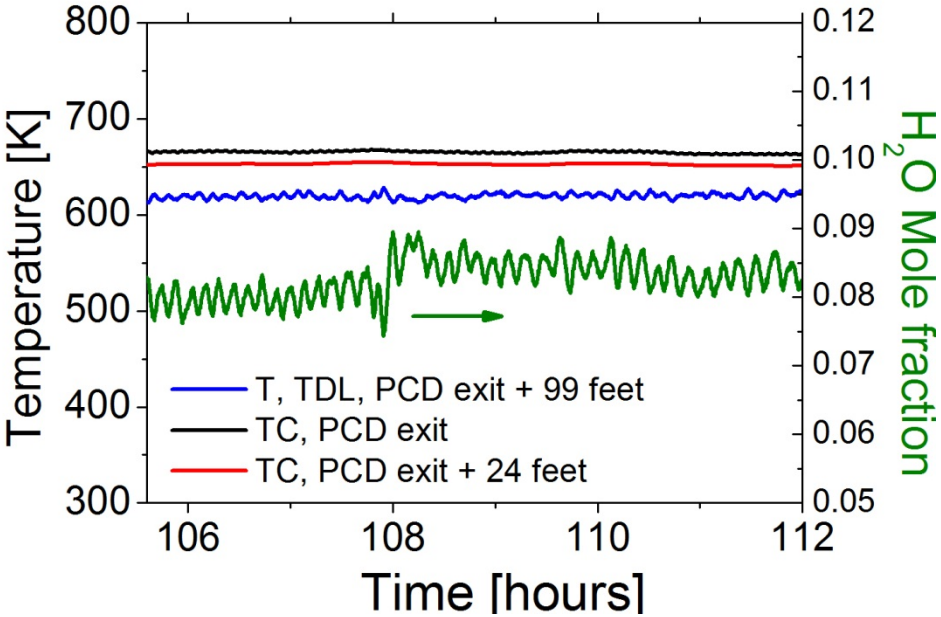

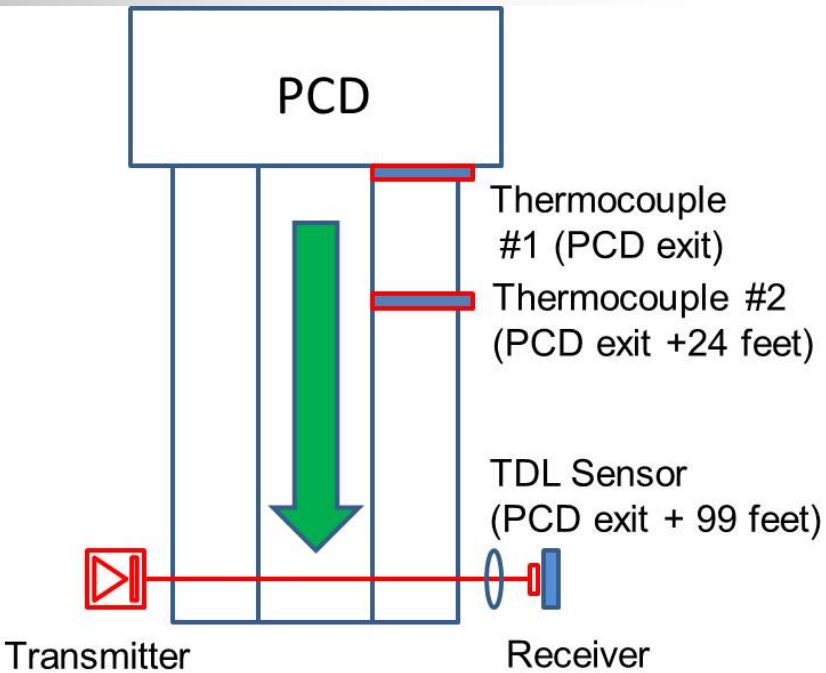

- Syngas temperature stable in agreement with post PCD TC's
- Time-resolved syngas moisture identifies transient and fluctuations

4. H_2O in Transfer Coal Gasifier @NCCC

TDL Sensor Captures Transient in Gasifier Reactor

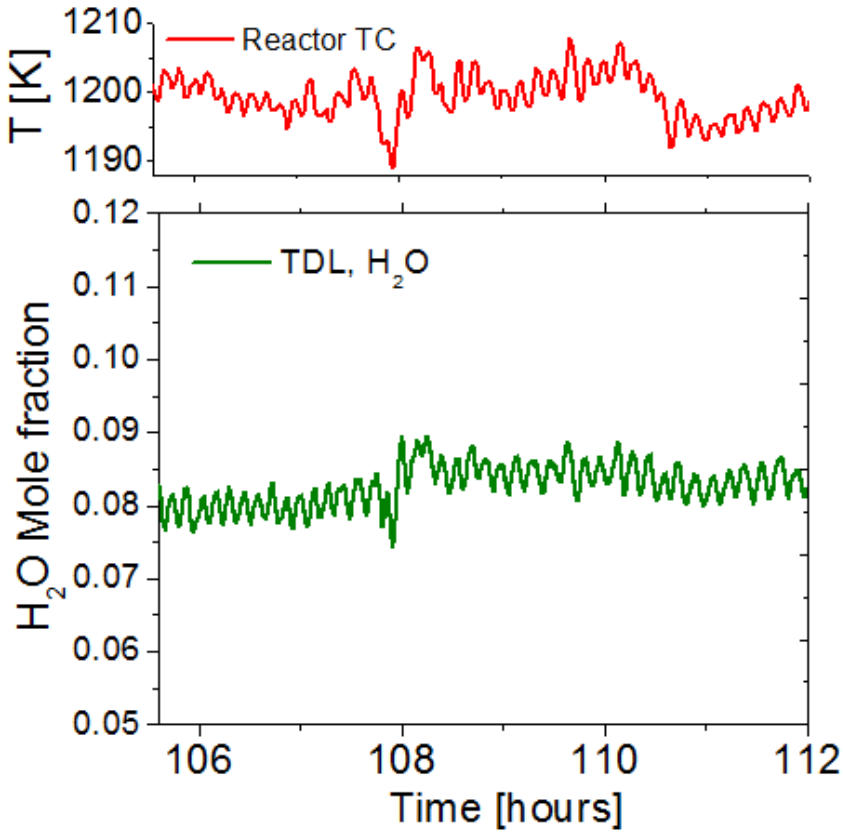

- Syngas temperature stable in agreement with post PCD TC's
- Time-resolved syngas moisture identifies transient and fluctuations
- Transient and fluctuations track the gasifier reactor TC

4. H_2O in Transfer Coal Gasifier @NCCC

Continuous Time-Resolved Unattended TDLAS

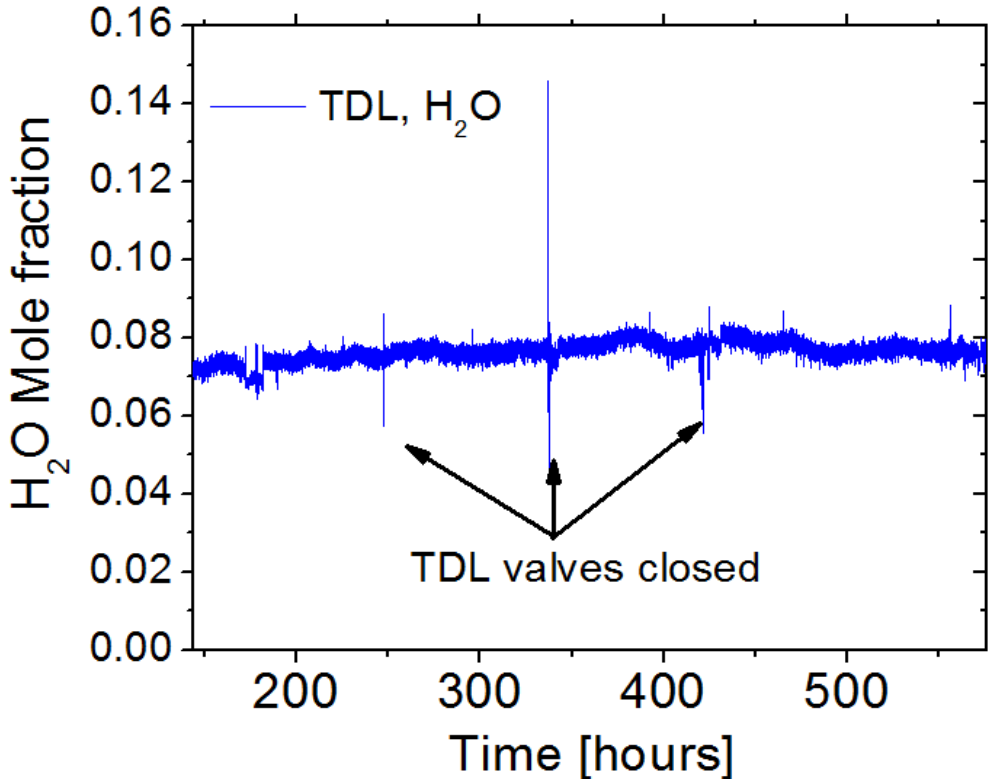

- Unattended operation yields continuous record of H_2O
- Values closed 3 times during run due to reactor upset not related to TDL
- Light transmission stable over entire campaign (depends on P)
  - No degradation of window transmission or laser performance

4. H_2O in Transfer Coal Gasifier @NCCC

TDL H_2O Compared to Liquid H_2O Samples

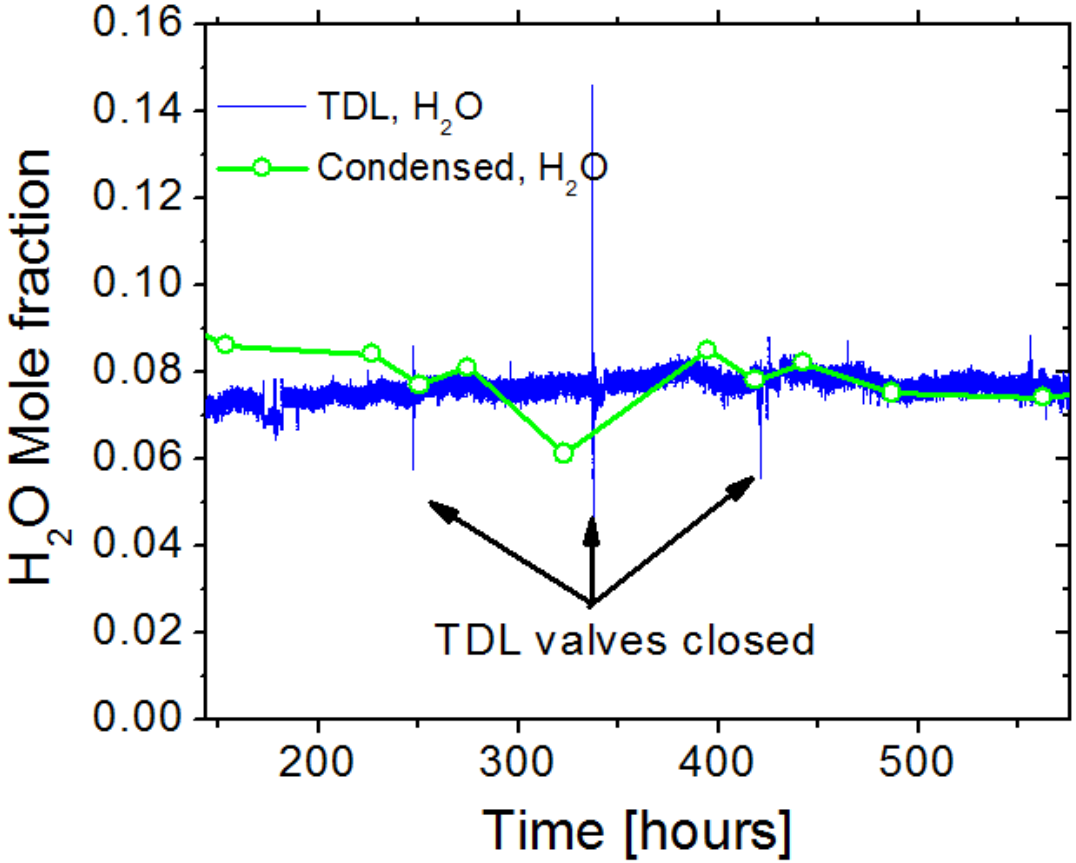

- Liquid H_2O samples taken from syngas every day or two
- TDLAS data in good agreement with samples

Can Sensor reveal real-time moisture fluctuations?

4. H_2O in Transfer Coal Gasifier @NCCC

Syngas H_2O Fluctuations Capture Reactor Conditions

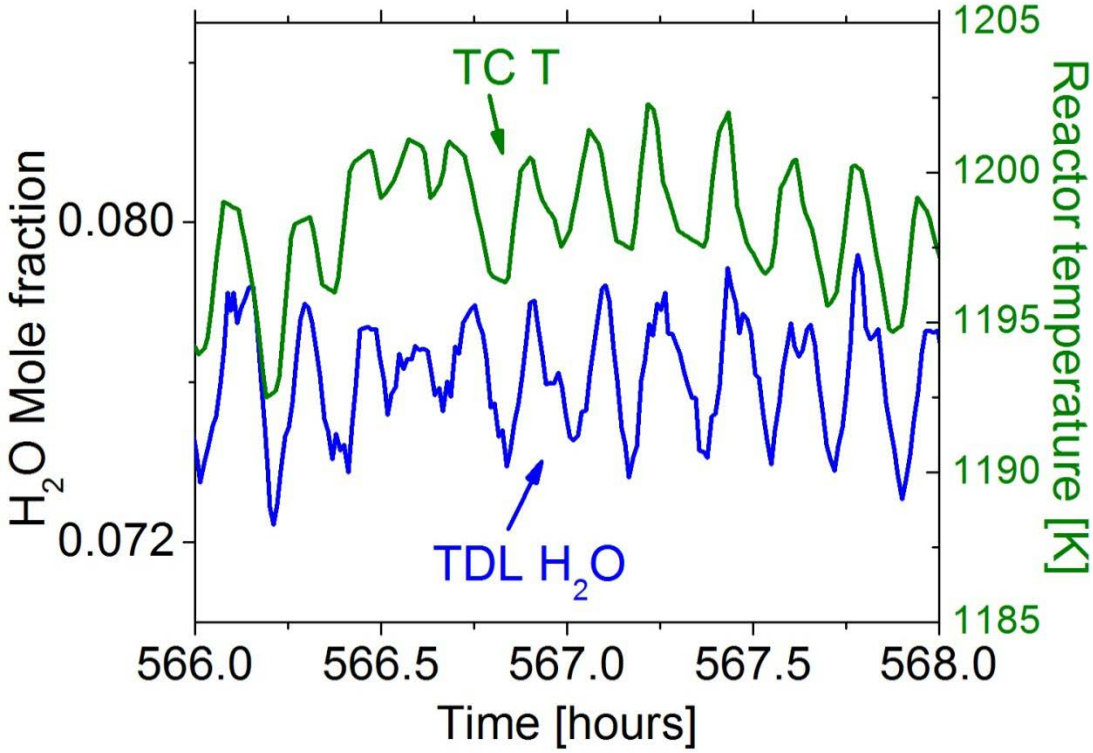

- H_2O fluctuation tracks the reactor thermocouple (note small ΔT)

Part 5: Measurements of NO and CO at exit of powerplant boiler

5. NO and CO in Coal-Fired Boiler Exhaust

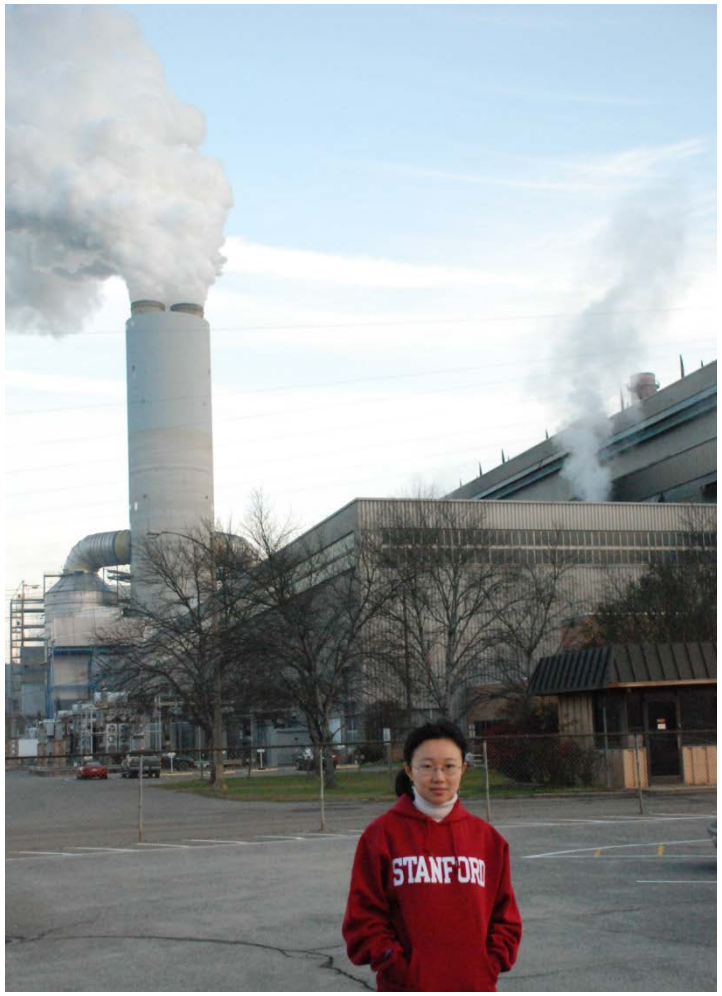

Xing Chao, 2009/10

5. NO and CO in Coal-Fired Boiler Exhaust

Emissions Sensing in Coal-Fired Powerplants

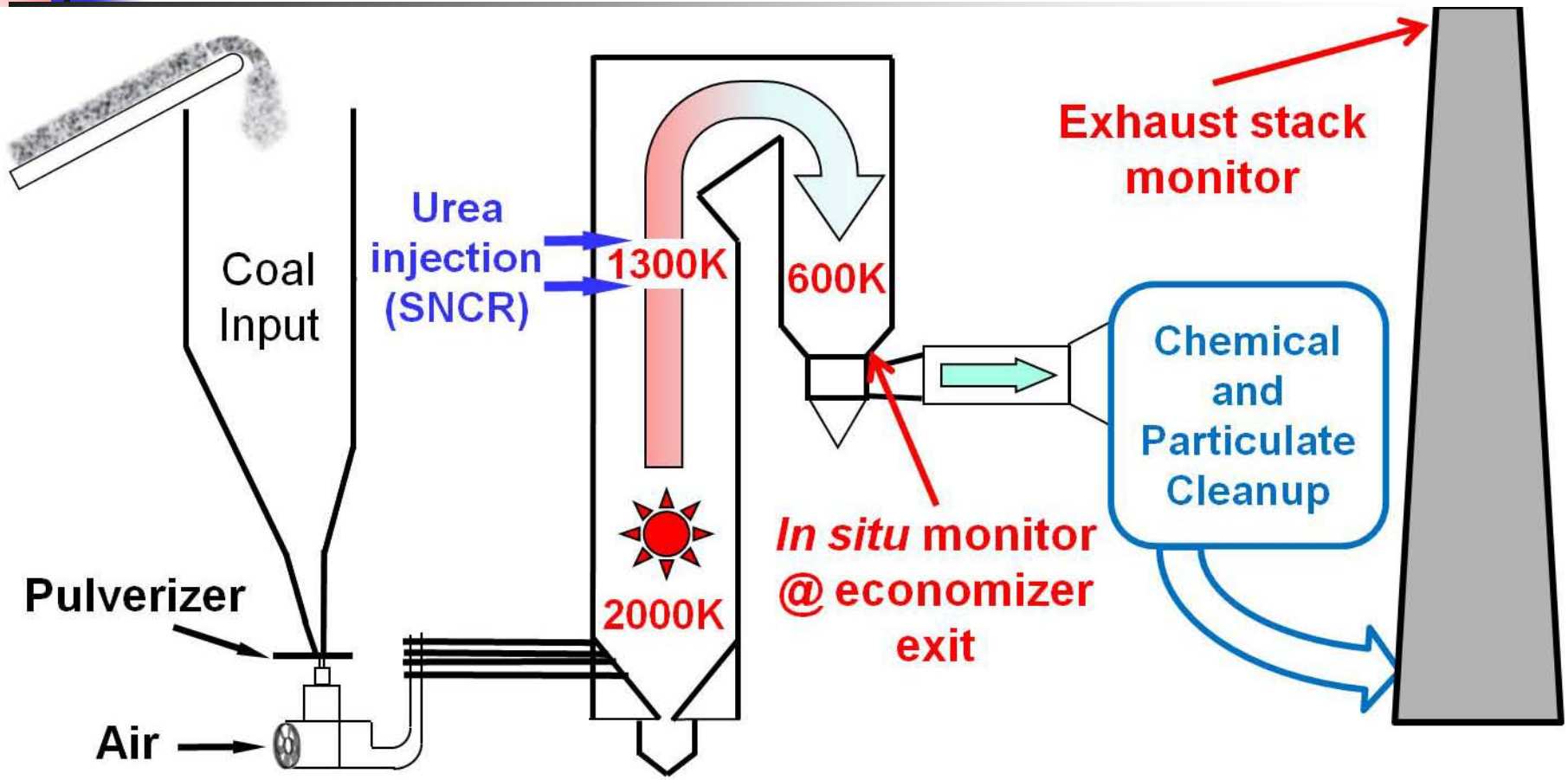

- *In situ* CO and NO measurements at economizer exit of pulverized coal boiler for characterization of SNCR

5. NO and CO in Coal-Fired Boiler Exhaust

Interference Absorption and Scattering Attenuation

- Measurement of other species must consider H_2O interference

CO

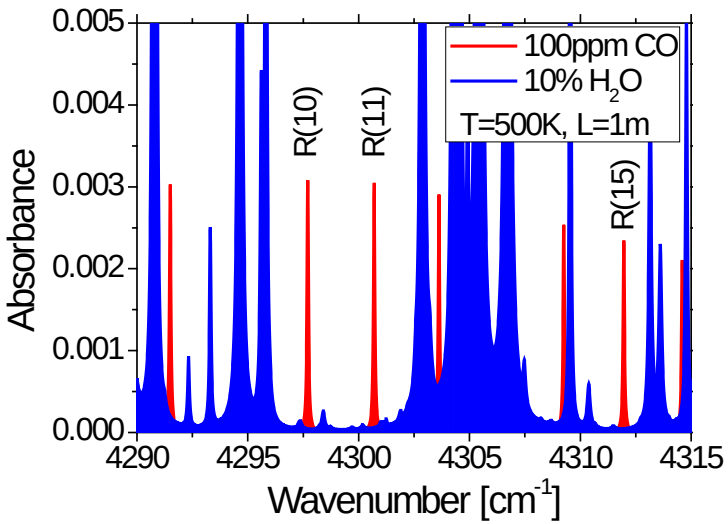

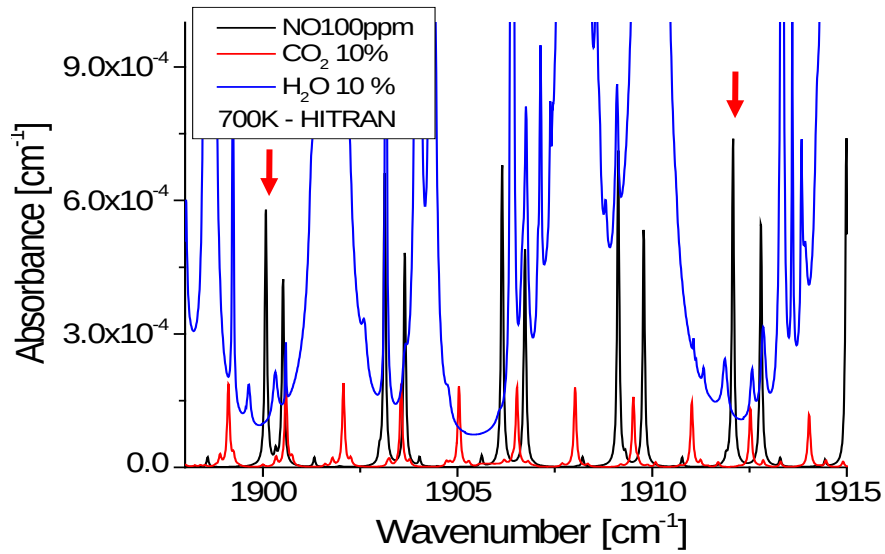

NO

- Several candidate CO lines found that are free of H_2O interference
- Two good candidate NO lines are found relatively free of interference

- Particulate in the flow (flyash, soot, etc) attenuates the beam, but Stanford's 2f/1f approach resolves the problem

5. NO and CO in Coal-Fired Boiler Exhaust

Sensing at the Economizer Exit

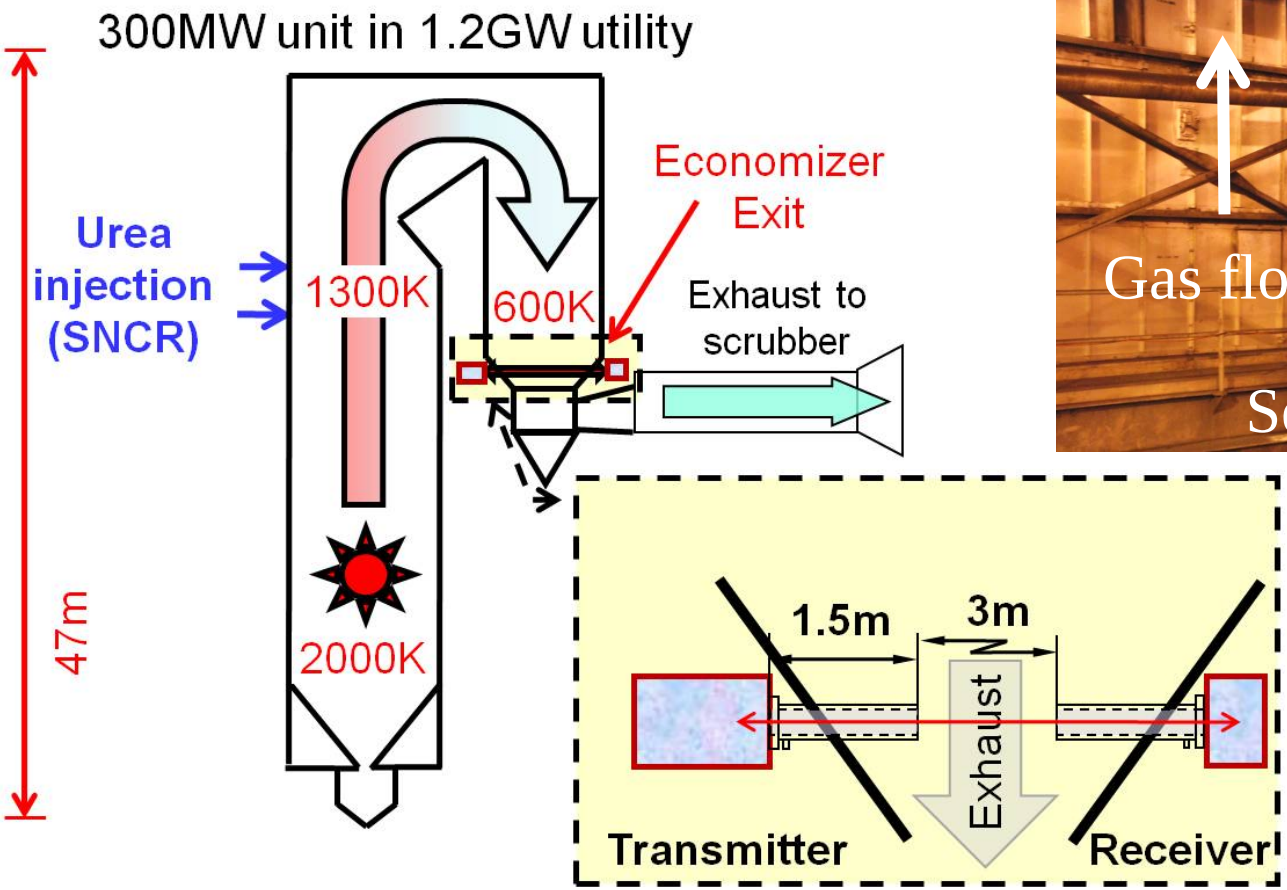

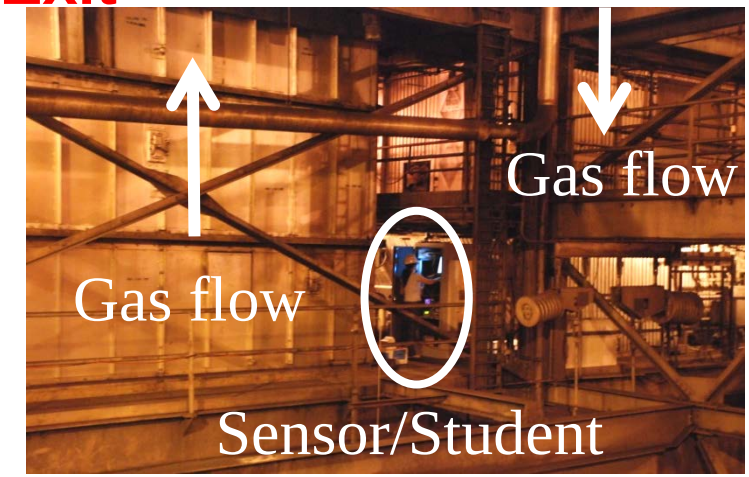

- **Utilizes 5.2μm QC for NO and 2.3μm TDL for CO**
- **Dusty environment results in large scattering losses**
  - **50-90% of incident light scattered**

5. NO and CO in Coal-Fired Boiler Exhaust

CO Sensing with 2.3 μm DFB Laser

- **Continuous monitoring of CO with varying excess air**

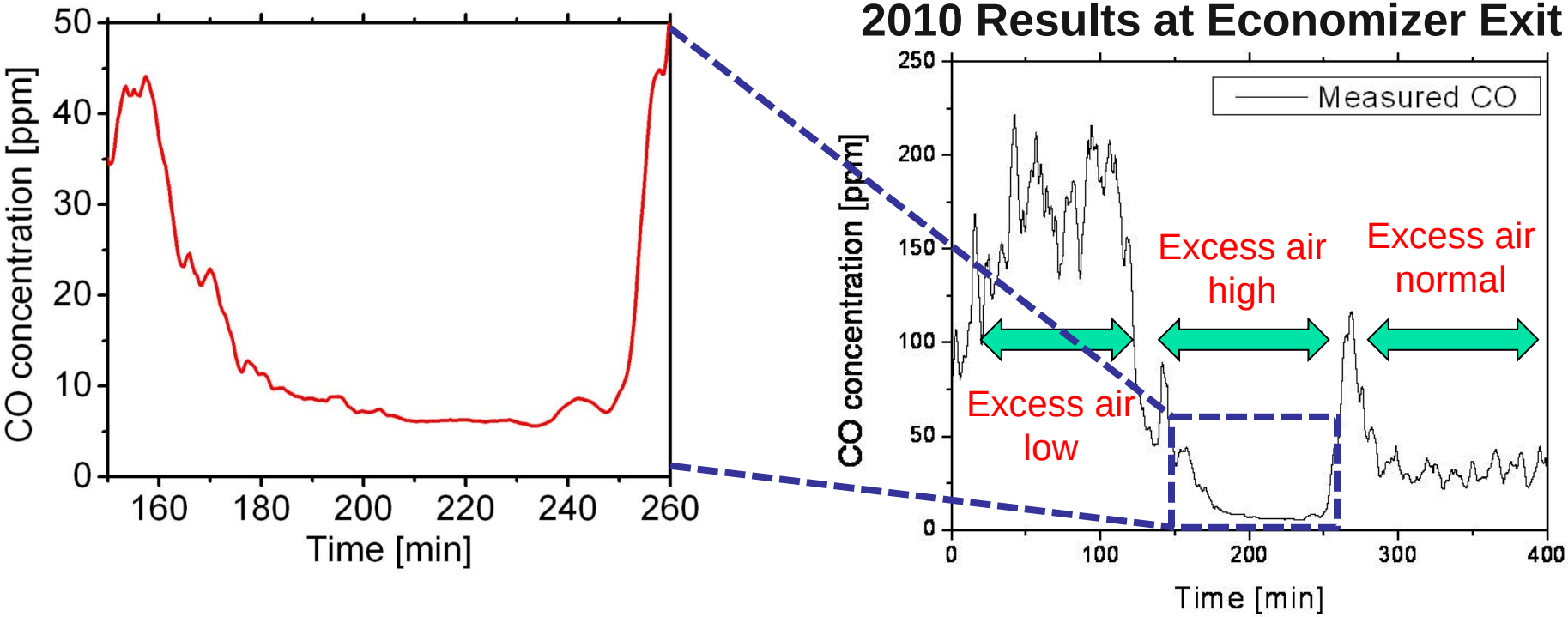

- **Correlates with excess air as expected**
- **Sensitive (ppm) time-resolved CO detection**
- ***In situ* sensor avoids delay/mixing of stack CEM**

Chao et al., *Proc Combustion Institute*, 2011

5. NO and CO in Coal-Fired Boiler Exhaust

NO Sensing with 5.2 μm QC Laser

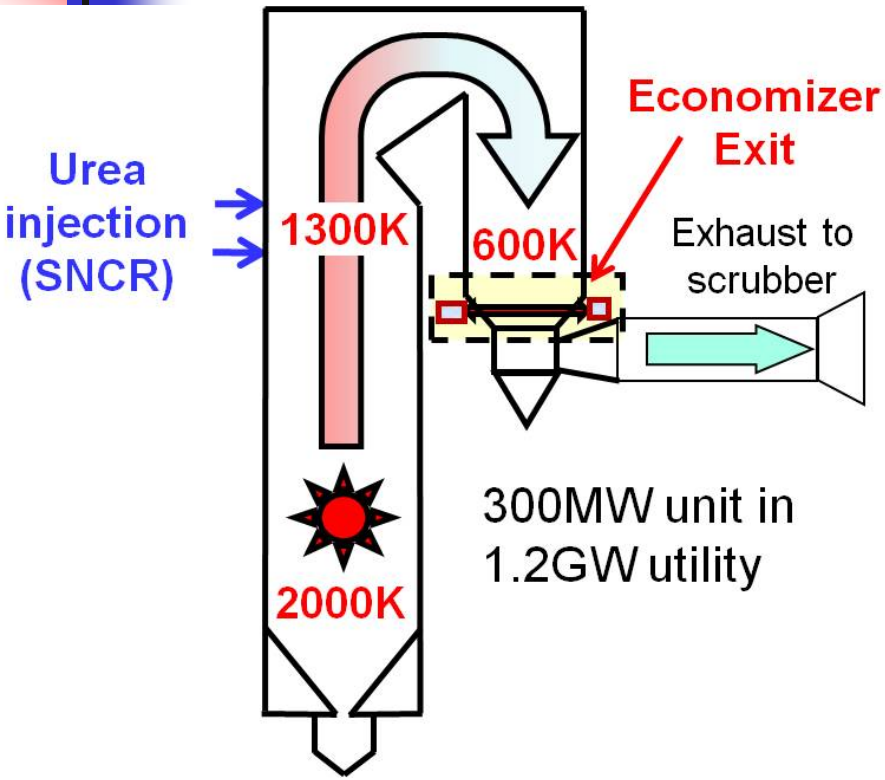

2010 Results at Economizer Exit of Pulverized Coal-Fired Plant

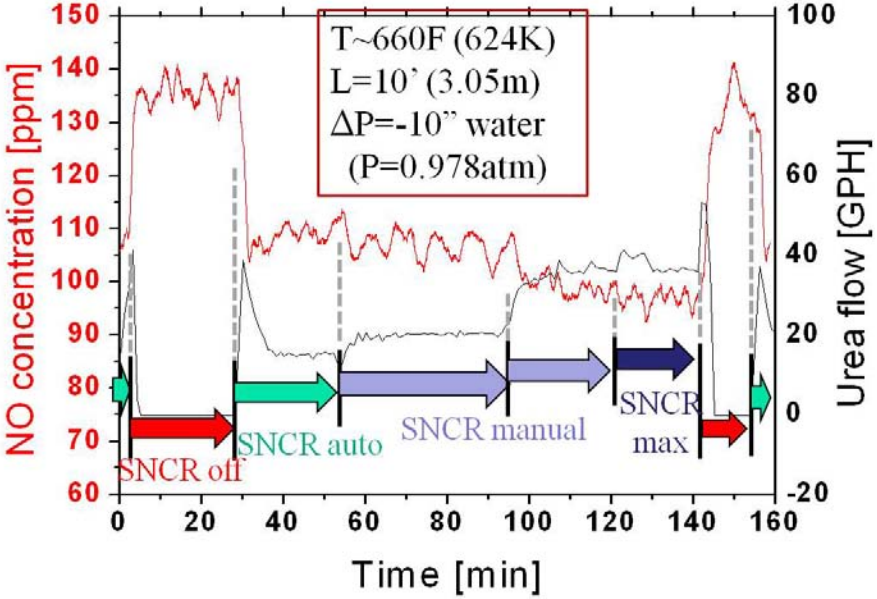

- **Sensitive (ppm) time-resolved NO detection**
- ***In situ* sensor avoids delay/mixing of stack CEM**
- **Potential for control of individual boilers**

6. TDLAS for Energy Conversion – Future Trends

- Portable TDL-based sensors useful for T, V, species and mass flux over wide range of conditions, industries
- Potential use as control variables for combustion emissions/efficiency
- Potential use for compliance monitoring of pollutant emissions

- Current and future topics:
  - Extension to UV and mid-IR to access new species

    → CO, CO_2, HC's, radicals, NO, NO_2
  - Advanced energy utilization: bio-fuels, gasification, liquifying natural gas

Next Lecture

Shock tubes and applications to combustion kinetics